Chem Soc Rev

REVIEW ARTICLE

View Article Online
View Journal

Cite this: DOI: 10.1039/c9cs00653b

Upgrading of marine (fish and crustaceans) biowaste for high added-value molecules and bio(nano)-materials

Thomas Maschmeyer, [a] Rafael Luque [b] and Maurizio Selva *[c]

Received 23rd December 2019

DOI: 10.1039/c9cs00653b

rsc.li/chem-soc-rev

Currently, the Earth is subjected to environmental pressure of unprecedented proportions in the history of mankind. The inexorable growth of the global population and the establishment of large urban areas with increasingly higher expectations regarding the quality of life are issues demanding radically new strategies aimed to change the current model, which is still mostly based on linear economy approaches and fossil resources towards innovative standards, where both energy and daily use products and materials should be of renewable origin and 'made to be made again'. These concepts have inspired the circular economy vision, which redefines growth through the continuous valorisation of waste generated by any production or activity in a virtuous cycle. This not only has a positive impact on the environment, but builds long-term resilience, generating business, new technologies, livelihoods and jobs. In this scenario, among the discards of anthropogenic activities, biodegradable waste represents one of the largest and highly heterogeneous portions, which includes garden and park waste, food processing and kitchen waste from households, restaurants, caterers and retail premises, and food plants, domestic and sewage waste, manure, food waste, and residues from forestry, agriculture and fisheries. Thus, this review specifically aims to survey the processes and technologies for the recovery of fish waste and its sustainable conversion to high added-value molecules and bio(nano)materials.

1. Introduction

In the past forty years, the average consumption of fish has significantly expanded from 12.6 kg per person in the early 1970s to 14.2 and 19.8 kg per person in the early 1990s and 2010s, respectively.[1] This impressive growth explains why the United Nations' 2030 Agenda for Sustainable Development and FAO have widely recognized the essential role of fisheries and aquaculture for food security and nutrition. However, it has also been highlighted that this sector has several challenges, including the reduction of fishing beyond biological sustainability, and the need to improve the recovery and upgrading of waste.[2]

The estimate discards from fisheries worldwide are still a matter of debate with yearly quantities varying in a rather wide range. Some analyses report amounts exceeding 20 million ton per year, corresponding to approximately 25% of the total production including by-catch (''non-target'' species) and fish processing waste.[3,4] In contrast, other studies claiming the use of a 'catch reconstruction' approach, which also comprises data missing from official (FAO) reports, indicate that global discards peaked at 18.8 million tons in 1989, and gradually declined thereafter to *ca.* 10 million ton per year, representing between 10% and 20% of the total reconstructed catches (reported landings + unreported landings + unreported discards).[5,6] This decrease in global discarding offers a good perspective, and efforts need to be enhanced worldwide to ensure that this trend continues. However, it has also been estimated that in 2014, high-seas fishing profits totalled $1.4 billion, which is much lower the governments subsidies of $4.2 billion afforded to this sector. This has led to the conclusion that companies operating in the high seas benefit from underreporting the catch, with an obvious underestimation of fishing revenue and profits.[7] This is a fact that was publicly denounced by an international broadcaster who cited the case of the fishing industry in Australia, one of the world leaders in the field, declaring officially only 65% of the total commercial fish catch.[8]

Although the emerging scenario is not clearly defined, beyond the accuracy of statistics and estimates, the resulting amount of fish biowaste is in the order of dozens of million tons per year, representing a resource of an extraordinary chemical richness, which is certainly worth valorising.[9]

In addition to capture fisheries, aquaculture offers another remarkable contribution to fish production. According to FAO

[a] *F11 – School of Chemistry, The University of Sydney, NSW 2006, Australia*
[b] *Department of Applied Chemistry, School of Science, Xi'an Jiaotong University, No. 28, Xianning West Road, Xi'an, 710049, P. R. China*
[c] *Dipartimento di Scienze Molecolari e Nanosistemi, Università Ca' Foscari Venezia, Via Torino, 155 – 30175 – Venezia Mestre, Italy. E-mail: selva@unive.it*

analysis, the global aquaculture production (including aquatic plants) in 2016 was 110.2 million tonnes, shared between 80.0 million tonnes of food fish and 30.1 million tonnes of aquatic plants with an overall first-sale value estimated at USD 243.5 billion (Fig. 1).[2]

Aquaculture continues to grow comparatively faster than other major food sectors, with a 5.8% annual growth rate in the past 15 years, implying another substantial input in the production of fish biowaste.

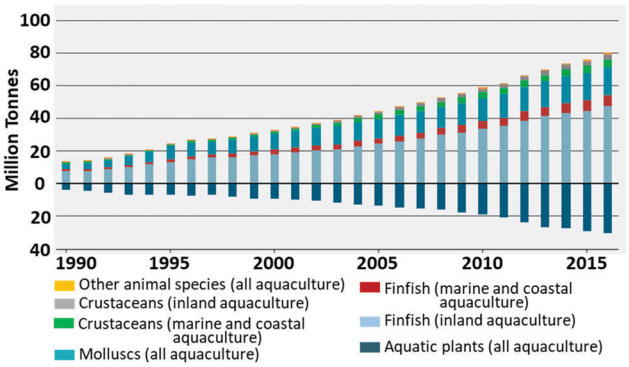

Fig. 1 World aquaculture production of food fish and aquatic plants from 1990 to 2016 (from ref. 2).

Thomas Maschmeyer

Prof. Thomas works in the School of Chemistry at University of Sydney. He is the Founder and Executive Chairman of Gelion Technologies (2015), Co-Founder of Licella Holdings (2007) and inventor of its Cat-HTR™ technology. He authored over 325 publications, including 26 patents, been cited 10 000+ times, and has an H-Index of 59. He serves on the boards of ten international journals and has received many awards, including most recently the Eureka Prize for Leadership in Innovation and Science (2018), Australia's Principle Science Prize, and the Federation of Asian Chemical Societies' Contribution to Economic Development Award (2019).

Before distribution, the processing of fish involves different operations aimed to remove their slime and scales, head, fins and bones, and the preparation of fillets for labelling and final packaging.[10] The generated fish residues are comprised of whole waste fish, fish head, viscera, skin, bones, blood, frames liver, gonads, guts, some muscle tissue, *etc.*, and the corresponding composition varies according to the type of species, sex, age, nutritional status, time of year and health. However, proteins, fats, fibre, ash, and different elements (in the form of minerals) are present in the proportions shown in Table 1.[11]

Therefore, fish biowaste contains several potentially valuable molecules including oils, a well-balanced mixture of amino acids and bioactive peptides, collagen, chitin, gelatin, and

Rafael Luque

Prof. Rafael Luque (PhD 2005 from Universidad de Cordoba, Spain) has significant expertise on biomass and waste valorisation practices, (nano)materials science, heterogeneous (nano)-catalysis and green chemistry (>450 publications, >25 000 citations, H-index 75), leading the NanoVal group at Universidad de Cordoba, (http://www.uco.es/users/q62alsor/index.html), an internationally consolidated group. Prof. Luque is also the Director of the Center for Molecular Design and Synthesis of Innovative Compounds for Medicine at RUDN University in Moscow, Russia (from 2018), Chair Professor from the Department of Applied Chemistry at Xi'an Jiaotong University (China) and more recently DFSP Distinguished Scientist at King Saud University in Saudi Arabia. Prof. Luque is the 2018 and 2019 Highly Cited Researcher (Clarivate Analytics) and received numerous awards including the most recent 2015 Lu Jiaxi Lectureship from the College of Chemistry and Engineering in Xiamen University (China) and 2018 ACS Sustainable Chemistry & Engineering Lectureship award.

Maurizio Selva

Maurizio Selva is a Full Professor of Organic Chemistry at the Department of Molecular Sciences and Nanosystems, University Ca' Foscari Venezia, Italy. The major research interests of Prof. Selva are focused on the implementation of eco-friendly synthetic protocols based on clean reagents, catalysts and solvents, including dense CO_2, dialkyl carbonates and multiphase systems assisted by ionic liquids, for the upgrading of bio-based chemicals and the functionalization of renewable-based materials. Prof. Selva has authored over 150 publications, including 15 book chapters and 11 patents.

Table 1 Average composition of fish waste (from ref. 11)[a]

(%)									ppm			
Crude protein	Fats	Crude fibre	Ash	Ca	P	K	Na	Mg	Fe	Zn	Mn	Cu
57.92 ± 5.26	19.10 ± 6.06	1.19 ± 1.21	21.79 ± 3.52	5.80 ± 1.35	2.04 ± 0.64	0.68 ± 0.11	0.61 ± 0.08	0.17 ± 0.04	100.00 ± 42.00	62.00 ± 12.00	6.00 ± 7.00	1.00 ± 1.00

[a] Values in % or mg kg^{-1} (ppm) on a dry matter basis.

pigments.[12] Accordingly, in recent years, various processes and technologies have been reported for their recovery/upgrade to high added-value products.[13,14] This approach has multiple benefits within the paradigm of the circular economy, not only affording desirable marketable products, but also promoting a more sustainable aquaculture and fisheries industry, lowering the impact of the anthropic exploitation of marine resources and helping to preserve coastal environments where these activities mostly occur. An interesting perspective recently focused on the concept of a shell biorefinery, where emerging technologies for the processing of crustacean shells providing chitin, calcium carbonate, and protein are expected to tremendously impact the market of bio-commodities and biomaterials within the next few years.[15]

However, there is still a way to go for the implementation of a biorefinery that can bridge the existing gap between the current practice for processing fish (both from capture and aquaculture) and the already available knowhow for the valorisation of related waste.[16–19] Indeed, low-tech solutions often continue to be the most popular options by which residues are treated through simple drying or cooking to get fishmeal (Fig. 2).[20]

Despite being rich in nutrients, fishmeal is a low-value product, which is mostly used in the animal feed and fertilizer sectors.

In light of these considerations, the present review aims to provide an insightful definition of the waste-to-wealth concept through a close inspection of the protocols to extract fish residues and upgrade extracts for the preparation of high added-value products with potential in the nutraceuticals, pharmaceuticals and cosmetics sectors and the fabrication of advanced materials. This analysis describes the chemical reactions involved in the treatment and upgrading processes of the waste, and the chemical engineering solutions available for this purpose.

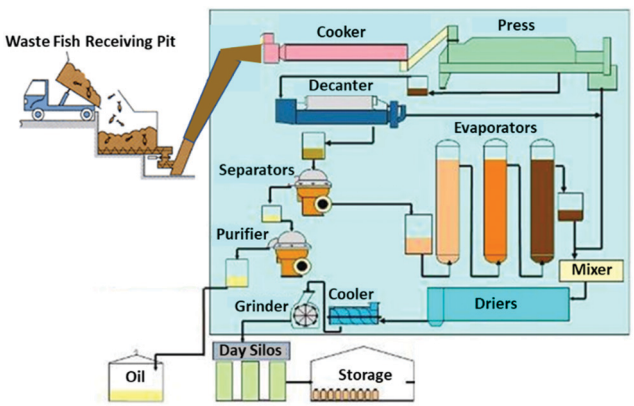

Fig. 2 Schematic of the large-scale production of fishmeal.

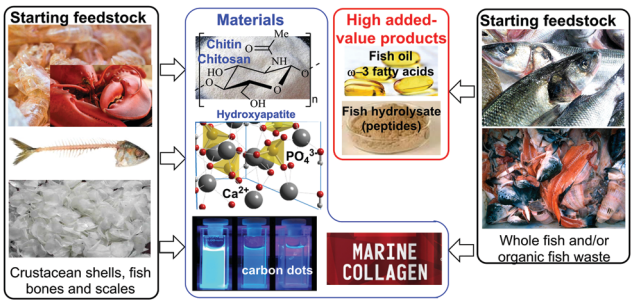

Fig. 3 Overview of the logic flow of the present review.

Fig. 3 presents an overview of the logic flow of the present review.

2. The process challenge: spoiling and preservation of waste

A major challenge in marine waste is the conservation of the product and strategies for treating the waste as close to capture as possible.

Highly variable degradation times is one of the major issues in the management of fish biowaste (besides the unpleasant odor). The organic portion of fish waste rapidly decomposes within hours or days depending on the storage conditions. Briefly, fish spoilage occurs mostly through bacterial and enzymatic autolysis (self-digestion) and lipid oxidation.[21] Physical handling accelerates autolytic changes even in chilled fish and fish entrails because membrane-bound packages, which usually compartmentalize autolytic enzymes, break down when subjected to physical forces, thereby allowing enzymes and substrates to come into close contact. Thus, physical damage of tissues should be avoided while conveying fish and during discharge from vessels.[22] Moreover, on dead fish, microorganisms usually found on their outer surfaces (skin and gills) and in the intestines proliferate freely, invading their flesh through the muscle fibres. Although the rate of spoilage depends on the texture of the tissues, particularly the dermis and epidermis of fish skin, microbial metabolism is accompanied by the production of biogenic amines such as putrescine, histamine and cadaverine, organic acids, sulphides, alcohols, aldehydes and ketones, which cause unpleasant and unacceptable off-flavours.[23] The extent of microbial attack can be determined

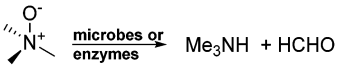

Scheme 1 Microbial or enzymatic reduction of TMAO.

based on the level of trimethylamine (TMA) coming from the reduction of trimethylamine oxide (TMAO) which many fish use as an osmoregulant to avoid dehydration in marine environments and tissue waterlogging in fresh water. Different classes of bacteria including *Shewanella putrifaciens*, *Aeromonas* spp., and *psychrotolerant Enterobacteriaceae* obtain energy by reducing TMAO to TMA (and HCHO), generating the typical ammonia-like fishy odour (Scheme 1).

The level of TMA in fresh fish is *ca.* 10–15 mg/100 g, but it rapidly increases during spoilage. Another important deterioration path is the oxidation of polyunsaturated acylglycerol-constituting fish lipids, which is a free radical process catalysed by light, heat, enzymes, metals, and metalloproteins.[24] This reaction generates glycerol together with a variety of oxidation products, including aldehydes, ketones, alcohols, hydrocarbons, volatile organic acids and epoxy compounds, some of which are responsible for undesirable odours and rancidity.

Storage under ice in anaerobic conditions and/or a CO_2 atmosphere helps to contain decomposition mechanisms due to microbial and enzymatic autolysis, but cannot prevent lipid oxidation, which requires the use of antioxidants (*e.g.* tocols and carotenoids) and metal chelators including phosphoric and citric acid and ethylenediaminetetraacetic acid (EDTA). The latter compounds inhibit the pro-oxidant catalytic effects of metal ions by forming stable complexes and reducing the metal redox potentials.

On the other hand, a remarkable portion of fish biowaste is represented by the exoskeletons of shrimps and crustaceans, which are usually more stable to chemical or enzymatic breakdown compared to other biomasses.

However, in this case, autofermentation phenomena may also incur, leading to the decay of the waste. The enzymes produced by the shrimp intestinal microflora are likely responsible for the generation of putrescent compounds, which make the residue no longer amenable for processing. Specifically, it has been shown that the decay of shrimp shells including that of the constituent chitin may occur within 72 h at 30 °C.[25]

This scenario clearly highlights how the treatment/valorisation chain of fish residues and side streams is characterized by significant differences due to the nature of the starting raw marine biomass.

Spoiling and oxidation of fish waste can be basically prevented through the same storage and preservation technologies available for fish products. This subject has been extensively reviewed by Samples, who described the pros and cons of conventional procedures including the use of flaked ice, the addition of ice to seawater, the use of water–ice systems and ice slurries with or without additives as natural antioxidants, ozone or organic acid mixtures (ascorbic acid, citric acid and lactic acid), and more sophisticated methods, for example, high-pressure (200 MPa) treatment combined with freezing to −18 °C to decrease the microbial contents and production of TMA, and vacuum packing under a controlled (CO_2) atmosphere.[26]

Furthermore, not only storage, but also transportation and delivery to biorefineries have to be examined to preserve the chemical richness of this type of biowaste and reduce the carbon footprint of the associated operations and infrastructure. This problem has been addressed in detail through specific actions within Horizon 2020, the biggest EU research and innovation programme.[27]

3. High added-value compounds

3.1 Fish oil

Fish oils are extremely popular in the nutritional sector due to their high content of the well-known long-chain ω-3 polyunsaturated fatty acids (PUFAs), the beneficial impact of which on human health, recognised 4 decades ago,[28] continues to fuel research programs and commercial interest.[29–33] With a current market above 2 billion US$ and projected to reach a minimum of 3.5–4 billion by 2025 estimated CAGR (compound annual growth rate) of 7.4%, ω-3-based PUFAs dominate the sector of dietary supplements and are distributed worldwide by companies with calibre including Cargill, FMC, Omega Protein, Arista Industries, and GOED Omega-3 in North America, Pharma Marine AS and GC Rieber Oils in Norway, Croda International PLC in the UK, Polaris in France, and Royal DSM in The Netherlands.[34,35]

The most relevant ω-3 fatty acids, docosahexaenoic acid (DHA) and eicosapentaenoic acid (EPA), are originally synthesized by microalgae and then accumulated in phytoplankton, which is part of the dietary intake of fish, particularly tuna, sardines, salmon, mackerel and herring.[36] Based on their lipid content, fish can be categorized as lean (*e.g.* cod, haddock and pollock), fatty (*e.g.* sole, halibut and red fish), medium fatty (*e.g.* most wild salmon), and high fatty (*e.g.* herring, mackerel and farmed salmon) species containing up to 2%, 2–4%, 4–8%, and 8–20% fat, respectively.[37] The (wide) degree of variability of the fat content, even within the same species of fish, depends also on the water where the fish lives, season and life cycle stage. On average, arctic sardines living in very cold waters contain significantly more fats and EPA and DHA than Mediterranean sardines. Moreover, smaller fish are preferable because a shorter life cycle in fish results in a lower level of heavy metals and organic pollutants to be accumulated in its flesh.

Scheme 2 shows the structure of the principal fatty acids (FAs) of the ω-3 family, highlighting the more relevant components of fish oil, EPA and DHA, in the dashed red rectangle.

None of the omega-3 FAs are synthesized *de novo* by mammals, and thus must be obtained from dietary intake. These compounds are characterized by having their first double bond at the third position from the terminal (or *n*th) methyl group in the molecule. They are labelled considering the total chain length and position of the unsaturated carbons. For example, **DHA (22:6)** is an omega-3 (n-3) fatty acid with six double bonds and 22 carbon atoms.

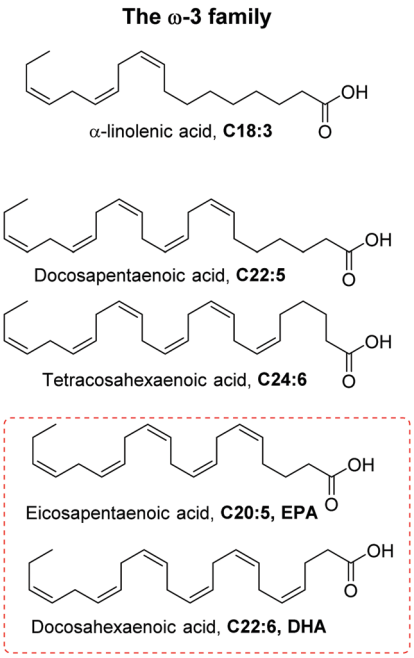

Scheme 2 Principal fatty acids of the ω-3 family. α-Linolenic acid (**C18:3**) is found in plant oils. Eicosapentaenoic acid (**C20:5, EPA**) and docosahexaenoic acid (**C22:6, DHA**) are present in fish oils.

It should be noted that a comparative GC-analysis of 46 marine oils commercially available as omega-3 supplements showed the presence of seventy-three fatty acid isomers, including n-6, n-4, n-3, and n-1 polyunsaturated fatty acids, with a concentration of EPA and DHA in the range of 7.8–45.4% and 5.5–44.1% of total fat, respectively.[38] Moreover, although the *cis*-configuration at the double bond is a generally accepted characteristic for PUFAs in natural oils and fats (Scheme 2),[39] this study also detected trans isomers of both EPA and DHA, mostly as mono-trans products (up to 20% of total trans acids), in amounts varying from 0.1% to 1.5% of total fats. These (*trans*) species were ascribed to the geometrical isomerization of the *cis*-FAs during the refining of the oils, particularly deodorization, which is a high-temperature processing carried out at 180–270 °C for the removal of unpleasant odours.[40] The presence of *trans* isomers of EPA and DHA was also noticed in other omega-3 products available in the European market, highlighting the caution needed when applying thermal treatments, such as to preserve the integrity of natural fish oils.[41] In this context, fish biowaste represents a rich source of ω-3 FAs, particularly the organic fraction including viscera, heads, tails, flesh residues, and specific wastewater with a high lipid (triacylglycerols, TGA) content. Table 2 summarizes the composition of oils extracted from common fish waste, reporting for specific cases, the amount of PUFAs present in fish liver oils. The latter (livers) may represent up to 10% of the viscera discarded during fish processing and are among the major reservoirs (between 30% and 40%) of lipids in fish.[42]

The following section will examine the commercial preparation of ω-3-rich fish oil as one of the high added-value chains for the exploitation of fish waste.

Table 2 Lipid composition of oils recovered from fish waste and PUFA content in fish liver oils

Entry	Raw material (waste)	TAG (wt%)	FFA[a] (wt%)	PUFA (wt%)	Ref.
1	Walleye pollock	92.15	3.28		43
2	Walleye pollock livers			20.40	
3	Pacific halibut	89.94	1.87		
4	Pacific halibut livers			21.59	
5	Sardine by-products	>99			44
6	Pink salmon livers			37.65	42
7	Tuna by-products		2.83	30.04[b]	45
8	Tuna livers		2.12	26.87[b]	
9	Cod liver			21.48[b]	
10	Sea bass and sea bream by-products		1.28	9.41[b]	

[a] FFA: content of free (non-esterified) fatty acids and. [b] Sum of **C20:5** and **C22:6** (**EPA** + DHA).

3.1.1 Large-scale production of ω-3-rich fish oil. The manufacturing of fish oils for human consumption generally follows the steps indicated in Fig. 4.

Using either whole fish or fish waste, cooking and pressing are used to initially separate the oil from a protein-rich solid residue, which ends up in fishmeal. These physical-thermal processes may take place on board the fishing vessel. The cooking step is designed for breaking down fat cells and releasing their oil content. However, the conditions also depend on the type and the size of fish, where heating is often carried out by continuously delivering the starting material to a cylindrical steam cooker in the form of a screw conveyor with hollow flights, operating at 95–100 °C for a relatively short period (15–30 min).[46,47] The resulting suspension is pressed to squeeze the liquid from the slurry, and the recovered water/oil emulsion is centrifuged to separate the stick water from the oil. The other refinement steps include:

(i) Degumming. Gums in raw fish oil are mostly comprised of phospholipids (PLs), which act as emulsifiers, coordinate metals favouring the oxidation of oil, and increase the viscosity. Degumming is often carried out at 60–70 °C by mixing the fish oil with acids such as phosphoric, acetic, citric, and oxalic acid,

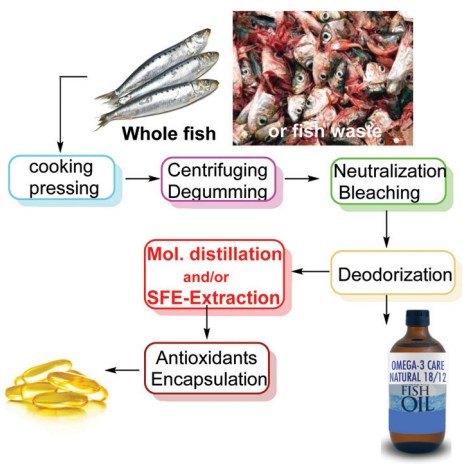

Fig. 4 Flowchart of the operations to produce ω-3-rich fish oil.

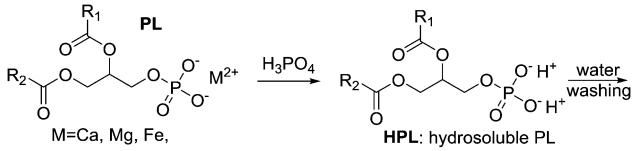

Scheme 3 Acid degumming of raw fish oil.

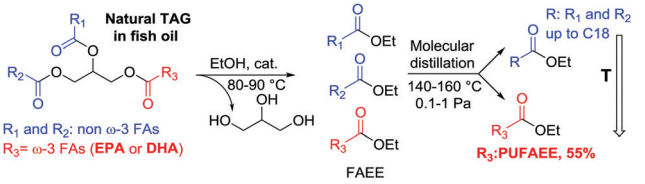

Scheme 4 Transesterification and molecular distillation of fish oil.

whose role is either protonating the gum and complexing bivalent metals in the gum to obtain hydrosoluble species, which can be removed by water washing (Scheme 3).[48]

(ii) Neutralization. This step removes acidity due to both the degumming treatment and the free fatty acids usually present in crude fish oils (1–3%, see Table 2), which is carried out by mixing oil with alkaline solutions (~10% aq. NaOH, 40–60 °C).[49] In some cases, winterization, *i.e.* fractional crystallization of saturated fatty acids at low temperatures (from −55 °C to −85 °C) has been proposed as a further step to reduce the FFA content.[50]

(iii) Bleaching. A light-coloured oil is produced by eliminating pigments, trace metals and other contaminants through adsorption on bleaching earth (Fuller's earth), activated carbon and synthetic silica.[51]

(iv) Deodorization. The refining of crude fish oils may induce undesirable changes in flavour quality due to the presence of secondary lipid oxidation products, mainly ketones, alcohols and aldehydes of various chain lengths and degrees of unsaturation including (*Z*)-1,5-octadien-3-one, (*E*,*Z*)-2,4-heptadienal, 1-penten-3-ol, and (*Z*)-4-heptenal, which influence the organoleptic properties of the oil.[52] Deodorization is performed by vacuum distillation of the oil at 5–50 mmHg with careful control of *T* and time, mostly below 200 °C and 1 h, respectively, to avoid the degradation of PUFAs.[53]

The above-described steps i–iv afford the so-called "18/12TG" ("18% EPA" and "12% DHA" in "triglyceride"), containing about 30% omega-3 fatty acids, with the residual 70% being a mixture of saturated fatty acids, cholesterol, some omega-6 fatty acids, and other oxidation products.[54,55] However, the fish oil omega-3 industry, particularly KD-Pharma GmbH in Germany,[56] has developed further expertise by which EPA and DHA can be produced on an industrial scale to concentrations greater than 95%. Molecular distillation (MD) and supercritical fluid extraction (SFE) combined with supercritical fluid chromatography (SFC) are the technologies used for this purpose.

3.1.1.1 Molecular distillation of 18/12TG. The principle of MD (or short-path distillation) is based on the transformation of natural triglycerides containing PUFAs into lighter molecules, which can be separated efficiently by vacuum distillation. This concept is illustrated in Scheme 4.

In natural triacylglycerols (TAGs), due to steric hinderance, only one long-chain ω-3-PUFA (EPA or DHA) can fit per molecule of glycerol. The other two ester functions bear shorter and more saturated alkyl chains. The 18/12TG mixture first undergoes catalytic transesterification with EtOH to release glycerol and obtain fatty acid ethyl esters (FAEEs) with boiling points much lower than that of the original oil. The FAAEs are then subjected to molecular distillation (140–160 °C, 0.1–1 Pa), by which a lighter fraction containing up to C18 fatty acid esters is separated from higher molecular weight compounds, including EPA and DHA ethyl esters (PUFAEEs). MD allows PUFAs to be concentrated from the initial 30% to approximately 55%, producing an oil readily available on the market.[57] However, MD cannot be repeated to further increase the amount of PUFAs because the thermal stress induced by repeated exposure to high temperatures degrades both EPA and DHA.

3.1.1.2 Supercritical fluid technology (SFT). A semi-continuous technology to refine and concentrate fish oils has been developed by coupling supercritical fluid extraction (SFE) and supercritical fluid chromatography (SFC) using compressed CO_2 as a solvent and a carrier, respectively. The KD-Pür® protocol trademarked by KD-Pharma[58] starts with SFE, where supercritical carbon dioxide ($scCO_2$) gently extracts THE ethyl esters produced in Scheme 4 from unwanted elements such as glycerides, free fatty acids, dyes, pollutants and cholesterol. Thereafter, SFC is performed, during which the extracted mixture of FAEEs is passed through a chromatographic column packed with silica xerogel, and the components (FAEEs) are separated selectively according to their size and degree of unsaturation. Both SFE and SFC operate at a low temperature (40–50 °C, slightly above the critical *T* of CO_2, 31 °C), thereby avoiding any alteration to the thermo-sensitive EPA and DHA. Moreover, the high diffusivity and low viscosity of $scCO_2$ allow the use of long chromatographic columns, which enable the industrial production of up to 99% pure fatty acids. The release of CO_2 by depressurization avoids any contamination of the product, although high-pressure operations at $p \geq 140$ bar (with $scCO_2$) imply high investments and running costs, which impact the final market price of the ω-3 concentrate. Table 3 compares some of the advantages and disadvantages of KD-Pür® technology and molecular distillation.

Table 3 Comparison of MD and KD-Pür® technology for the purification of ω-3 PUFAs

Entry	Conditions	MD	KD-Pür®
1	*T*/°C	140–160	35–50
2	*P*/bar	10^{-5}–10^{-6}	>140
3	Solvent/carrier	None	CO_2
4	Selectivity	Medium	Very high
5	Max viable concentration	65–70%	99%
6	Flexibility on EPA/DHA ratio	Limited	Very high
7	Costs	Limited	High

It should be noted that some nutritional studies indicate that after the ingestion of PUFAs as ethyl esters (FAEEs), these compounds are converted into the original triglyceride form found in fish oil, which is the only one that can be metabolized by the human body. The assimilation of triglycerides shows a 70% increase in the omega-3 index, which is defined as the percentage of EPA + DHA in red blood cell membranes compared to ethyl ester derivatives.[59] This is why manufacturers prefer the commercialization of fish oil in the triglyceride form.

3.1.1.3 Anti-oxidants and encapsulation. The presence of initiators such as heat, light/ionizing radiation and metal ions/metalloproteins is one of the most common pathways by which unsaturated omega-3 molecules easily undergo oxidation with atmospheric oxygen, generating unstable peroxyl radicals, which break down into a range of secondary oxidation products, including aldehydes, ketones, alcohols, hydrocarbons, volatile organic acids and epoxy compounds.[60] These species are responsible for the bad smell and rancidity of oil.

Among the methods to prevent the oxidation of the omega-3 oils, both the use of antioxidants and protection techniques such as microencapsulation have been described. Primary antioxidants are generally phenolic compounds that can scavenge free radical intermediates by either donating hydrogen atoms or co-generating resonance-stabilized radicals, which favour the termination step of oxidation. Accordingly, natural antioxidants are becoming more preferable than synthetic molecules because of their double action in preventing oxidation and imparting a pleasant aroma to oil. Some of the natural phenol-based molecules investigated for fish oils are shown in Scheme 5 and compared to BHT (butylated hydroxytoluene) as one of the most common synthetic antioxidants.

Quercetin, a common flavonoid found in fruits, and quercetin-3-*O*-glucoside (500–1000 μM) have demonstrated better antioxidant activity than BHT in bulk fish oil, while several studies have proven the efficiency of rosemary extracts as oxidative stabilizers of omega-3 compounds.[61]

Microencapsulation of omega-3 compounds is another strategy to minimize oxidative deterioration and facilitate the use of fish oil in a stable and easy-to-handle form. The existing literature on this subject was recently reviewed by Dowling *et al.*, who detailed the two most commonly used commercial processes, complex coacervation and spray-drying emulsions, and described several other emerging techniques such as spray chilling, extrusion coating and liposome entrapment.[62] In spray drying, a selected source of omega-3 oil (core material) is initially dispersed in a solution of a polymer chosen among proteins, carbohydrates, lipids and gums either alone or in combination. The emulsion/dispersion is then pumped through an atomizer and the atomized droplets are finally dried to produce microcapsules. In coacervation, the oil component is dispersed in a gelatine solution, which, by pH adjustment, coacervates, forming a coating over the oil droplets. A subsequent cooling step hardens the coating and encapsulates the oil. The classic hydrocolloids employed in the complex coacervation of omega-3 oils include gelatine and whey proteins and oppositely sodium polyphosphate, carboxymethyl cellulose and charged arabic gum.

3.1.2 Extraction of oil from fish waste by different methods. Fish oil is obtained directly from the waste of fish processing using different techniques based on chemical, enzymatic, and supercritical extractions. Chemical protocols typically involve the Soxhlet or Goldfisch, Folch, Bligh and Dryer method and acid digestion, employing apolar solvents, including petroleum or diethyl ether, hexane, chloroform and hexane, or mixtures of polar and non-polar compounds comprised of chloroform and methanol or water.[63] Hexane is among the few solvents also reported for large-scale extraction; however, oil contamination with even solvent traces has limited its use in the processing of nutraceuticals.[64] Enzymatic procedures make use of commercially available enzymes including Alcalase, Neutrase, Lecitase Ultra, Protex and Protamex to break down the protein portion of the waste and recover the released oil by centrifugation.[65] The majority of supercritical extractions use compressed carbon dioxide (see previous section) due its non-toxicity, low cost, mild critical conditions (T_c = 31 °C, P_c = 74 bar), high diffusivity and low viscosity. However, other supercritical fluids, particularly dimethyl ether, have been and are currently under investigation.[66] This section will examine some comparative assessments of the results obtained by the different extraction methods.

In one example, the skin of Indian mackerel, one of the most popular marine fish in Malaysia, was freeze dried (−47 °C, 0.133 bar, final moisture: 6.3%), ground into particle sizes of 0.2–0.5 mm, and then extracted either continuously by $scCO_2$ at 45–75 °C and 20–35 MPa (2 mL min^{-1}) or Soxhlet extraction (40 mL of petroleum ether per g of dry fish powder, 6 h; vacuum distillation at 65 °C; and drying at 45 °C).[67] The application of a pressure swing technique, holding CO_2 in contact with the sample matrix before depressurization, proved effective to allow the penetration of the solvent and minimised its consumption, providing an extraction yield of up to 52.3/100 g sample (dry basis) with a PUFA content of 27.74% as the sum of EPA and DHA. Both the yield and the composition of fish oil were similar to that obtained by the Soxhlet method.

In another investigation, different fish by-products including cuts from orange roughy (OR) and salmon (S) were subjected to wet reduction (WR, cooking), enzymatic extraction (EE), and supercritical fluid extraction (SFE).[68] The skin with stuck muscle collected from fish peeling was frozen at −20 °C, cut into uniform

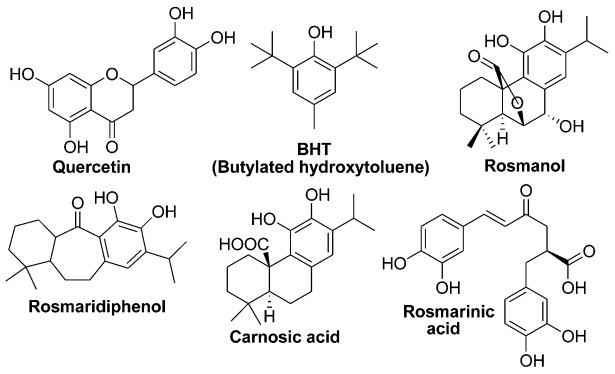

Scheme 5 Structures of natural antioxidants compared to the synthetic BHT.

Table 4 Comparison of the methods for the extraction of fish waste (from ref. 65)

Entry	Amount of sample (g)	Extraction method	Conditions	Collected oil[a] (kg/100 kg)
1	100	WR	Heating (water), 95 °C, 15 min; centrifuging (104 rpm, 20 °C, 10 min)	12
2		EE	Aq. protease (enzyme/substrate = 0.05 w/w), (56 °C, 120 min); centrifuging (104 rpm, 20 °C, 10 min)	25
3		SFE	Freeze drying, 72 h; 25 MPa, 40 °C, 10 Kg CO_2/h, 3 h	29

[a] Estimated based on the extraction of 100 kg of raw material. Results were comparable for both OR- and S-derived waste.

pieces (1–10 mm), and extracted according to the conditions in Table 4.

Compared to the WR and EE methods, SFE proved to be superior not only due to the amount of the extracted oil (Table 4), but also the quality of the product. Specifically, the SFE-extracted oil showed a lower acidity (content of FFAs of *ca.* 1.5% of oleic acid, AOCS Official protocol), consistent with the reduced hydrolysis of triglycerides during the treatment, and a lower amount of hydroperoxides, light aldehydes, and ketones (total oxidation value, TOTOX between 8 and 15), indicating the non-oxidizing conditions of the method due to its mild temperatures, non-oxidizing atmosphere and darkness, and low amounts of heavy metals including Cd, Hg and Pb below the detectable limits (by ICP). However, economic analysis led to the conclusion that because of the expensive freeze-drying step, SFE extraction is less competitive than EE and WR unless the supercritical technology is integrated in the whole omega-3 processing, involving the use of $scCO_2$ in the extraction, fractionation, and omega-3 concentration and/or formulation to produce high-value ingredients in functional foods or as active principles in pharmacology.

The simultaneous extraction and fractionation of fish oil with $scCO_2$ was described in several studies, demonstrating the suitability of this approach to enrich the product in EPA and DHA components.[69,70] Recently, this method was followed starting from tuna waste, particularly from tuna heads, which were first freeze-dried to reduce the moisture content to 2.3%, ground into particle sizes of 0.2–0.5 mm, and finally subjected to fractional extraction at 65 °C and 40 MPa using a mixture of CO_2 and ethanol (3 mL min^{-1}: 2.4 mL CO_2 and 0.6 mL ethanol min^{-1}, v/v) for 120 min.[71] Control of the moisture was critical because of the adverse entrainer effect of water, which acts as a barrier against CO_2 diffusion into the sample, reducing the extractability of the oil.[72] The latter was extracted in 3 fractions, and further subdivided in 6 different samples collected at times of 20, 40, and 60 min, which showed a progressive increase in PUFA content up to 50% in the latter fractions. Combined extraction/fractionation with $scCO_2$ also proved to be efficient for the enrichment of ω-3 FAs in oils obtained from freshwater fish (speckled fish from Brazilian rivers), which are a poorer source compared to marine fish oils.[73] The best compromise between selective fractionation and solubility of oil in $scCO_2$ was found between 33 °C and 40 °C at a pressure of 200 bar.

The liver wastes discarded during the processing of rock lobster (*Jasus edwardsii*) from southern Australia were recently investigated for the production of ω-3 oils.[74] These residues had

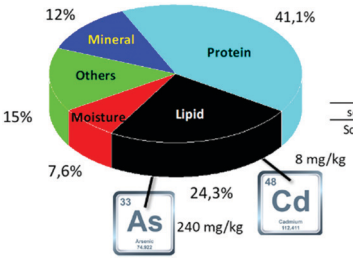

Extraction of lobster livers

	Extraction Yield (%)	PUFAs (%)	As (mg/kg)	Cd (mg/kg)
$scCO_2$	22.8	31.3	2.2	0.01
Soxhlet	24.3	7.8	33.0	0.27

Fig. 5 Left: Composition of freeze-dried Australian rock lobster liver highlighting the contamination of As and Cd in the lipid fraction (from ref. 74). Table (right): Yield of extraction, PUFA and As and Cd contents in extracted oils.

a high content of PUFAs (24.3% w/w), but were found to be contaminated by As (240 mg kg^{-1}) and Cd (8 mg kg^{-1}) (Fig. 5).

After freeze-drying (−85 °C, 15 mTorr, 48 h), the lobster liver samples were extracted either continuously by $scCO_2$ at 50–60 °C and 30–35 MPa and a flow rate of 0.434 kg h^{-1} or by Soxhlet using diethyl ether (9 mL g^{-1} dry sample, 4 h, 40 °C). The table in Fig. 5 summarizes the results. Compared to the Soxhlet protocol, $scCO_2$ extraction gave a slightly lower yield; however, the content of PUFAs was *ca.* 4-fold higher (31.3% *vs.* 7.8%) and the amount of Cd and As was 27 and 15 times lower than that in the Soxhlet-extracted lipids, respectively.

As mentioned above, the development of CO_2-based SFE at the production scale is limited by the costly freeze-drying pre-treatment of the raw materials. Thus, in search for alternative extraction methods, subcritical dimethyl ether (DE: T_c = 126.85 °C, P_c = 53.7 bar) has been recently proposed as a solvent for extracting tuna livers discarded during fish processing.[75] Indeed, contrary to common extraction solvents, DE has good solubility in both water and oil, a property which allows the issue of controlling the moisture content of samples before SFE to be overcome. The tuna livers were frozen at −18 °C, minced and then extracted with subcritical DE in a semi-continuous apparatus operating at 42 °C and 0.8 MPa. The process parameters including T, p, time (50 min) and stirring speed (925 rpm) were optimised by a response surface method. Under these conditions, water and lipids could be extracted together by DE even starting from crude tuna liver samples with more than 60 wt% moisture content. The yield of extracted fish oil was in the range of 17% with a content of PUFAs of *ca.* 21%. The values of both yield and oil composition were substantially comparable to that achieved by SFE with CO_2 (35 MPa and 50 °C; CO_2 flow = 3 mL min^{-1}) of the same liver waste, thereby

indicating that DE was not only an effective replacement for CO_2, but the DE-based process was successful without any energy-consuming freeze-drying pre-treatment. Notably, DE has been approved as a safe solvent in the food industry by the Food Safety Authority of Europe.

Biological processes for the extraction of fish oil have been described by enzymatic treatments of a variety of fish waste including salmon heads, mixed salmon-derived by-products (head, frame and viscera), and mackerel parts.[76–79] Both autolysis (silage) using enzymes already present in fish viscera and hydrolysis catalysed by the addition of commercial exogenous enzymes such as Alkalase, protease, Sea-B Zyme and Flavourzyme in variable concentrations (0.5–2%) have been used. The reactions were performed at 30–50 °C with the extraction yields varying between 15% and 20%. Although these methods claimed advantages such as low energy requirement, no use of solvents and low investment costs, they have the drawbacks of the intrinsic high costs of enzymes, long processing time, which reduces the hydrolyzate quality, and deterioration of the products due to hydrolytic conditions favouring the formation of free fatty acids (FFAs) and oil/water emulsions.

3.1.3 Additional examples. Besides the examples detailed in Section 3.1.2, other information on the extraction and purification of ω-3-enriched oil from whole fish and fish waste by $scCO_2$ is summarized in Table 5.

Moreover, for further information, it should be mentioned that vast literature is also available on the exploitation of marine macroalgae as sources of polyunsaturated fatty acids (PUFA) for nutritional purposes.[86]

3.1.4 Lipids extracted from fish waste as biofuels. Extensive literature reports the use of fish oils as biofuels. Although this topic is not related to the valorisation of fish waste for added-value molecules for human consumption and use, it is briefly mentioned in this review to provide a more complete scenario on fish oil exploitation. The extraction, refinement and commercialization of ω-3 oils as nutritional supplements are challenging when fish processing facilities are located in remote areas and limited infrastructure and plants are available. Under these conditions, oil from fish by-products is obtained during the production of fishmeal, and the more sustainable and economically viable use of this resource (oil) is generally the co-generation of energy as an in-house or regional fuel. Indeed, processes for the upgrading of fish oil for fuels are both less energy intensive and less subjected to stringent specifications than that in the food and pharmaceutical industries.[87]

The initial steps for the conversion of fish waste into fuels are basically the same as that described in Fig. 3, including cooking, pressing, and other refining processes such as degumming, and neutralization. Studies have confirmed that fish oils can be used as fuels in convectional combustors or diesel engines in boilers and furnaces that can accommodate low-grade fuels.[88] However, in most cases, transesterification with MeOH or EtOH is required to convert fish oil in a biodiesel as a mixture of fatty acid methyl or ethyl esters (FAMEs or FAEEs), fulfilling standard fuel specifications. One example reported started from a heterogeneous mixture comprised of heads, skins, fatty layers and tails of different fish, which were cooked in boiling water and filtered. Oil was then obtained in a separating funnel and subjected to transesterification with both methanol and ethanol at the corresponding reflux temperatures (6 : 1 alcohol to oil molar ratio) in the presence of KOH as a catalyst.[89] The yields of FAMEs and FAEEs were 95 and 92 wt%, respectively, and the properties of these fish-derived fuels were perfectly within the limits prescribed by ASTM D6751 biodiesel. Another study investigated the production of fuel from tilapia (a carp) fish waste. The residues were heated under pressure (at 110 °C) and the resulting suspension was squeezed in a tank equipped with a screw to crush the solid and release oil.[90] The viscera of the tilapia gave the highest oil content (22.02%) compared to the heads (9.23%) and fins (4.33%), but the viscera-derived product also had the highest FFA content due to its hydrolysis catalysed by endogenous enzymes in the starting material (see above, biological processes). Therefore, neutralization was required before base-catalysed transesterification to produce biodiesel. In a different approach, the fish waste derived from mixed residues (viscera, eyes, fins, tails and maw) discarded from Indian carps was dried (102 °C, 40 min), crushed, and forced through a mechanical expeller. The resulting oil was finally purified by extraction in a Soxhlet apparatus using *n*-hexane as the solvent.[91,92] Due to the high acid content (acid value: 11.89 mg KOH per g oil), the fish oil was neutralised by the esterification of FFAs with MeOH (MeOH : oil = 6 : 1, 1.0 wt% H_2SO_4, 120 min, 55 °C), and then subjected to base-catalysed transesterification (MeOH : oil = 6–10 : 1, 1.5–2.5 wt% β-tri-calcium phosphate or CaO, 90–120 min, 55–65 °C). The water content (0.001–0.03%), kinematic viscosity (4.99 $mm^2\ s^{-1}$) and flash point (150 °C) of the obtained biodiesel (FAMEs) met the standard ASTM D6751 specifications; however, the low density and cloud point of 0.84–0.86 g cm^{-3} and 1 °C, respectively, indicated that the fuel was suitable for moderately cold climatic conditions.

Table 5 Procedures for the extraction and purification of ω-3-enriched fish oils

Entry	Starting material	Procedure	Ref.
1	Sardine heads	CO_2-based SFE	80
2	Atlantic mackerel	CO_2-based SFE	81
3	Various sources	CO_2-based SFE	82
4	Tuna oil	CO_2-based SF-chromatography	83
5	Tuna oil	CO_2-based SFE	84
6	Sardine, anchovies and mackerel oil	CO_2-based SFE	85

3.2 Fish hydrolysate

In recent years, significant efforts have been directed to investigating and implementing technologies to improve the production of the so-called fish protein hydrolysates (FPHs) by converting fish waste into peptides containing 2–20 amino acids. This topic has been examined in different review papers highlighting the relevance of FPHs in food chemistry, particularly as functional ingredients of dietary supplements, due to their potent biological activities such as antihypertensive, antioxidant, antimicrobial, immunomodulatory and anticancer effects.[93–96] Some of the trademarked nutraceuticals based on FPHs include Seacure®, Amizate®, Protizen®, Vasotensin®, and Peptace®, which are products available commercially to alleviate body stress, support muscular and vascular functions, lower blood pressure, and control weight disorders (Fig. 6).

Among the biological activities promoted by these products, their antihypertensive and antioxidant properties have been the most investigated. FPHs act in the reduction of arterial blood pressure by inhibiting the ACE enzyme, which is responsible for the conversion of the peptide hormone Angiotensin-I into the powerful vasoconstrictor Angiotensin-II, and the inactivation of the neurotransmitter nonapeptide bradykinin, which contributes to vasodilation and hypotension in the systemic circulation.[97] These effects are mediated by the type of amino acids and their position the C-terminus in the peptide sequence of FPHs.[98]

For example, a prolonged antihypertensive action was reported after administration of the pentapeptide Leu-Lys-Pro-Asn-Met and the dipeptide VY (H-Val-Tyr-OH) obtained from bonito mackerels and sardine protein hydrolysate, respectively.[99,100] Similar ACE inhibitory activity was described for FPHs derived from the discards of Mediterranean fish species, particularly, 14 novel ACE-inhibitory peptides were identified in horse mackerel and small-spotted catshark hydrolysates. For the latter (catshark-PHs), one of the most promising peptides was VAMPF (Val-Ala-Met-Pro-Phe), for which an IC50 value (concentration of hydrolysate needed to inhibit 50% of ACE activity) as low as 0.44 μM was obtained by a QSAR-model.[101] On the other hand, although there is still a lack of evidence to explain the relationship between the structural characteristics of the peptides of FPHs and their antioxidant properties, a peptide size in the range of 0.5–3 kDa and the presence of hydrophobic amino acids together with residues of histidine, proline, methionine, cysteine, tyrosine, tryptophan and phenylalanine have been recognised as critical factors. It has been hypothesised that the hydrophobic sequences interact with lipid molecules by donating protons to scavenge the radicals responsible for oxidative mechanisms.[102] Literally, dozens of amino acids sequences have been identified in FPH peptides obtained from fish waste with potent antioxidant activity.[103]

3.2.1 Production of FPHs. The large-scale production of FPHs is based on chemical and biological processes. Fig. 7 illustrates the processing steps, summarising the major advantages and disadvantages of these methods.

Although chemical methods are relatively inexpensive and easy to implement, they are often poorly selective since they require (harsh) conditions, which result in the uncontrolled breakdown of raw materials and production of mixtures of peptides with reduced nutritional quality. On the contrary, there is a consensus that enzymatic hydrolysis (EH) is the most viable strategy to obtain food-grade protein hydrolysates with bioactive properties.[104,105]

EH usually starts by heating the raw material at 85–95 °C to terminate the endogenous enzymes still active in the organic fraction of both whole fish and fish waste.

Subsequently, exogenous enzymes must be carefully chosen and added to the solid to optimize the selective cleavage of its protein content into peptides. A variety of enzymes have been reported for this purpose including Alcalase®, Flavourzyme®, Protamex®, bromelain, thermolysin, proteinase K, pepsin, papain, and chymotrypsin. Therefore, treatment conditions may be largely different, for example, pepsin works at pH = 2.0, and T = 37 °C, while trypsin and chymotrypsin require much higher pH and T of 8.0 and 60 °C, respectively.

Fig. 6 Examples of some commercial nutraceuticals based on FPHs.

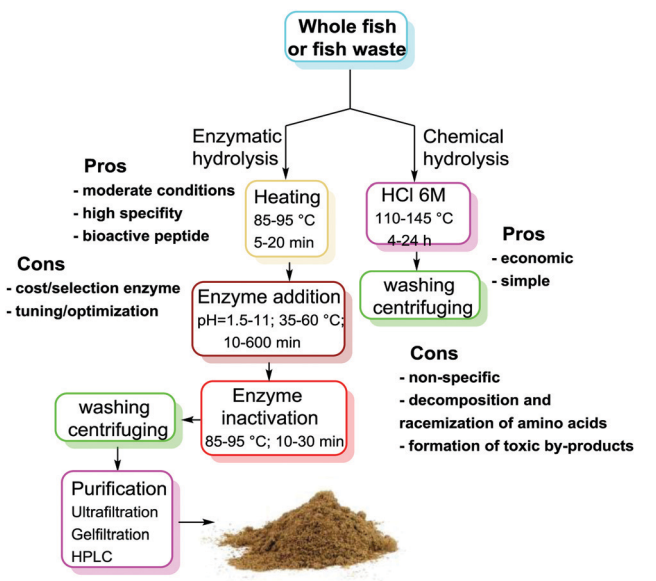

Fig. 7 Schematic of chemical and enzymatic hydrolysis to produce FPHs.

This influences the reaction kinetics, impacting the reaction times and enzyme concentration, which vary in typical ranges between 10 and 600 min and 0.01–5.00%, respectively. The response surface methodology (RSM) approach is often used to reduce the number of experimental trials required to optimize hydrolytic conditions. Once the desired degree of hydrolysis is achieved, the enzymatic reaction is quenched by either heating at 85–95 °C or acidifying the hydrolysated slurry. Different fractions comprised of sludge of solids and non-soluble proteins, an aqueous and lipid layer are then separated by centrifugation. Although the hydrolysated solid can be used as a source of bioactive compounds, purification is a further crucial step to improve the quality and the biological activity of peptides for commercial use.

Among the purification techniques, ultrafiltration, gel filtration, ion exchange chromatography, and reverse-phase high performance liquid chromatography (RP-HPLC) has been reported to be the most effective. This section will describe some representative examples of the enzymatic hydrolysis of different typologies of fish waste.

In one case, the production of bioactive peptides was investigated starting form tuna dark muscle waste, a common by-product of canned tuna processing.[106] After steam cooking at 100–105 °C, the solid waste was subjected to enzymatic hydrolysis using both orientase (OR) at pH 7.0 and 50 °C and protease (PR) enzymes (pH 7.5 and 37 °C) for up to 6 h. Subsequently, the hydrolysates were heated (100 °C, 20 min), centrifuged (12 000 rpm, 15 min), and purified *via* gel-filtration (Sephadex G-25) followed by HPLC (MICRA NPS RP-18). The purification allowed the initial mixture to be fractionated into major components with their molecular weight distributed between 4500 and 1400 Da, 1400 and 390 Da, and <390 Da, and their antioxidant activity was measured against the scavenging of the 2,2-diphenyl-1-picrylhydrazyl (DPPH) radical and the lipid peroxidation inhibition assay using linoleic acid as the standard reagent. The amino acid sequence of the best performing peptides was then determined by Q-TOF mass spectrometry, and the results are presented in Table 6.

Compared to conventional antioxidants such as *t*-butyl-4-hydroxyanisole (BHA), α-tocopherol, L-ascorbic acid, and short hepta/octa-peptides showed good antioxidant properties for food and nutraceutical applications, confirming that hydrophobic amino acids such as Leu, Val, Tyr, and Met likely interacted with lipids and scavenged lipid-derived radicals especially due to the Tyr-residues acting as proton donors.

Another study investigated the hydrolysis of fresh salmon backbones using eight different proteolytic enzymes including Corolase1 PP, Corolase1, Protamex, Papain, Bromelain 400, Trypsin, Protex 6L, and Seabzyme L200.[107] After mincing, the residual solid was centrifuged (2250 rpm, 15 min) to separate the oil fraction from a mixture of stick water and sediments (defatted material), which were used for hydrolysis. This was performed at 50 °C by adding distilled water and the enzyme dose of 0.1% (w/w of raw material mixture). After 120 min, deactivation of the enzyme (M_w-heating, 5 min, $T > 90$ °C) followed by freezing at −80 °C afforded a fish protein hydrolysate (FPH), which was characterized and investigated for its ACE inhibiting effect and *in vitro* antioxidative activities. The highest antioxidative ability (DPPH scavenging ability, 38 ± 0.5%) was obtained using Protamex during hydrolysis, while the trypsin-catalysed process yielded the best ACE-inhibiting peptides. The latter showed IC_{50} values in the range of 0.2–0.9 mg mL^{-1} and FPLC analysis confirmed an average size of up to 1200 Da including 14 amino acids.

In a different approach, the design and the selection of techniques for the fractionation of the protein fractions obtained by the enzymatic hydrolysis of solid waste from tuna canning industry were investigated.[108] The study referred to an industrial-scale installation of typical size for tuna processing with a capacity of 10 000 ton per year, a 46% yield of primary product (canned tuna), and an amount of fish waste available for hydrolysis of 5400 ton per year. Under the continuous production of 300 day per year, the plant co-generated 1.5 m^3 h^{-1} of clarified hydrolysate, the composition of which is shown in Table 7.

The separation of this complex mixture, especially for the valorisation of the medium protein fraction (1–4 kDa), which is the most promising one for high-added value products of nutraceutical and pharmaceutical interest, was studied through advanced membrane configurations. Process optimization was modelled by transport equations and mass balance using membrane cascades based on the integration of ultrafiltration (UF) and nanofiltration (NF) methods, which resulted in a yield of 62.5% with a maximal product purity of 49.5%. Moreover, operating with an overall UF-membrane area as low as 185 m^2, the coupling of the UF/NF system to a water recovery membrane stage avoided the need for supplementary freshwater inlet streams with a reduction in the total running

Table 6 Comparison of the antioxidant activity of the purified peptides obtained from tuna dark muscle and conventional antioxidants

Entry	Enzyme[a]	Antioxidant	DPPH radical scavenging capacity[b] (%)	Relative antiox. activity (days)
1	OR	Leu-Pro-Thr-Ser-Glu-Ala-Ala-Lys- (978 Da)	79.6	7.13
2	PR	Pro-Met-Asp-Tyr-Met-Val-Thr (756 Da)	85.2	7.89
3		BHA[c]	nd[d]	6.93
4		α-Tocopherol	nd[d]	5.88
5		L-Ascorbic acid	88.6	nd[d]

[a] Enzyme used to extract peptides from tuna muscle. [b] All sample concentrations at 100 μg mL^{-1}. [c] *t*-Butyl-4-hydroxyanisole. [d] nd = not determined.

Table 7 Composition of clarified protein hydrolysate from tuna processing waste

Entry	Protein fraction	Mol weight (kDa)	Amount (wt%)
1	Ultra-heavy	>7	11.5
2	Heavy	4–7	3
3	Medium	1–4	19
4	Light	0.3–1	28.5
5	Ultra-light	<0.3	38

costs, varying between 25% and 49% for total protein limits of 100 and 250 g L^{-1} respectively.

4. Advanced materials and devices

4.1 Bio-materials

The definition of a biomaterial is a constantly evolving concept.[109] From the early description coined in 1986, as 'a non-viable material used in a medical device and intended to interact with biological systems', the radical changes undergone by medical technologies, which now include drug and gene delivery systems, tissue engineering and cell therapies, nanotechnology-based imaging and microelectronic devices, have imposed a complete new vision for biomaterials. Currently, the consensus is towards widening the definition by encompassing any substance engineered to interact with biological systems either for therapeutic (body tissues repair) or diagnostic purposes.[110] Under this umbrella, representative biomaterials derived from fish waste are discussed in this section.

4.1.1 Collagen. Collagen is the predominant protein in the extracellular matrix (ECM) of human tissues, constituting up to 30% of the dry weight of the body. This protein displays a triple helical structure, where three α-chains repeat a characteristic $(Gly\text{-}X\text{-}Y)_n$ sequence, with the X and Y positions mostly occupied by proline and hydroxyproline, respectively (Fig. 8).[111]

Although the reported types of genetically different collagens vary between 28 and 29,[112,113] the most common ones are the fibril-forming proteins, usually labelled as type I, II, III, V, and XI collagens, which auto-assemble into highly oriented fibres with diameters ranging between 25 and 400 nm and banding pattern with a periodicity of approximately 70 nm.[114] Fibrils are the basic unit of collagen responsible for the robust nature of skin, tendons and bones. They are formed due to intra- and inter-molecular covalent cross-linking among the residual amino-acids (mostly lysine, hydroxylysine, and their aldehyde derivatives) present in the short N- and C-terminal regions of the α-chains.

The most common procedure to obtain collagen is the extraction of a variety of animal connective tissues using acidic, alkaline, or neutral solubilization or enzymatic treatments. Biomaterials fabricated with naturally derived collagen display limited evidence of local or systemic toxicity, non-immunogenicity, biocompatibility, low antigenicity, and capability to promote cell adhesion and proliferation.[115–118] However, drawbacks in collagen extraction may arise from the batch-to-batch variability, the need for good manufacturing practices eliminating potential contamination of pathogens, and ethical issues with animal experiments. For example, collagen of mammal origin from bovine and porcine hides and bones has been associated with a high risk of transmitting diseases such as spongiform encephalopathies (BSE and TSE), and avian/swine influenza.[119] Thus, alternative syntheses have been explored using recombinant human collagen (rhCol), but their application are still limited due to the high cost of protein expression.[120]

In search for other natural and cheap starting materials, the use of biowaste, especially the organic fraction of fish discards, has been investigated. Some representative results are described in the next section.

4.1.2 Collagen from fish-biowaste. Studies on the extraction of collagen from fish waste date back to more than 20 years ago.[121,122] Subsequently, vast literature on this subject has evolved,[123,124] but only in the past five years investigators have been focused not only on improving extraction methods for large scale production, but also achieving advanced (bio)materials with enhanced properties. Although marine collagens generally show lower molecular weights and lower denaturing (melting) temperatures than terrestrial animal collagens,[125] studies based on genomic, molecular cloning, biochemical, and structural investigations have demonstrated similar characteristics between fibrillar collagens from marine and human sources.[126] Moreover, marine-derived proteins are zoonosis-free.

Extraction procedures. As mentioned before, combined alkali/acid solutions or enzymatic treatments are typically employed to extract collagen from fish residues (mostly scales and skin).[127–131] Fig. 9 presents a flow chart of the required basic operations, which highlights how the used strategies

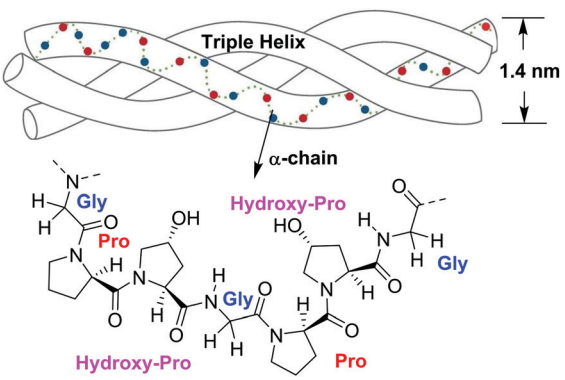

Fig. 8 Pictorial view of the structure of collagen.

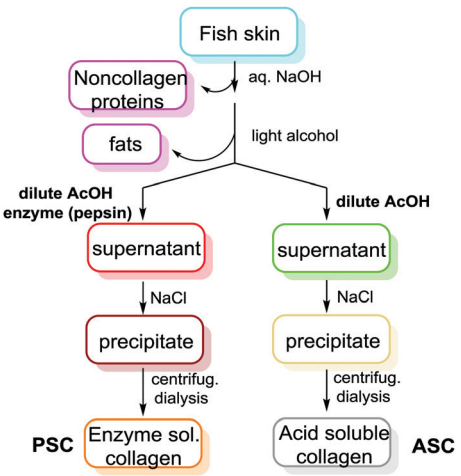

Fig. 9 Flowchart of the basic operations for the conventional extraction of collagen from fish skin with acid and acid/enzyme treatments (top and bottom, respectively).

comprise multi-step, time-consuming operations, which are often unsuitable for process scale-up.

Specifically, in one case, the treatment of fish residues from Indian carp (*Catla catla*) and rohu (*Labeo rohita*) has been considered. India ranks second in the world freshwater aquaculture, a business generating millions tons per year of products with 30–35% (w/w) of discards in fish processing, which represents a realistic source of collagen.[132] The enzymatic digestion of an aqueous suspension of defatted swim bladder waste of rohu was carried out using a mixture of acetic acid containing pepsin [EC 3.4.23.1; 3000–3500 NF U mg^{-1}; solid : liquid ratio of 1 : 10 (w/v)]. Pepsin soluble collagen (PSC) was achieved with a yield of 465.2 g kg^{-1} (dry weight basis). The enzymatic breakdown was carried out at 4 °C for 48 h, producing an extract that maintained the triple helical structure and exhibited high fibril-forming ability.[133]

However, innovation in extraction procedures has been implemented by engineering new reactors, conditions and solvents. In one example, the extraction of defatted samples of flatfish skin was carried out in acetic acid (0.05 M; 1 : 100, sample : acetic acid, w/v) using industrial ultrasonicating equipment (8 L, 20 kHz operational frequency). Native type I collagen was obtained in a collagen yield of 46% after 4.5 h at 4 °C.[134]

The unprecedented use of deep eutectic solvents (DESs), particularly derivatives of biodegradable and non-toxic choline chloride (ChCl), was recently described for the extraction of collagen peptides from cod skins.[135] Among the tested DESs, mixtures of ChCl with lactic and acetic acid proved successful for the extraction of type I collagen, while the combination of ChCl and oxalic acid was the best option to obtain collagen peptides with an M_w of around 11 kDa with extraction efficiencies of up to 91% at 65 °C. The driving force for extraction was the formation of ammonium salts at the N-sites of both proline and hydroxyproline amino acids in collagen, which was proved by UV-vis and FT-IR analyses (Fig. 10).

A conceptually similar, although different in practice, approach was devised using ionic liquids (ILs) as solvents for collagen extraction from the waste scales of carp fish.[136]

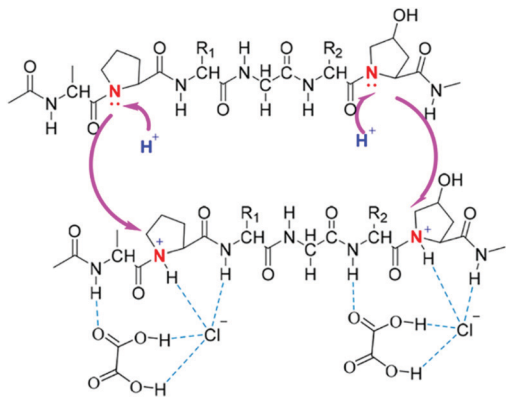

Fig. 10 Ammonium salts of both proline and hydroxyproline amino acids formed during extraction of cod skin with DESs. The case of ChCl and oxalic acid is shown. Reprinted from ref. 135 with permission from the American Chemical Society, Copyright 2017.

A COSMO-RS computational model was implemented to compare the activity coefficients (AC) of collagen in ILS. Accordingly, the best performing solvent was 1-ethyl-3-methylimidazolium acetate ([C_2C_1im][Ac]), which showed low AC (inverse of solubility) and the best fit Sigma profile. The extracted collagen was precipitated (from the IL) employing an NaCl solution (2 M) after pre-treatment at 100 °C for 12 h and eventually collected (3.1 ± 0.5% yield).

Here, it is worth mentioning another procedure, which although not related to fish residues, was employed for the extraction of collagen-rich marine biomass from sponges (*Porifera*). Under mild conditions (37 °C), lyophilized samples of sponge materials derived from *Thymosea* sp., *Chondrosia reniformis*, and *Chondrila nuculla* were suspended in water and pressurised in a batch vessel (autoclave) with CO_2 of 50 bar.[137] Without added acids or extra solvents, a collagen/gelatine powder was obtained with a yield of approximately 50%, more than 30% higher than that obtained with conventional extraction using dilute acetic acid. FTIR, CD, and DSC characterizations indicated not only the high purity of the extract, but consistent similarities to collagen/gelatine samples from other marine sources. *In vitro* cytotoxicity tests carried out using the ISO/EN 10993 protocol on mouse lung fibroblasts did not demonstrate any toxic effects. In a continuation of this study, the extraction method based on water acidification with pressurised CO_2 was further optimised at a low pressure of 10 bar, thereby widening its perspectives for large-scale applications.[138]

In an effort to improve the standard extraction protocols shown in Fig. 3, a response surface methodology (RSM) with integrated Box-Behnken design (BBD) was developed.[139] Starting from only fish skin waste, the extraction yield of collagen was optimized up to 19.27 ± 0.05 mg g^{-1} skin under specific conditions (1.90 M NaCl, 8.97 mL g^{-1} solvent/solid ratio, 0.54 M acetic acid and 36 h). SEM analysis proved the presence of irregularly linked fibrils, displaying large pores suitable for the incorporation of chemicals and drugs.

The massive growth of the jellyfish population is impacting marine ecosystems worldwide.[140] Thus, although it is not a fish residue, with the aim of both preventing/minimizing this environmental risk and identifying innovative sources of collagens from marine biomass, an investigation was undertaken considering jellyfish as a feedstock.[141] Starting from the fresh umbrella and oral arm tissues of *Catostylus mosaicus* jellyfish, conventional acid extraction in 0.5 N acetic acid allowed collagen (JASC) to be obtained in yields ranging from 14 to 22 mg g^{-1} dry weight. JASC was a type I collagen with triple helical molecular signatures comparable to industry-standard collagen. Moreover, the JASC collagen solution-formed fibrils (Tris buffer, pH 7.5–8; 4–25 °C) were characterized by AFM and BCARS spectroscopy, which further confirmed a structure nearly identical to the fibrils of the standard type I collagen (Fig. 11).

Statistical analysis showed that the proliferation of MC3T3-E1 preosteoblasts on JASC-coated with polystyrene dishes surpassed that of standard collagen. Finally, the blend of agarose 1% (w/w) and fibrillised JASC offered a sufficiently rigid scaffold (*ca.* 50-fold stiffer than hydrogel of pure JASC)

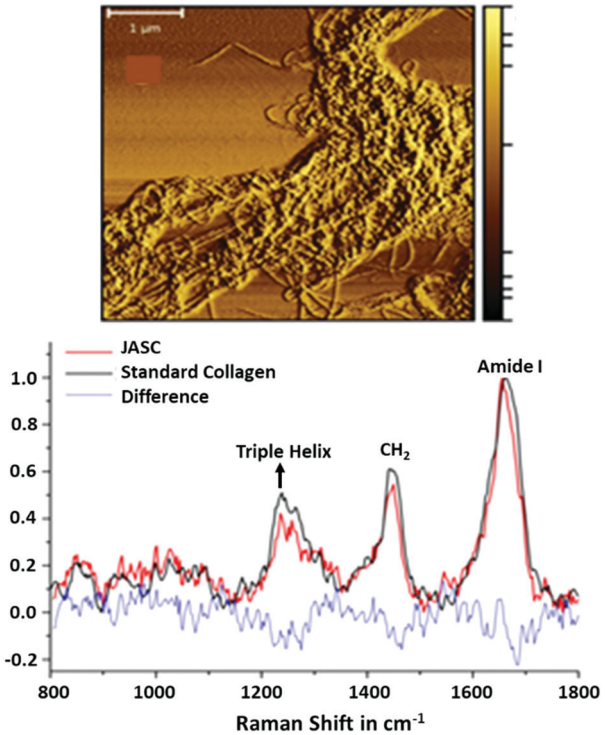

Fig. 11 Top: AFM images of fibrillized JASC at room temperature. Line profiles show a width of 25–78 nm. Bottom: Raman-like spectra (BCARS) of *in situ* fibrils of JASC and standard collagen normalized on amide I band. This band is a marker for the secondary structure of the polypeptide backbone associated with C═O and N–H stretching and bending. Adapted from ref. 141, with permission from the American Chemical Society, Copyright 2018.

that could promote cell adhesion and proliferation, potentially suitable for bone tissue engineering applications.

The final procedure described here refers to the application of extrusion, a well-known technique in the food industry. An innovative extrusion-hydro-extraction (EHE) process was implemented to extract tilapia fish scales (TFS).[142] The synergistic effect of high heat (135 °C), high pressure, and high mechanical force during the process broke the chemical bonds between collagen and hydroxyapatite, affording type **I** collagen (up to 16 g protein/100 g crude protein content yield (dry basis)). Further benefits of the extrusion technique include continuous production, ease of operation, and low waste formation.

Marine fish-derived collagen (MFC) has been extensively used to formulate cosmetics for skin repair and regeneration. Besides the dozens of self-styled websites claiming the benefits of marine collagen,[143] scientific reports on this subject suggest that oral administration of MFC hydrolysates inhibits collagen loss and collagen fragmentation in chronological aged skin with a statistically significantly higher skin elasticity level in elderly women.[144,145] A recent investigation on the properties of collagen extracted from cod and salmon skins highlighted that both materials had good moisturizing effect through water adsorption, preventing skin dehydration and irritation, as confirmed by topic exposure and cytokine evaluation.[146]

However, there are much more attractive perspectives for fish collagen in the fabrication of biomaterials and biodevices.

4.1.3 Fish collagen-derived biomaterials and biodevices. The richness of hydrolysed fish collagen (HFC) in glycine, proline, glutamic acid, and aspartic acid and a variety of peptides has prompted researchers to investigate its ability to promote the multidirectional differentiation of several stem cell types. One example focused on HFC extracted from tilapia scales by enzymatic hydrolysis (0.1–0.3% complex protease, 60 °C) and used as a dried powder.[147] The sample (M_w in the range of 700 to 1300 Da) was mainly comprised of glycine, proline, and hydroxyproline (rates of 333/1000, 115/100 and 117/1000 residues, respectively) and promoted the viability of model mesenchymal stem cells derived from rat bone marrow. This aptitude was ascribed either to the moderate molecular weight of the peptides, which could expose more active sites for the growth regulation of the cells, or the remarkable amount of proline as a key amino acid for the synthesis of polyamines, which are regulators of cell proliferation and differentiation. HFC inhibited chondrogenic and adipogenic differentiation (no effects on neural differentiation), thereby providing a solid principle for the use of HFC in biomaterials and biological coatings, and as a differentiation-inducing agent.

The poor mechanical strength and somewhat low thermostability (denaturing temperature, T_d) of fish-derived pure collagen hamper its use in the fabrication of scaffolds for tissue engineering (TE). Thus, to overcome this issue, strategies based on reinforcement with fillers or cross-linking agents have been developed. For example, the presence of [*N*-(3-dimethylaminopropyl)-*N*′-ethylcarbodiimide hydrochloride] (EDC·HCl), a known peptide coupling agent, during fibril formation of salmon atelocollagen increased its Td from 18 to 47 °C, and further improved its capability for the proliferation of human periodontal ligament cells. Similarly, it was demonstrated that jellyfish-extracted collagen cross linked with EDC·HCl/*N*-hydroxysuccinimide (EDC/NHS) exhibited a higher cell density and enhanced cell proliferation compared to bovine collagen.[148] A similar protocol was used to improve the mechanical strength of poly(lactic acid) (PLA), a remarkable biomaterial for sutures, implants for bone fixation, and drug delivery, by grafting collagen extracted from fish bone.[149] In the presence of EDC·HCl, both NMR and FTIR analyses proved that a collagen/poly(lactic acid) composite (C–PLA) was formed through amide covalent bonds between both components. The addition of 5–10% of collagen provided a formidable enhancement of both tensile strength and elongation at break of C–PLA up to 88.60% and 176.88%, respectively, with respect to pure PLA, indicating a new avenue for the fabrication of PLA-based composites with high impact resistance.

An alternative option has been recently proposed by grafting type I collagen extracted from the fish scales of *Labeo rohita* (Rohu) and *Catla catla* carp, on graphene oxide (GO), which is well-known in TE for its positive effects in cell proliferation and differentiation.[150] Grafting was carried out by mixing a GO solution in MES buffer (pH 6.5) with collagen dissolved acetic acid in the presence of EDC·HCl and NHS, both acting as

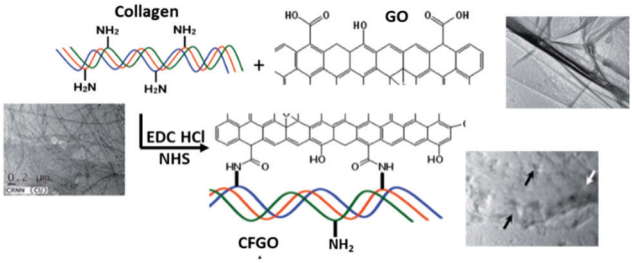

Fig. 12 Schematic view of amide bond formation between collagen and graphene oxide. TEM images of collagen (left), GO (top right) and CFGO (bottom right). The black and white arrows indicate GO sheets and collagen fibres, respectively. Adapted from ref. 150 with permission from the Royal Society of Chemistry, Copyright 2015.

activators of surface carboxyl groups on GO. FTIR and UV analyses substantiated the formation of amide bonds between GO and collagen in the collagen-functionalised graphene oxide (CFGO), as shown in Fig. 12.

TEM images proved the close contact of randomly distributed GO nanosheets and collagen fibres. This plausibly explained why the tensile strength of the CFGO scaffold (3.19 MPa) was significantly improved with respect to native collagen (0.09 MPa). *In vitro* investigations using NIH 3T3 embryonic mouse fibroblast cells revealed no cytotoxicity, while SEM images demonstrated that after a prolonged cultured time (12 days), the fibroblasts displayed the typical spindle-shaped morphology, suggesting that the cells infiltrated the scaffold and proliferated there. Finally, to test for antimicrobial activity, curcumin (diferuloylmethane, a component of *Curcuma*) was adsorbed in CFGO. Both Gram +ve and Gram −ve organism growth was considerably reduced, thereby further confirming the potential of synergistic effect of collagen and GO in CFGO for tissue engineering applications.

Another investigation focused on collagen extracted from tilapia (an abundant freshwater fish) skin.[151] The combination of acid dissolution and pepsin digestion was used to prepare collagen sponge, which had a content of glycine, hydroxyproline, and proline (31.9%, 7.7%, and 11.3%, respectively) consistent with type I protein. Thereafter, the sponge was subjected to electrospinning at 16–18 kV to fabricate a membrane of collagen nanofibers, which mimicked the reticular structure of extra cellular material (ECM). This was confirmed by SEM analyses, showing smooth collagen nanofibers of 310 ± 117 nm (diameter) similar to the native topographical features of natural ECM. Both the tensile strength (6.72 ± 0.44 MPa) and thermal stability of the collagen nanofibers met the requirements for human skin. The system elicited no immune responses. Moreover, after culturing human keratinocyte cells (HaCaTs) on the collagen nanofibers for 5 d, the proliferation rate of the HaCaTs was 11.4%, indicating good capability for both the adhesion and proliferation of key cells involved in skin wound re-epithelialization and healing. Tests on epidermal differentiation proved that tilapia collagen nanofibers significantly upregulated the expression of proteins such as involucrin and filaggrin, and TGase1 genes responsible for the formation of integrated epidermis. Overall, the biomimetic electrospun tilapia skin collagen nanofibers are a promising biomaterial for skin regeneration.

In a different approach, a bioinspired piezoelectric material based on fish skin as an energy harvester was proposed to transduce deformations of human skin.[152] Biowaste fish skin (FSK) from *Catla catla* carp was demineralised through acid/base washings followed by treatment with aq. EDTA (20 mM) to remove metal traces. Then, FSK was laminated by polydimethylsiloxane (PDMS) to fabricate a robust nanogenerator (FSKNG) with a layer thickness of 20 μm (Fig. 13, top). FESEM analyses proved the presence of collagen nanofibrils with a D-periodicity of ∼50 nm (Fig. 13A, bottom).

The extended polypeptide chain hydrogen bonding network in FSK accounted for the improved dielectric properties of the material ($\varepsilon_r \sim 50$, and loss tangent, $\tan\delta \sim 0.6$ at 1 kHz).

Moreover, –CONH hydrogen bonding motifs acted as molecular dipoles, inducing spontaneous polarization, which, through a nonlinear electrostriction effect, was the origin of the piezoelectricity in the nanofibrils. As a result, FSKNG proved to be suitable to engineer a self-powered wearable healthcare monitoring device for detecting minute mechanical pressures generated by human physiological signals (arterial pulses, Fig. 13B, bottom). FKSNG showed a sensitivity of ∼27 mV N-1 and fast response time of ∼4.9 ms, producing 2 nA of short-circuit current (I_{sc}) and 200 mV of open-circuit voltage (V_{oc}), with long-term stability (75 000 cycles) under 7.5 N of contact force.

A similar bio-piezoelectric nanogenerator was fabricated starting from fish swim bladder (FSB, a fish processing waste), composed of well-aligned natural collagen nano-fibrils (diameter of *ca.* 64–65 nm; D-periodicity of 61 ± 3 nm).[153]

FSB with an average thickness of 253 ± 10 μm was sputtered on both sides of a gold electrode, paying attention to not heat/damage the collagen crystals. Subsequently, fine copper wires were attached to the Au–FSB system, which was encapsulated by PDMS. The thickness of the PDMS layer on either side of the FSB was 374 μm. An external mechanical vibration acting on

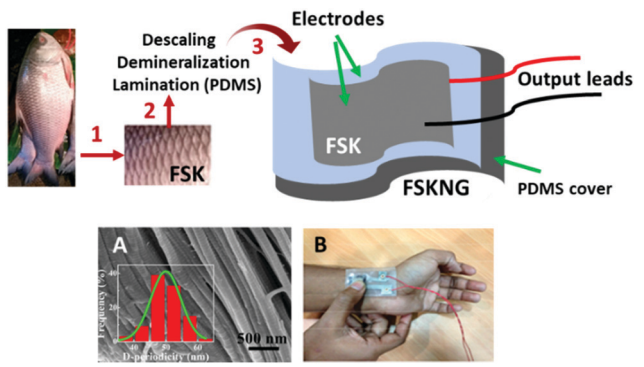

Fig. 13 Top: Steps 1–3 for the fabrication of FSKNG. Bottom: (A) FE-SEM image of demineralised skin. FSK with the histogram profile of D-periodicity in the inset. (B) FSKNG as a pressure sensor for radial artery. Adapted from ref. 152, with permission from the American Chemical Society, Copyright 2017.

Table 8 Biomaterials and biodevices from fish-derived collagen

Entry	Starting material	Prepared biomaterial or biodevice	Ref.
1	Fish scales, barramundi	Burn/wound dressing material	154
2	Swim bladder, sturgeon fish	Artificial cartilage, bone defect repair	155
3	*Arothron stellatus* fish	Scaffold for wound healing	156
4	Echinoderm connective tissues	Membranes for tissue regeneration	157
5	Fish scale, tilapia	*In vivo* wound healing material	158
6	Fish scale, tilapia	Anti-inflammatory biomaterial	159
7	Grass carp skin	Scaffold for biomedical applications	160
8	Salmon skin	Bone tissue engineering	161
9	Fish scales, *Lates calcarifer*	Tissue regeneration applications	162
10	Chinese catfish skin	Tissue engineering	163
11	Fish scale	Bio-piezoelectric nanogenerator	164

the BPNG caused a piezoelectric potential, which moved electrons *via* an external load (not through the dielectric FSB) to neutralize the potential difference between the electrode sides. This generated a positive peak voltage and current pulses. Releasing the vibration resulted in the quick disappearance of the piezopotential, causing electrons to flow back to the opposite electrode with a negative peak voltage. Under compressive normal stress by a human finger (1.4 MPa), the BPNG produced an open-circuit voltage of 10 V and short-circuit current of 51 nA with repeated compressions. The as-generated electricity with an output power density of 4.15 μW cm^{-2} was enough to turn on more than 50 commercial blue LEDs, paving the way for applications in portable electronics and implantable biomedical sensors.

4.1.4 Miscellaneous examples. Besides the examples detailed in Section 3.1.3, other relevant studies on the fabrication of biomaterials and biodevices based on fish-derived collagen are summarized in Table 8.

4.2 Chitin

Chitin is the second most abundant natural polymer after cellulose. Similarly to the latter in plants and collagen in higher animals, chitin plays a vital structural role in the form of ordered crystalline microfibrils as components of the exoskeleton of arthropods and crustaceans, and the cell walls of fungi and yeasts.[165] Chitin is an analogous cellulose polymer, comprising β-(1-4)-2-acetamido-2-deoxy-β-D-glucose and β-(1-4)-2-deoxy-β-D-glucopyranose structures, which lead to poly(β-(1-4)-*N*-acetyl-D-glucosamine). Depending on the source, the number of glucosamine molecules varies between 5% and 10% (Fig. 14).

Chitin is mostly obtained from crustacean waste in the fishing industry, essentially from the shells of prawns, crab, shrimp, and lobster.[166] The total annual production of chitin

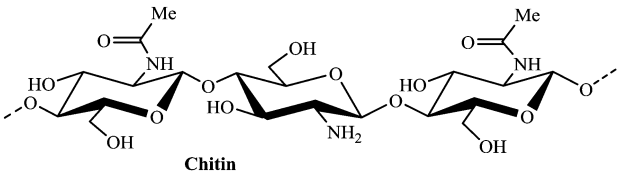

Fig. 14 Structure of chitin with intercalating *N*-acetylglucosamine (end) and glucosamine (mid) units.

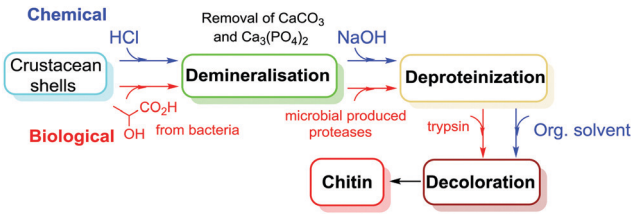

Fig. 15 Flowchart of the operations for the conventional extraction of chitin from fish crustacean shells with chemical and biological treatments (blue and red, top and bottom, respectively).

has been estimated to be 2.8 × 10^7 and 1.3 × 10^9 tonnes from the freshwater and marine ecosystems, respectively.[167] Although there is a certain variability due to species, size and season, crustacean exoskeletons usually comprise *ca.* 20–30% chitin together with 30–50% minerals (mainly calcium carbonate), 30–40% proteins and others including lipids (up to 14%) and pigments (*e.g.*, astaxanthin).[168] The isolation of chitin from these residues requires consecutive steps of deproteinization, demineralization, and discoloration to remove protein, inorganic components and pigments (astaxanthin, canthaxanthin, astacene, lutein and β-carotene).[169] Accordingly, chemical and biological (microbial) methods have been implemented for this purpose (Fig. 15).[170]

Due to protein degradation inside the shells, for high purity chitin, the waste needs to be processed within a few hours of its generation.

Under chemical conditions, demineralization (removal of inorganic salts) is generally carried out with diluted HCl, although other acids such as HNO_3, HCOOH, H_2SO_4, and CH_3COOH have been reported. Then, deproteinization is performed with aq. NaOH solutions (1–10%) at 65–100 °C and finally, discoloration is achieved at room temperature by solvent extraction with acetone, ethanol, ethyl acetate or their mixtures.[171] In search for alternative solvents, supercritical CO_2 has been also described for the decolouration step.[172] However, although chemical methods have been recognised to be uneconomical and eco-unfriendly, with potential adverse effects on the properties of extracted chitin, they are still the preferred commercial treatments due to their short processing time. Nonetheless, biological treatments are under development and promise to offer alternative extraction pathways using lactic acid-producing bacteria for

the demineralisation process and proteases such as *Pseudomonas aeruginosa K-187*, *Serratia marcescens FS-3*, and *Bacillus subtilis* for the fermentative deproteinisation of crustacean biowaste.[167,170] Recently, proteolytic enzymes such as trypsin from cod and blue fish have been proposed to carry out the decoloration process, particularly for the removal carotenoproteins (astaxanthin).[173,174]

The final extract, crystalline chitin, displays biocompatibility, biodegradability, antimicrobial activity, low immunogenicity, and eco-safety, making it one of the most promising biomaterials. Exhaustive reviews have been reported on this subject, describing the variety of uses and potential applications of chitin in wastewater treatment, purification processes, food additives, packaging, controlled agrochemical release, pulp and paper treatment, cosmetics, tissue engineering wound healing, *etc.* (Fig. 16).[110,175–177]

Pertinent to the context of this review, selected examples of chitin extraction and applications for the synthesis of high added-value molecules and/or the fabrication of advanced materials and devices will be detailed in the following section to offer a view on the potential and challenges of the most recent strategies in this sector for the valorisation of fish biowaste.

4.2.1 Innovative extraction of chitin. As mentioned above, the conventional chemical-based extraction of chitin is not without drawbacks mostly due to the environmental and economic impact of the procedure. For example, ~1 L (972 mL) concentrated HCl (35 wt%) is required to demineralize 100 g of chitin from crab shell waste, generating 220 g (112 L at STP) of carbon dioxide in the atmosphere.[178]

Further issues are related to the quality of the product, which often displays inconsistent characteristics, as determined by variable molecular weight, irregular degree of acetylation, and non-uniform chain scissions.[179] Besides the use of biological methods, recent efforts have addressed the design of alternative solvents for chitin, whose extended hydrogen-bonded structure

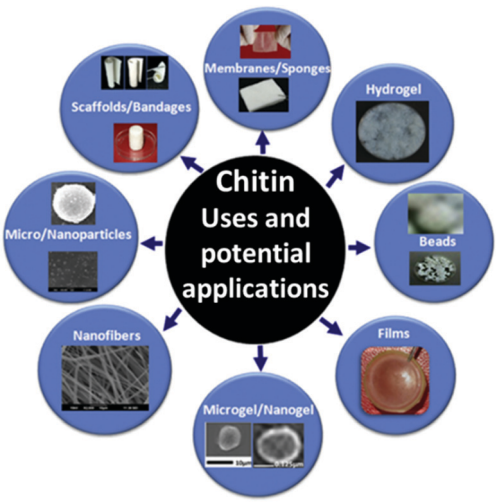

Fig. 16 Processing of chitin into gels, membranes, nanofibers, beads, micro- and nanoparticles, scaffolds, and sponges. Adapted from ref. 176 with permission from Elsevier, Copyright 2014.

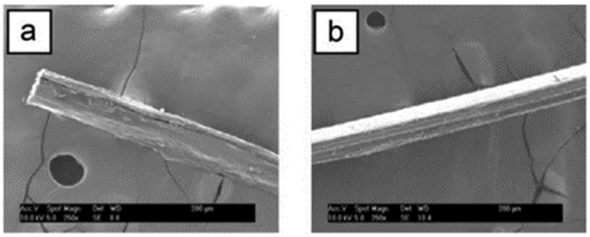

Fig. 17 SEM micrographs of the chitin fibres: (a) from shrimp shells and (b) from practical grade chitin. Reprinted from ref. 180 with permission from the Royal Society of Chemistry, Copyright 2010.

results in extremely poor solubility, if any, in most organic solvents and water. A valuable approach was conceived by the combined application of microwave energy and ionic liquids, particularly 1-ethyl-3-methylimidazolium acetate ([Emim][OAc]), which proved to be effective not only to dissolve chitin, but also raw crustacean (shrimp) shells at a loading of *ca.* 0.3 wt% (at least 94% of the available chitin) with a total irradiation time of 2 min.[180] The basicity of the acetate anion of the IL was plausibly involved in this good solubilising capability. In addition, chitin fibres could be spun directly from the solution through a dry-jet wet-spinning method followed by the addition of water as a coagulant. The SEM images of the fibres are shown in Fig. 17.

Characterisation tests proved that the extracted chitin had a higher M_w, purity and degree of acetylation than that obtained by the conventional industrial multistep chemical process. Starting in 2016, this technology was implemented for the extraction of crustacean biomass in a production plant operated by Mari Signum MidAtlantic, LLC in Richmond (VA).[181]

This represents a concrete step towards the development of the chitin market, which is rapidly expanding and forecasted to triple to $2941 million by 2027.[182] Further investigations have also highlighted that the original IL ([Emim][OAc]) can be replaced by a cheaper IL such as hydroxyammonium acetate ([NH_3OH][OAc]), which allowed the isolation of native chitin with >80% purity and a degree of acetylation of >70%.[183] Interestingly, a recent theoretical study based on a molecular dynamics (MD) approach investigated the mechanism of the dissolution of chitin in ILs in 1-allyl-3-methylimidazolium bromide (AMIMBr), showing that Br cleaves the chitin hydrogen bonds, and AMIM+ could prevent it from regaining crystallinity.[184] A cost-effective and environmentally benign method based on water solvent for the preparation of chitin was recently described starting from grounded shrimp shell waste.[185] In a typical procedure, the solid material was first deproteinized in hot water (0.1 g mL^{-1}, autoclave, 180 °C, 15–30 min), and subsequently, demineralisation was carried out in an aq. suspension under CO_2 pressure (20 bar, 15 min). Both steps occurred with an efficiency of >90%, and the resulting chitin had a viscosity average molecular weight M_w (~390 K) slightly lower than that (~570 K) of chitin obtained by the conventional chemical-based extraction method. In addition, a techno-economic analysis developed by Aspen Plus V10 proved that the total capital investment and

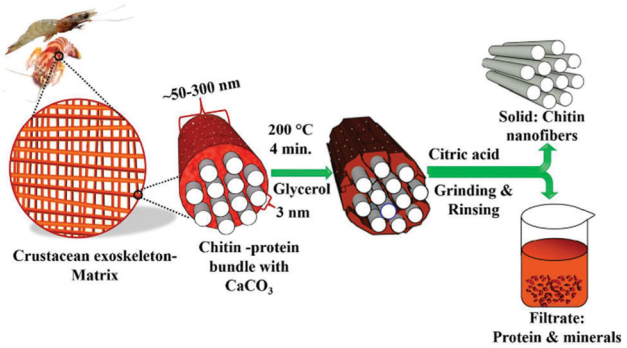

Fig. 18 Scheme for the isolation of chitin by hot glycerol and citric acid. Reprinted from ref. 186 with permission from the American Chemical Society, Copyright 2018.

total operating cost calculated for the H_2O/CO_2 method were *ca.* 1.4 and 2.8 times lower, respectively, that that of the traditional procedure.

In a conceptually similar approach, both a renewable solvent and a reagent such as glycerol and citric acid were used. The steps of deproteinization and demineralisation of prawn shell waste were carried out with hot glycerol (200 °C, 4 min, ambient pressure) and citric acid (ambient T and p, 20 min), respectively, to obtain chitin in yields of 30–40 wt% with respect to the starting raw material (Fig. 18).[186] Glycerol was recycled while co-product calcium citrate could be used as a dietary supplement without further purification.[187]

The isolated chitin was free of $CaCO_3$ and it showed a residual protein content (0.24%) nearly half the amount (0.41%) present in the chitin obtained by the classical chemical method. Moreover, HRSEM analyses demonstrated the formation of chitin nanofibers with a width and length in the range of 20–100 nm and several hundred nanometres, respectively.

In the development of sustainable strategies for dissolving/extracting chitin, deep eutectic solvents (DESs) have received increasing attention in recent years.[188] DESs are hybrid systems, where molecular ionic clusters are found within a complex and disordered hydrogen-bonding network. This unique combination of coordinating hydrogen-bonding ions and molecules confers excellent solvent properties comparable to that of ionic liquids.[189] However, in contrast to the majority of ILs, which are toxic compounds, most common DESs obtained from choline chloride (ChCl) possess low-to-moderate cytotoxicity, are non-phytotoxic and readily biodegradable.[190] The first report on the use of DESs for chitin extraction dates back to 2017, where the comparison of four different eutectics demonstrated that the best-performing one was a 2 : 1 mixture of ChCl and malonic acid (CCMA).[191] A 7 wt% suspension of grounded lobster shell waste in CCMA was heated at 50 °C for 2 h, centrifuged in water, and the resulting solid decolourised (10% H_2O_2, 80 °C). The overall procedure allowed the separation of two chitin samples (S and P) of different crystallinity (67.2% and 80.6%) in a total yield of 20.63% ± 3.30%, higher than that (16.53% ± 2.35%) obtained by treating the same waste through the conventional chemical method (6% HCl, rt, 2.5 h; 10% NaOH, 90 °C, 3 h; 10% H_2O_2, 80 °C). Although S and P solids displayed different thermal stability, the spectroscopic patterns and surface morphology analysed by FTIR and SEM proved their similarities to commercial chitin. In a continuation of this investigation, a closer comparison showed that the purity (93%) and the residual protein content (*ca.* 2 wt%) of the S and P samples was nearly identical to chemically extracted chitin, but the latter displayed a M_w (576 kDa) and crystallinity index (87.48%) ~1.75 and 1.1–1.3 times higher, respectively.[192] These differences were attributed to the higher temperature used during the CCMA-based extraction, which plausibly favoured the breaking of the glycosidic bonds and intra/inter-molecular hydrogen bonds in chitin, causing a decrease in its M_w and the generation of some amorphous solid.

Another approach to improve the sustainability of DESs-based extractive protocols was designed using an NADES (natural deep eutectic solvent) comprised of an equimolar mixture of ChCl and malic acid (2-hydroxybutanedioic acid), a naturally occurring compound as an L-enantiomer and produced by all living organisms.[193] Combined with M_w irradiation (700 W, 9 min), the extraction of a 4% suspension of shrimp shell waste in the selected NADES allowed demineralization and deproteinization processes with an efficiency of 100% and 93.8%, respectively. The short processing time due to M_w positively impacted the quality of the final extract. The mechanism of the NADES-based chitin extraction considered that once the minerals (mostly $CaCO_3$) from the shrimp shells were removal by malic acid, a void space was formed between the residual proteins and chitin fibres, with overall weakening of the linkages within the structural framework. Then, (competing) hydrogen bonding between the NADES and the glucosamine units of chitin favoured its dissolution and extraction. Very recently, the same group also proposed a two-step extraction of shrimp shell waste based on demineralization carried out with citric acid and subsequent removal of the protein content *via* the combined use of M_w energy and four DES as mixtures of betaine hydrochloride (betaine HCl)–urea, choline chloride (ChCl)–urea, ChCl–ethylene glycol, and ChCl–glycerol, demonstrating that in all cases the yield (of chitin, 22–25%) was higher than for conventional chemical procedures (17%).[194]

4.2.2 Valorisation of chitin in nano- and hybrid materials. Although the applications of chitin are limited by its poor solubility in most solvents, several processing techniques have been recently developed for the fabrication of nano-, bio-, and hybrid materials based on chitin. One example is the preparation of chitin nanofibers (ChNFs), which are considered among the best biocompatible candidates for wound dressing, tissue engineering, soft contact lenses, membranes for water filtration, *etc.*[195,196] A study compared three new methods for the preparation of ChNFs by drying a solution (0.4–0.8% w/v) of squid pen-derived chitin in HFIP (hexafluoro-2-propanol) solvent, through cold press (CP), vacuum drying (VD), and vacuum-assisted filtration (VF).[197] The films obtained *via* the self-assembly of chitin nanofibers fabricated by CP, VD, and VF had elastic moduli of 1.3 GPa, 1.5 GPa, and 2 GPa, respectively. Moreover, the corresponding

stress–strain curves showed no slipping, early breakage, breakage at the grips, or inhomogeneity. These mechanical properties are suitable in materials for biomedical use. The same solvent (HFIP) was used to dissolve chitin and prepare nanofibers with diameters of less than 100 nm through different procedures including self-assembly, microcontact printing, and electrospinning.[198] Alternatively, ChNFs (from dried shrimp shell) of high molecular weight were successfully electrospun using 1-ethyl-3-methylimidazolium acetate as an ionic liquid solvent.[199]

A wet-spinning process was described as an unprecedented technique to spin pure chitin fibres from a chitin aq. solution (6 wt%) containing NaOH (11 wt%) and urea (4 wt%).[200] Pure chitin nonwoven fabrics were then obtained by removing the water with acetone, and subsequent hot pressing (60 °C, 0.1 MPa, 4 h, Fig. 19).

Compared to chitin fibres spun from other solvents or blended with cellulose, ChNFs from aq. solution exhibited superior mechanical properties. Specifically, the fineness of the material decreased (from 10.3 to 5.8 dtex), with an increase in tenacity (0.75 to 1.36 cN dtex) at increasing hanging gravity from 0 to 500 g. Notably, no extra (chemical) binders were used to stick the fibres to each other. Only non-covalent interactions (hydrogen bonds, van der Waals forces and hydrophobic interactions) were exploited for self-aggregation, with advantages to secure biocompatibility upon contact with living tissues for medical applications. This was confirmed for wound dressing. Not only the tensile strength (1.2 MPa) and elongation at break (1.0%) of the chitin nonwoven fabrics met the mechanical requirements of traditional gauze, but they displayed increased wound contraction and accelerated wound healing in rabbits.

In a substantially different approach, ChNFs were used to fabricate a piezoelectric nanogenerator (PENG).[201] Once chitin was extracted from crab shells, uniform nanofibers of 10–20 nm width were mixed with an organic polymer such as poly(vinylidene fluoride) (PVDF, 5 wt%) to prepare a thin film of 2.4 × 1.8 cm and 47 μm thickness, which was finally covered on both sides with aluminium foil as electrodes and incapsulated on polydimethylsiloxane (PDMS). It was demonstrated that ChNFs as dopants of PVDF were able to maximize by up to 84.3% the nucleation of the β-phase in the organic polymer, resulting in the maximum piezoelectricity (35.56 pC N^{-1}). Under human finger impulse imparting and releasing and axial pressure of 27.5 N (av. frequency 6 Hz), the PENG charged a 2.2 mF capacitor to 3.6 V within a short time (20 s) and illuminated 25 blue LEDs connected in series. These features make it suitable for application in *in vivo* biomedical devices harvesting energy from heart beats and blood flow, and charging devices capturing mechanical energy from moving cars, sea waves, and even rain drops and body movements.

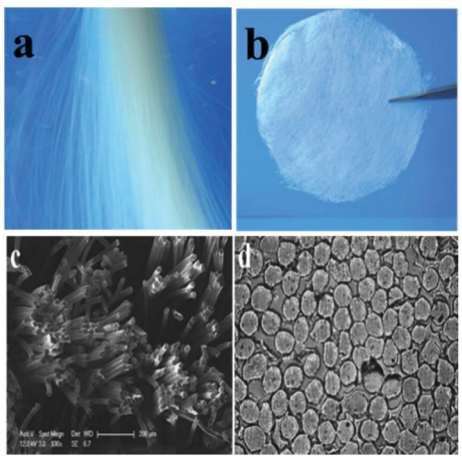

Fig. 19 Photographs of freshly spun chitin fibres in (a) water and (b) chitin nonwoven fabrics in the dry state. (c) SEM image (scale bar 200 nm) and (d) optical microscope photograph (d) of a bundle of the air-dried chitin fibres. Adapted from ref. 196 with permission from the Royal Society of Chemistry, Copyright 2013.

Hybrid nanomaterials have been developed to improve the mechanical strength and stability of chitin by the addition of biocompatible fillers. Accordingly, the preparation of chitin-graphene oxide (GO) nanosheets was reported by mixing the two components in a mass ratio in a wide range, from 24 : 1 to 0.3 : 1.[202] The FTIR, ^{13}C solid-state NMR and DSC analyses were consistent with the absence of covalent interactions between chitin and GO, the latter acting as a filler to induce structural rearrangements in chitin with new hydrogen bonds among the chains. The cohesion of the hybrid material and its mechanical stirring stress resistance were proportional to the GO quantity in the material (up to a chitin : GO ratio of 12 : 1). The measured rheological properties and storage and loss moduli (G' and G'') with angular frequency showed that the behaviour of the composites turned from gel-like to solid-like with a progressive increase in the content of GO. Finally, the addition of GO did not interfere with the lysozyme activity on the chitin chains, thereby indicating that the polymeric matrix of these materials preserved their biodegradability.

Other multi-functional hybrid bio-aerogels were described based on cellulose nanofibers (CNFs) decorated with chitin nanocrystals (ChNCs).[203] After the extraction of CNFs and ChNCs from corn husks and shrimp shell waste, respectively, a sustainable freeze-drying methodology was envisaged. Specifically, a mixture of an aqueous solution of CNFs with dispersed ChNCs was firstly frozen in a dry ice–isopropanol mixture (−73 °C), and subsequently freeze-dried in a lyophilizer for 4 days (−88 °C under vacuum). The FESEM images of three CNFs aerogels with different amounts of ChNCs (0%, 1%, and 2% referred to as neat AR, AR1 and AR2, respectively) are shown in Fig. 20 (top).

The morphology of the material changed with the amount of ChNCs, which tended to locate between the CNFs, reducing the intermolecular interactions between the fibres. This was particularly evident for AR2 and explained its superior ability for the removal of dyes (MB: methylene blue and Rh6G: rhodamine 6G) from aqueous solution compared to AR and AR1. The interactions of the positively charged dye molecules with the acetamide-enriched AR2 favored adsorption (Fig. 20: bottom, dotted lines). The same reason accounted for the superior antibacterial and antioxidant activity of AR2 over AR and AR1.

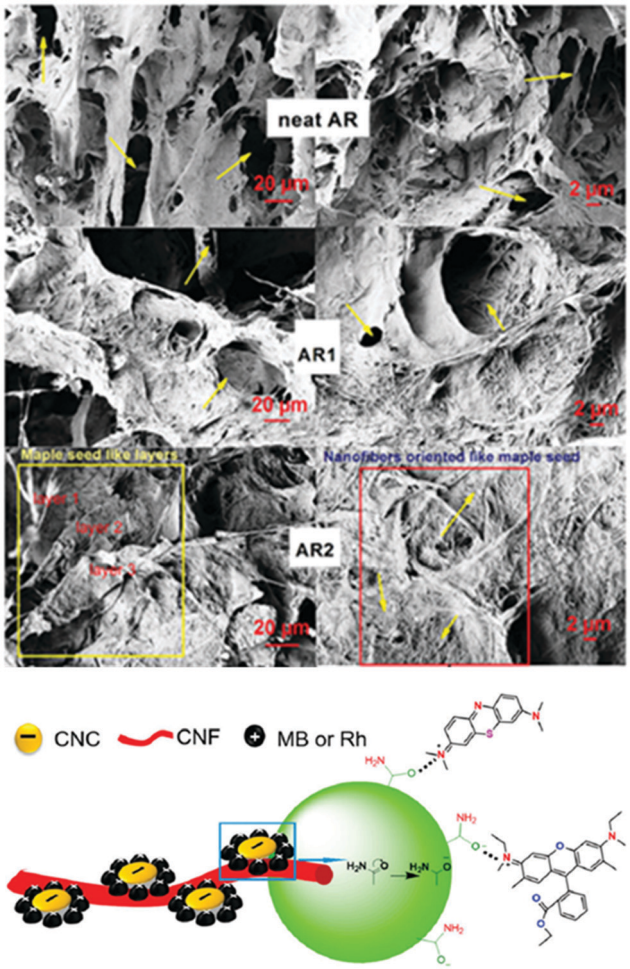

Fig. 20 Top: FESEM images of the different aerogels and bottom: mechanism for the adsorption of dyes (MB and Rh6G) into AR2. Adapted from ref. 203 with permission from the Royal Society of Chemistry, Copyright 2017.

A similar concept was developed in the layer-by-layer spray coating of cationic CNF and anionic ChNC suspensions onto poly(lactic acid) (PLA) films.[204] The attractive electrostatic forces between CNFs and ChNCs induced strong adsorption of thin alternating layers, while self-repulsion in each layer provided more efficient packing. As a result, the films with at least two alternating coated layers, consisting of PLA-(ChNC-CNF)*n*, were significant less permeable to O_2 compared to PLA alone, even at an elevated relative humidity of 70%. This potential targets engineering applications aimed to fabricate 100% bio-renewable barrier packaging for foods, pharmaceuticals and electronics, where oxygen permeability is a key issue.

4.2.3 Chitin-based nano-carbons, nanocomposites and C-dots. Nanocarbons include fullerenes, nanotubes and nanoscrolls, 2D-honeycomb-arranged graphene, nanodiamonds and activated carbon nanoparticles and fibers.[205,206] The properties of nanocarbons including mechanical flexibility, stability, ultra-high surface area, low toxicity, biocompatibility and tunable electrical, physical and chemical behaviour have contributed to its increasingly popular use as fillers in functional materials (hybrids and composites), chemical- and bio-sensing in medicine, energy conversion and storage, and preparation of bioelectronics platforms, supercapacitor electrodes, plant-growth promoters, and catalyst supports.[207,208]

Carbon dots are a different class of carbonaceous nanomaterials comprising nano-sized (<10 nm) quasi-spherical functionalized C particles with hydroxyl, carbonyl and carboxylic moieties.[209] Usually abbreviated as C-dots, these materials were fortuitously discovered in 2004, and since then, have been widely applied due to their ability to integrate the optical properties of semiconductor-based quantum dots with the electronic properties of carbon materials.[210] C-dots have been extensively investigated for applications in biosensing, bioimaging, drug delivery, photocatalysis, photovoltaic devices, and optoelectronics.

The following section will highlight some selected contributions reporting the recent uses of chitin as a starting material for the preparation of both nanocarbons and C-dots.

It has been demonstrated that the efficiency of carbon-based electrodes in supercapacitors is substantially enhanced by the introduction of N-based dopants.[211] Accordingly, chitin containing ~6.9 wt% nitrogen from structural NH_2 and *N*-acetyl groups has been considered as a source for these materials. In one example, nanocrystalline chitin was used as a soft template for the preparation of mesoporous nitrogen-doped carbon materials with a layered structure.[212] The deacetylation and hydrolysis of chitin fibrils isolated from king crab shells allowed chitin nanocrystals (ChN) with a diameter and length in the range of 10–18 nm and 300–500 nm, respectively, to be obtained. An aq. suspension of ChN was then mixed at rt with $Si(OCH_3)_4$ to functionalise the chitin surface. After drying, silica/NCh composite films were achieved and subjected to carbonization at 900 °C under nitrogen. Silica was finally etched (aq. NaOH, 90 °C) to fabricate layered mesoporous nitrogen-doped carbon (NC) materials. The major features of one of the best-prepared samples are shown in Fig. 21.

Elemental and EDX analyses confirmed the presence of C, N, H, and O in *ca.* 83, 4.6, 1.4, and 11.5 wt%, respectively. TEM showed partially aligned porous networks with the pore channels oriented parallel to each other within each layer, while SEM highlighted how the material was formed through the assembly of the carbon nanorods in a true replica of the layered nematic organization of the starting nanocrystalline chitin films. Silica proved crucial to preserve this (nematic) organization and introduce mesoporosity, which is essential for rapid

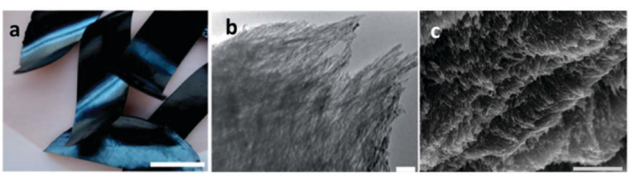

Fig. 21 Mesoporous nitrogen-doped carbon. (a) Photograph (scale bar, 1 cm), (b) TEM image (scale bar, 100 nm), and (c) SEM image (scale bar, 500 nm). Adapted from ref. 212 with permission from the Royal Society of Chemistry, Copyright 2014.

electrolyte diffusion in electrodes. Tin oxide particles were then embedded in the material to improve its electrochemical properties, particularly its specific capacitance (C_s), which was enhanced by up to up to 202 F g^{-1} at a current density of 230 mA g^{-1}, confirming the superior performance of the supercapacitor electrodes.

A similar approach was used to design materials with a totally different scope in the field of adsorbents and catalytic systems. In this study, the carbonization of α-chitin was followed by on-line thermogravimetry coupled with Fourier transform infrared spectroscopy, which proved that the deacetylation/decomposition of chitin mostly occurred at 300–450 °C, releasing volatile carbonyl products and nitrogen-containing compounds.[213] Further increasing the carbonization temperature in the range of 400–1000 °C decreased both the O- (from 12.7 to 6.7 wt%) and N- (from 8.4 to 3.1 wt%) contents of the obtained materials, indicating extensive degradation of the surface functional groups. Moreover, the crystal structure of chitin was progressively replaced by a more regular layered carbon-sheet structure with the formation of a graphitic phase. Consistent with these structural/morphological properties, the carbon prepared at 400 °C could remove up to 92% of Cr(VI) from aq. solutions (10 ppm, pH = 10), while the sample obtained at 1000 °C was no longer an adsorbent. Both the amino and pyrrolic N groups at the surface of materials were responsible for their metal chelating effects. However, high-temperature carbonization (at 800–1000 °C) provided carbons with a large content of graphitic nitrogen, which acted as excellent catalysts for the epoxidation of olefins.

Other strategies to synthesize N-doped carbonaceous materials from chitin were devised to obtain photoluminescent C-dots. Although this subject is still in its infancy, original approaches are emerging based on the concept that N-dopants cause a fluorescence enhancement. Increasing interest has been focused on fish scale waste as a source of chitin.[214] One example described a hydrothermal method by which an aqueous suspension of fish scale waste of grass carp was heated at 200 °C (24 h, autoclave) to afford homogeneously sized C-dots of 2 nm with a remarkably high N-content of 14.6% (by XPS) (Fig. 22).[215]

After excitation at 365 nm, the aq. dispersions of C-dots showed a PL emission peak at 430 nm with a quantum yield as high as 17.08% due to nitrogen doping. The PL effect was so strong that even at a very low concentration, the aq. dispersion of C-dots gave very bright violet-blue luminescence (top inset of Fig. 21). Notably, the fluorescence could be selectively quenched by the addition of ClO^- (up to 10 mM), making the fish scale-derived C-dots a sensing system for this anionic species.

In a recent variant of this protocol, the hydrothermal treatment of both prawn and crab shells waste was described in the presence of urea (2 wt%), acting as a denaturant.[216] The method allowed the isolation of pure chitin together with the concurrent formation of an aq. suspension of N-doped C-dots (Fig. 23).

At 150 °C (1 h), the protein content of the shell waste was removed by urea-assisted hydrolytic cleavage of the amide

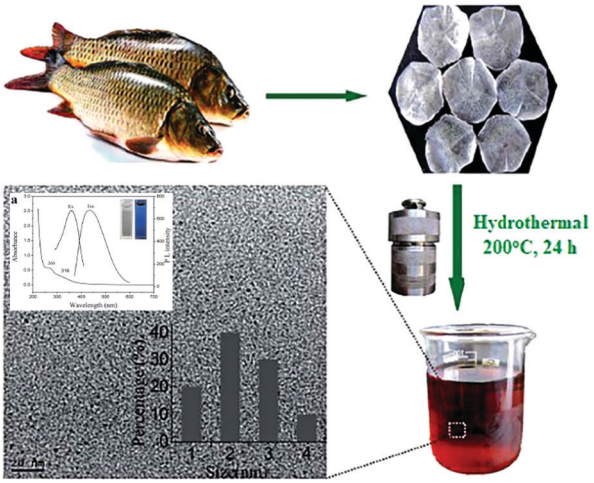

Fig. 22 C-Dots from the hydrothermal treatment of fish scales. In the TEM image, the insets show the particle size distribution histogram of the C-dots (bottom) and their UV-vis absorption, excitation and emission spectra (top). Reprinted from ref. 215 with permission from the Royal Society of Chemistry, Copyright 2015.

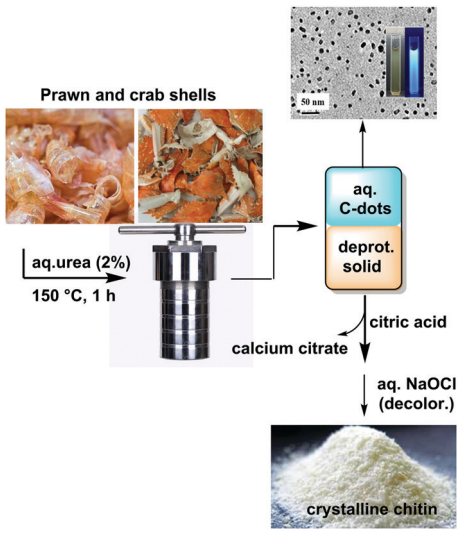

Fig. 23 Chart of the hydrothermal method for the concurrent synthesis of chitin and N-doped C-dots.

bonds. This produced a supernatant liquid phase containing C-dots and a solid residue, which was demineralized and decolourised using citric acid and NaOCl, respectively (see Section 3.2.1). Chitin was then isolated in yields of 21% and 31% from crab and prawn shells, respectively.

The formation of quasi-spherical C-dots with a size in the range of 7–15 nm was confirmed by TEM. After excitation at 355 nm, the PL spectrum showed a maximum emission intensity at 415 nm with a quantum yield of 5.84%, which is consistent with PL-behaviour described in the literature for aq. C-dots suspensions. The spectroscopic characterization of chitin indicated that the degree of acetylation and the crystallinity index (CrI) were 93.6% and 93.7%, and 84.5% and 85.1%,

Table 9 Transformation and applications of fish-derived chitin

Entry	Transformation/processing	Prepared chemicals/materials	Ref.
1	Catalytic conversion of chitin	Acetic acid and pyrrole	217
2	Selective thermal degradation	*N*-containing furan derivative	218
3	Thermal treatment in ionic liquids	*N*-containing furan derivative	219
4	Chitin nanocrystals	Aqueous foams	220
5	Universal solvents for chitin	Hydrogels as functional material	221
6	Deep eutectic solvents	Wound healing films	222
7	Pyrolysis of squid chitin	Carbon for supercapacitor electrodes	223
8	Mechanochemical amorphization	Oligomers of *N*-acetyl-D-glucosamine	224
9	Porous chitin microbeads	Sustainable cosmetics	225
10	Enzymatic hydrolysis	*N*-acetyl-D-glucosamine	226

for the product isolated from prawn shells and crab shells, respectively. Both the molecular weight and CrI of the hydrothermally prepared chitin were higher than that of chitin obtained by conventional chemical extraction. Overall, the simultaneous synthesis of chitin and C-dots proved to be cost-effective, fulfilling the requisites of energy-, time-, and water-saving for large-scale applications.

4.2.4 Additional examples. Besides the examples discussed in Sections 4.2.3 and 4.2.4, the other recently reported studies on fish-derived chitin are summarized in Table 9.

Chitin has also been reported to be converted into several derivatives (*i.e.* N- and O-sulfonated chitin) *via* chemical modification. These are relevant compounds in terms of similarity to heparin (blood anticoagulant), dibutyryl- and carboxymethyl-chitin for biomedical applications.[227–229]

4.3 Chitosan preparation and control of its molecular weight

Chitosan is derived from the partial deacetylation of chitin, specifically, when the degree of acetylation (DDA) or number of *N*-acetylglucosamine units in its polymeric structure is less than 50% (compare Fig. 14).[230] DDA is a structural parameter that influences the overall charge, reactivity, biological and physicochemical properties of chitosan, including its hydrophilic characteristics, macromolecular chain flexibility, polymer conformation, and viscosity.[231]

The deacetylation of chitin is traditionally carried out by alkaline hydrolysis of the acetamide groups under either heterogenous conditions with a concentrated base (aq. NaOH, 40–50%; 100 °C) and inert atmosphere to limit (oxidative) depolymerization, or homogeneous conditions at 25–40 °C, by freezing–pumping–thawing (FPT) cycles of an alkaline aqueous suspension of chitin until dissolution. Homogeneous-type conditions can be more effective since they involve moderate alkali concentrations ($\leq$13 wt%) and provide chitosan with no chain compositional dispersion.[171,232] However, besides deacetylation, the nucleophilic attack of the base to the glycosidic bonds of both chitin and chitosan induces partial depolymerization. The resulting chitosan usually displays good DDAs (from 70% up to >90%), but medium-sized molecular weights in the range of 80 to 800 kDa. Different strategies have been explored with the double aim to enhance the M_w of chitosan (and improve its mechanical properties),[233] and implement greener and safer processes.

It should be noted that various molecular weight averages are defined in polymer science. Herein, either M_w or $(\overline{M_w})$ is used. The first one (M_w) refers to the number average molecular mass of the polymer, which is determined by measuring the molecular mass of n polymer molecules and evaluating the arithmetic mean of the molecular masses of the individual macromolecules. Viscosimetry and the Mark–Houwink equation are generally used for this purpose. The second definition $(\overline{M_w})$ refers to the mass average molar mass and considers that the contribution of macromolecules (containing more mass) with larger molecular size is greater than that of smaller molecules. This average is mostly determined using light or X-ray scattering and differential refractometry.

One example reported a new process where the alkaline deacetylation of β-chitin was assisted by ultrasound (USAD).[234] After extraction from squid pens, chitin was ground in particles with a diameter in the range of 0.125–0.250 mm, suspended in aq. NaOH (40%, 50 mL) and subjected to ultrasound irradiation at 60 °C for 50 min (ν = 24 kHz; irradiation pulse and surface intensity of 0.5 s and 52.6 W cm^{-2}). The chitosan product (Ch1) was isolated in 88% yield with a degree of acetylation of 36.7% and an average molecular weight $(\overline{M_w})$ and dispersity ($Đ$) of *ca.* 12 × 10^5 g mol^{-1} and 1.4, respectively. Repeating the USAD protocol twice on Ch1 provided another sample (Ch3) with DAA, $\overline{M_w}$ and $Đ$ of 4.3%, 9 × 10^5 g mol^{-1} and 1.3, respectively, thereby confirming that this technique allowed the synthesis of high molecular weight chitosan with a low degree of acetylation without the use of extra additives, inert atmosphere and long reaction times. In the above Section 3.2.1, ionic liquids have been described to dissolve chitin. However, in the presence of water, the solvent power of ILs for chitin and more generally for polysaccharides is quite limited because the hydrogen bonding accepting ability of ILs is strongly decreased.[235] It was discovered that a peculiar class of ionic liquids comprised of basic tetraalkylammonium hydroxides in aqueous solutions ([Nx,x,x,x][OH]; X = 2–3; 25 wt%) was not only able to dissolve chitin (0.2 wt%) at room temperature, but also promote its deacetylation, yielding chitosan with a DDA of 91%.236 The product was quantitatively recovered by precipitation with the addition of excess water to the solution.

The combined use of mechanochemistry, *i.e.* the use of mechanical energy to activate chemical transformations, and

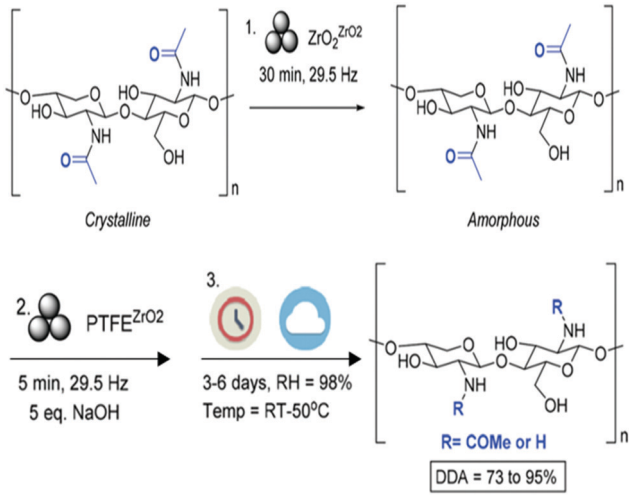

Fig. 24 Combined mechanochemical (amorphisation) and aging conditions for the deacetylation of chitin. Adapted from ref. 237 with permission from the Royal Society of Chemistry, Copyright 2019.

aging techniques has been successfully reported for producing high-M_w chitosan (Fig. 24).[237]

Commercial chitin was initially subjected to planetary ball milling, which reduced its crystallinity index from 65.8% to 14.3%. This loss of crystallinity (amorphization) improved the access to the acetyl sites of chitin through increased internal permeability.

Amorphous chitin was mixed with NaOH (1 : 1 wt%) and further milled at low energy in a PTFE jar with a ZrO_2 ball (5 min). Thereafter, the solid was aged in a controlled humid environment. At a relative humidity (RH) of 98%, a DDA of 73–98% was reached in 3–6 days, with the formation of chitosan of very high M_w of up to 4040 kDa. It was demonstrated that the energy usage of the milling/aging process at 50 °C was 3739 J g^{-1}, about ten times lower than that of solvothermal treatment, requiring 35 748 J g^{-1} for 3 h at 133 °C.

On the other hand, different applications require chitosan of low molecular weight (LMWC, M_w = 5 and 10 kDa), which, due to enhanced solubility even in neutral water, becomes more suitable for some biomedical and pharmaceutical uses or material synthesis, for example, drug and DNA delivery, grafting, crosslinking, fabrication of coatings.[238,239] Therefore, methods have been developed to promote the deacetylation of chitin concurrently to a controlled degree of depolymerisation. Mechanochemistry also proved to be effective in this case. One example reported that repeated ball milling cycles (up to 12) of mixtures composed of equivalent amounts of chitin and NaOH at a speed of 700 rpm resulted in the formation of chitosan with M_w and DAA distributed in the range of 7.7–12.8 kDa and 39.1–83.3%, respectively.[240] Control experiments with model compounds suggested that the ball mill-induced depolymerisation occurred through a base-catalysed hydrolysis mechanism without free radical or oxidative pathways. The proposed one-pot methodology exhibited various advantages including reduced environmental impact and base consumption (to about 1/10) as well as increased efficiency compared to multi-steps protocols. Curiously, in an almost parallel study, the ball-milling of α-chitin and kaolinite allowed depolymerisation without simultaneous deacetylation. It was also possible to isolate water soluble chitooligosaccharides (oligomers of *N*-acetyl-D-glucosamine) with a degree of polymerisation between 1 and 5.[241] Furthermore, by replacing kaolinite with H_2SO_4, chitin was mechano-catalytically converted to *N*-acetyl-D-glucosamine in a yield of 53%.[242]

Another method for the preparation of low-to-medium molecular weight chitosan started with the traditional extraction of chitin from shrimp shells *via* chemical deproteinization (NaOH, 80 °C, 3 h), demineralization (HCl, rt, up to 6 h), and discoloration processes. Thereafter, chitin was suspended in aq. NaOH (12.5 M), ultra-frozen at −83 °C (24 h), and finally heated at 115 °C (4–6 h). The resulting chitosan showed good solubility in acetic acid (1%), a low ash content (0.063%), molecular weight between 230 and 280 kDa, crystallinity index of *ca.* 40%, and DAAs above 90%.[243]

Combined chemical/biochemical approaches were also investigated. In one example, biological chitin (Bio-C) chitin was produced through the lactic acid fermentation (LAF) of shrimp waste in a packed bed column reactor with demineralization and deproteinization efficiencies of up to 92% and 94%, respectively, after 96 h.[244] Bio-C had a crystallinity index of 86% and M_w of 1200 kDa, both higher than that obtained *via* the classical chemical extraction method using the same shrimp shells. The subsequent deacetylation reaction was carried out by freeze–pump out–thaw (FPT) cycles, during which a reactor containing a suspension of chitin in 50% (w/v) NaOH was immersed in liquid nitrogen, degassed under vacuum, and allowed to thaw at ambient temperature for 6–7 times. The mixture was then heated at 90–100 °C for 5–120 min under stirring and chilled in liquid nitrogen. Chitosan was produced with a mid-range M_w (*ca.* 400 kDa) and a degree of acetylation (DA) of *ca.* 80%.

Other methods have been also explored in search for greener and safer chitin deacetylation procedures. For brevity, only a few of these are cited including steam explosion,[245] high temperature and pressure,[246] microwaving,[247] and intermittent water washings,[248] which generally afford chitosan with high DAA (70–90%) and M_w typically under 500 kDa.

4.3.1 Valorisation of chitosan. Chitosan is soluble in dilute acid aqueous solutions (up to 1 g L^{-1} at pH ≤ 6, for molecular weights up to *ca.* 400 kDa), where it is in the form of a cationic polysaccharide due to the easy protonation of its free amino groups.[249,250] This improved solubility has made chitosan far more accessible than chitin as a feedstock for the biomedical, pharmaceutical, food and textile industries and environmental applications in a variety of fields spanning from drug and gene delivery to heavy metal extraction, tissue engineering and development of anti-microbial and anti-tumour agents.[251,252] There are hundreds of papers published on chitosan. Thus, in an attempt to demonstrate the size of this subject and the vast topics that it encompasses, Table 10 summarizes a selected list of 43 review articles appearing in only the last five years (2015–2019) on the different uses of chitosan. The scenario

Table 10 A selected list of review articles on the uses of chitosan published in the last five years (2015–2019)

Entry	Publication year	Subject/application	Ref.
1	2015	Biomedical	256
2		Catalysis	258
3		Nanocomposites	260
4		Age prevention	262
5		Packaging	264
6		Organocatalysis	266
7		Wound healing	268
8		Drug delivery	270
9		Adsorption	272
10		Coatings	274
11		Food coating	276
12	2016	Wound healing	278
13		Biocomposites	280
14		Tissue engineering	282
15		Wastewater treatment	284
16		Tissue regeneration	286
17		Drug delivery	288
18		Water treatment	290
19	2017	Antimicrobial activity	292
20		Environmental applications	294
21		Food preservation	296
22		Functional materials	298
23	2017	Biomedical	257
24		Antimicrobial activity	259
25		Heavy metals adsorption	261
26		Antimicrobial wound healing	263
27		Adsorbent hydrogels	265
28	2018	Biomedical	267
29		Drug delivery	269
30		Hydrogels	271
31		Wastewater treatment	273
32		Antimicrobial activity	275
33		Drug delivery	277
34		Extraction modification	279
35		Tissue engineering	281
36		Packaging	283
37		Cosmetics	285
38		Tissue repair	287
39	2019	Chemical modification	289
40		Food technology	291
41		Composite coatings	293
42		Heavy metal adsorption	295
43		Nano composites	297

traces the features of a biopolymer fitting heterogeneous area, whose development requires challenging cross-disciplinary approaches. This also highlights how both an assessment of current applications and forecasting of future trends for the valorisation of chitosan are challenging tasks. However, in this section, examples of cutting-edge results and technologies are presented to help the reader appreciating the degree of progress achieved in the representative fields of chitosan-based hydrogels and adsorbent materials.

4.3.1.1 Chitosan-based hydrogels. Chitosan-based hydrogels (CBHs) have been widely recognised as biomaterials due to their excellent biocompatibility, biological activity, safety, and biodegradability. However, the ''Achilles' heel'' of CBHs limiting their practical applications is their poor mechanical strength. Approaches to overcome this issue have been proposed by coupling dissolution techniques specifically developed for chitosan with chemical modification. One example described the use of an unconventional new solvent system comprised of 4.5 wt% LiOH, 7 wt% KOH, and 8 wt% urea aqueous solution to solubilize chitosan by a freezing-thawing (FT) process (from −30 °C to rt).[253] ^{13}C NMR studies confirmed that dissolution took place due to the extended H-bonding network between the biopolymer and aq. alkali/urea, which formed macromolecular complexes that were stable at low temperature. Thereafter, casting of the chitosan alkaline solution on a glass plate followed by coagulation in warm water (40–60 °C) yielded a chitosan physical hydrogel. The mechanism for the formation of this gel was studied by SEM, TEM, AFM, and laser light scattering. Specifically, after initial parallel self-assembly parallel of the chitosan chains in the alkaline solution, heating induced the formation of nanofibers, which rapidly aggregated to construct a physical hydrogel through entanglement and cross-linking. Consequently, a homogeneous and compact network architecture was formed, woven by nanofibers with a mean diameter of 24 nm. The alkaline-solubilised chitosan was then chemically functionalised using epichlorohydrin [ECH, 2-(chloromethyl)oxirane], which was promptly subjected to nucleophilic displacement with both the –OH and –NH_2 functions of glucosamines units to form cross-linkages among the biopolymer chains. The reaction did not alter the mean diameter of the nanofibers (23 nm), but it reduced the pore size of the framework, indicating that cross-linking was compacting the structure. The mechanical properties such as compressive fracture stress and strain of both the physical and cross-linked gels reached 3.3 MPa and 85.9%, and 4.8 MPa and 77.7%, and were nearly 100 times better than that of the conventional gels fabricated from acid-solubilised chitosan (0.06 MPa and 12.2%), respectively. Additionally, its superior biocompatibility was proven, where *in vitro* cytotoxicity tests showed that myoblast C2C12 cells not only had 100% viability, but they could adhere, spread, and proliferate well on the new gel. In a follow-up study, the same alkali/urea solution was used to dissolve chitosan by the FT process. This was followed by chemical functionalisation using aq. 3-chloro-2-hydroxypropyltrimethyl ammonium chloride (CHPTAC; 60 wt%, 30 °C, 24 h). Both the –OH and –NH_2 functions of chitosan were alkylated by a polar tether ending with an ammonium salt, which imparted further aq. solubility and charge density to the resulting material (AC = alkylated chitosan) (Fig. 25).[254]

The intrinsic viscosity ($[\eta]$ = 6523 mL g^{-1}) and the ζ-potential (45 mV in deionized water) of AC certified its high charge density and typical electrostatic chain–chain repulsion effect. As a final step, stable polyelectrolyte complex (PEC) hydrogels were obtained *via in situ* polymerization of AC with different amounts of acrylic acid (12–45 wt%) in the presence of *N*,*N*′-methylene bisacrylamide (MBAA) as the initiator (60 °C, 3 d). Consequently, an AC/poly(acrylic acid) was fabricated (Fig. 18, bottom). Depending on the quantity of acrylic acid, PEC hydrogels show variable water contents (23–60 wt%), different tensile fracture nominal stress (1.99–5.96 MPa), Young's modulus (0.89–3.58 MPa), and deformation toughness (2.95–8.79 MJ m^{-3}). These tunable mechanical properties

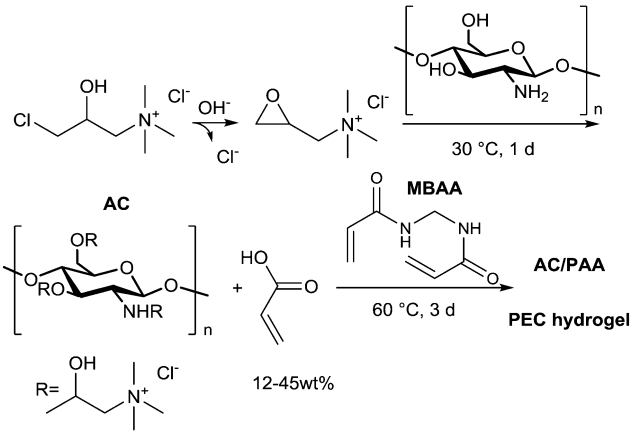

Fig. 25 Functionalisation of alkali-dissolved chitosan by CHPTAC followed by *in situ* polymerization of AC with acrylic acid.

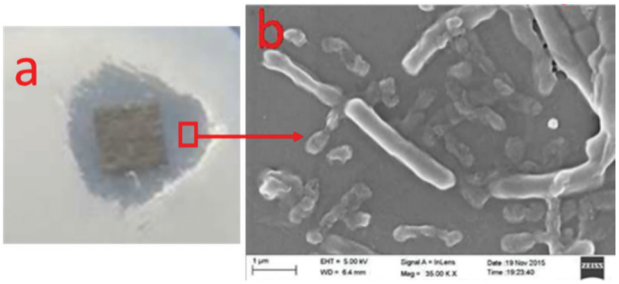

Fig. 26 (a) Photograph of the antimicrobial activity of the chitosan hydrogel nanocomposite (GO and IO-NPs) films against MRSA and (b) SEM images of the dead bacterial cells after treatment. Adapted from ref. 255 with permission from the American Chemical Society, Copyright 2016.

indicate the great potential of these gels for applications in load-bearing artificial soft tissues.

An approach to improve the antimicrobial properties of chitosan relies on the preparation of composites incorporating nanomaterials such as graphene oxide (GO, chemically exfoliated from oxidized graphite) and metals (Cu, Fe, Ni, and Zn) oxides. An example was described in the fabrication of chitosan-iron oxide coated graphene oxide hydrogels.[255]

The surface of GO was initially decorated with iron oxide nanoparticles (IO-NPs) by mixing an aq. solution of Fe^{3+}/Fe^{2+} in a 2 : 1 ratio with a dispersion of graphene oxide. SEM images confirmed the deposition of IO-NPs on the surface of the GO nanosheets. The suspension was then added to a chitosan solution (0.1 M AcOH and glycerol in a ratio of 3 : 2), stirred (1000 rpm, 2 h), neutralised (NaOH, 5 M), washed thoroughly, and casted on glass slides. After heating at 60 °C, the films of the nanocomposite hydrogels were peeled off and kept in a vacuum oven for further drying. During gel formation, glycerol acted as a chain extender and cross-linking agent by promoting electrostatic interactions with the $-NH_2/NH_3^+$ groups of chitosan and H-bonding with glucosamine units. The consequence of these aggregating forces and the increase in polar groups in the hydrogel matrix system conferred to the composite thermostability up to 274 °C, a swelling ratio in water of up to 75%, and tensile strength and modulus of 29 ± 2 and 2.3 ± 0.3 MPa, respectively, which were all well above that of a hydrogel of pure chitosan (180 °C, 45%, 17 ± 2 and 0.8 ± 0.1 MPa, respectively). Most importantly, the films exhibited antimicrobial activity against methicillin-resistant *Staphylococcus aureus* (MRSA), which is one of the most robust infecting bacterial strains in wounds and food products. At various bacteria concentrations (107, 106, and 105 CFU mL^{-1}), the iron oxide nanoparticles available on sharp GO nanosheet of sterilized films were able to penetrate the bacterial membrane, thereby inducing oxidative stress and disruption of the cells. Fig. 26 presents the FESEM analysis of the dead bacterial colony.

In a different approach, polydopamine was used as a cross-linker for a material comprised of chitosan and graphene oxide to generate a hydrogel with fast self-healing ability, good adhesiveness, and enhanced biodegradability.[299] Once chitosan was dissolved in AcOH and mixed with an aq. GO suspension (1 mg mL^{-1}), slow gelation occurred at rt in the presence of different amounts of dopamine (DA) and ammonium persulfate. A schematic chart of the procedure is shown in Fig. 27.

The presence of a typical –C=N stretching (Schiff base groups) supported the reaction of an *o*-quinone intermediate (from dopamine) with $-NH_2$ groups on chitosan. Also, Michael reactions could graft covalently quinoid species originating from DA monomers and oligomers to the chitosan backbone.

TEM and SEM showed an interconnected porous structure in the hydrogels with a pore size in the range of 120–500 μm containing nanofibrils plausibly originating from the penetration of PDA in the intercalated GO layers. The synergic effect of the three components of the nanocomposite was then proven. Using pig skin to simulate human dermis, the adhesive strength of the composite hydrogel was up to 0.95 MPa, 6 times higher than the gel without DA, while, the conductivity of the composite was up to 1.22 mS cm^{-1}, more than double that of the gel without GO. Additionally, experiments with HEF1 fibroblasts and cardiomyocytes demonstrated that an appropriate GO loading (lower than 0.75 mg mL^{-1}) was beneficial for cell proliferation and viability.

4.3.1.2 Chitosan as an adsorbent for water treatment. Chitosan is one of the most promising bio-sorbents for heavy metals in water. Due to its high degree of deacetylation, chitosan shows a metal chelating capability 5–6 times greater than chitin. Current research in this field is focused on maximising the exposure of the biopolymer functional groups to metals and fabricating chitosan nanomaterials easily recoverable from aqueous solutions. This approach has been followed in the preparation of magnetic nanobeads of chitosan *via* a solvothermal reduction protocol using a suspension of $FeCl_3{\cdot}6H_2O$, ethylene glycol, sodium acetate, and different amounts of chitosan powder (DAA = 80–95% M_w = 3.0 × 10^5 g mol^{-1}).[300] Both glycol and acetate salt were crucial for the formation of Fe_3O_4 instead of Fe_2O_3. After prolonged heating at 185 °C in an Ar atmosphere (48 h), cooling and washing, Fe_3O_4–chitosan composites (MCC)

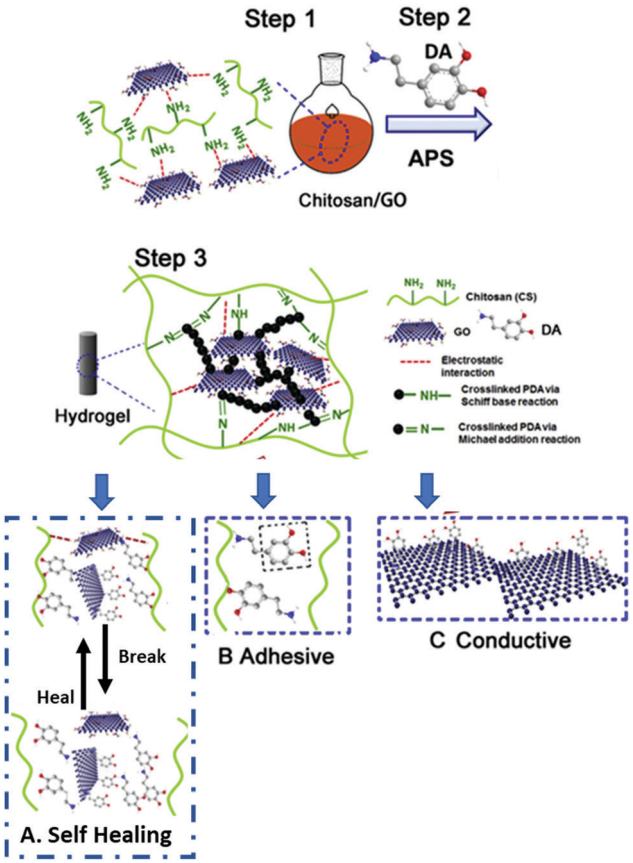

Fig. 27 Schematic protocol for the fabrication of the composite hydrogel from chitosan, GO, and DA. Electric interactions (step 1) and covalent bonding (step 3) between chitosan, GO and DA are highlighted, together with self-polymerization of DA. (A) Self-healing induced by non-covalent bonds between the catechol groups of DA and electrostatic interactions between chitosan and GO. (B) Self-adhesiveness imparted by the catechol groups. (C) Conductivity due to GO nanosheets. Adapted from ref. 299 with permission from Elsevier, Copyright 2017.

were obtained as spherical particles with an average diameter of *ca.* 200 nm, in which the Fe_3O_4 nanobeads were coated by a chitosan shell. The corresponding TEM images are shown in Fig. 28.

XPS spectra confirmed the presence of N-species, whose binding energy (398.0 eV) was consistent with the interaction of $-NH_2$ groups and Fe_3O_4, which likely stabilised the composite. Gel permeation chromatography (GPC) showed that the solvothermal treatment (185 °C) reduced the M_w of chitosan by about 4-fold to 9.05×10^4 g mol^{-1}. The Fe_3O_4–chitosan composites were selective for the adsorption of aq. Cu(II) with a maximum capacity of 129.6 mg g^{-1} of beads. Due to the fine particle size, the adsorption equilibrium was only 10 min, *ca.* 60-times shorter than that observed for analogous magnetic chitosan-cellulose beads. The saturation magnetization of the MCC material was up to 39.5 emu g^{-1}, which allowed its rapid recovery from aq. solution under a low magnetic field (<0.035 T, 30 s).

Although the blending of magnetic micro/nanoparticles with chitosan is efficient for the fabrication of easily separable composites, this method usually results in a decrease in the adsorption capacity of chitosan due to the strong interactions of the paramagnetic metal species on the biopolymer surface.[301] This has prompted researchers to investigate the preparation of magnetic chitosan through co-precipitation techniques. One example described a protocol in which three aq. solutions containing $FeCl_3 \cdot 6H_2O$, $FeCl_2 \cdot 4H_2O$ (40 °C), and NH_3/EtOH (1.10 v/v) were sequentially added to an aq. solution of chitosan to induce rapid precipitation.[302] The morphological characterization showed that the resulting composite was comprised of loose, porous blocks with a large pore size and particle size of around 10 μm. According to the mechanism for the formation of Fe_3O_4 nanoparticles in the presence of ammonia, the following steps occurred (Scheme 6).

Specifically, Fe^{3+} ions were expected to form a chelate complex with the hydroxyl group (–OH) of chitosan. The ions were limited in their mobility, but they were homogeneously distributed on the surface of the polymer. Thereafter, the addition of Fe^{2+} and $NH_3 \cdot H_2O$ produced uniformly distributed Fe_3O_4 nanoparticles. The presence of EtOH strongly reduced the solubility of chitosan, thereby inducing the fast precipitation and solidification of chitosan, which did not leave enough time for the densification of the final material. This was consistent with the observed porous blocks structure with large particles and explained the excellent adsorption capacity of the solid, which was up to 242.1 mg g^{-1} ($\sim$468.6 mg g^{-1} of chitosan) for aq. Cr(IV). The use of an intraparticle diffusion model confirmed that fast pore diffusion (the rate-controlling step) of aq. Cr(IV) ions in the composite occurred. Additionally, the saturation magnetization of the solid was 11.8 emu g^{-1}, which was large enough for good magnetic separation.

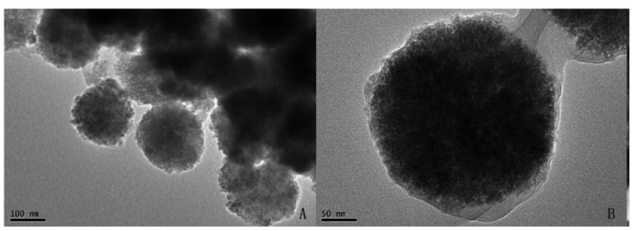

Fig. 28 TEM image of the Fe_3O_4–chitosan composite (mass ratio $FeCl_3 \cdot 6H_2O$: chitosan = 3 : 1). Adapted from ref. 300 with permission from the American Chemical Society, Copyright 2014.

$$NH_3 \cdot H_2O \rightleftarrows NH_4^+ + OH^-$$

$$Fe^{3+} + 3OH^- \rightarrow Fe(OH)_3$$

$$Fe^{2+} + 2OH^- \rightarrow Fe(OH)_2$$

$$2Fe(OH)_3 + Fe(OH)_2 \rightarrow Fe_3O_4 + 4H_2O$$

Scheme 6 Formation of Fe_3O_4 nanoparticles in the presence of aq. Ammonia.

Adsorbent materials are also largely employed for the selective removal of contaminant organic dyes released in wastewater effluents from the textile and food industries. A recent approach illustrated the fabrication of chitosan/polyamide nanofibers (CPNFs) using Forcespinning®, a technology based on high centrifugal forces.[303] Chitosan (DAA = 85%, M_w = 150 kDa) obtained from shrimp waste was solubilised in HCOOH in the presence of different amounts of commercial polyamide, and the mixture was subjected to 12 000 rpm (10 min) in dedicated Forcespinning equipment. The as-prepared CPNFs showed a diameter ranging from 100 to 500 nm, with a homogeneous and bead-free smooth structure. This study proved that these composites were effective for the removal of aq. model dyes such as Reactive Black 5 (RB5) and Ponceau 4R (P4R), with an adsorption capacity of up to 456.9 mg g^{-1} and 502.4 mg g^{-1}, respectively. The latter (capacity) was maximised under acidic conditions (pH = 1), where the protonated NH_2 groups of chitosan exerted the highest electrostatic attraction for the negatively charged dye molecules. Notably, the mixing of dye-loaded nanofibers with NaOH (0.5 M, 20 min, rt) allowed the release of dyes and the reuse of CPNFs for up to four times, without loss of adsorption capacity.

Another method for the preparation of a dye-adsorbent material was described starting from an aq. solution of chitosan (450 = kDa, DAA = 90.2%) in AcOH (0.2 wt%), to which aq. sodium tripolyphosphate ($Na_5P_3O_{10}$, NaTPP; 1.2 wt%), and $CaCl_2$ (0.1 M) were sequentially added at rt.[304] After the addition of TPP, the ionization degree of CS was 0.8 due to the increase in pH (from 3.5 to 6.0). This induced ionotropic gelation, leading to the spontaneous formation of CS-TPP nanocomplexes *via* intra- and inter-molecular linkages between the negatively charged TPP anions and positively charged CS. Then, upon the addition of $CaCl_2$, the CSTPP nanocomplexes served as a template to allow the in-situ mineralization of $Ca_2P_2O_7$ in the form of hybrid microflowers, which were recovered by centrifugation. Both SEM and TEM images showed the formation of CSTPP nanocomplexes and the final hybrid material, as presented in Fig. 29.

The microflowers had a diameter of 3–5 μm and were composed of well-defined 70 nm-thick nanosheets, with porous, hierarchical structures of plate-shaped microparticles. Further characterization proved that the material consisted of 23% CS–TPP nanocomplexes and 77% $Ca_2P_2O_7$ crystals. The microflowers displayed an adsorption capacity for Congo Red (CR, a model dye) of 520 mg g^{-1}, higher than that of many materials used to remove the same dye from aq. solutions. Indeed, the ζ-potential of the hybrid solid was 39.7 mV at pH 7.0, indicating that it had a positive surface charge suitable for the electrostatic attraction of CR.

4.4 Hydroxyapatite

Hydroxyapatite (HA), which has the formula $Ca_{10}(PO_4)_6(OH)_2$, is among the most attractive materials as bone fillers and scaffolds for biomedical implants, not only because its chemical composition resembles the mineral component of bone tissue, but also due to its bioactivity, biocompatibility,

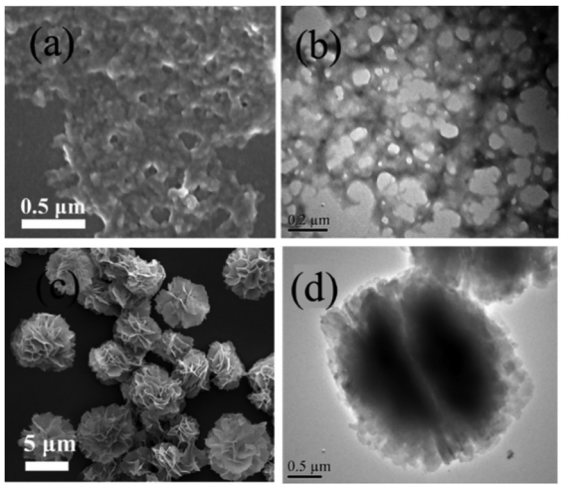

Fig. 29 SEM and TEM images of chitosan–TPP nanocomplexes (a and b), and hybrid microflowers (c and d), respectively. Adapted from ref. 304, with permission from the American Chemical Society, Copyright 2014.

high osteoconductive and/or osteo-inductive non-toxicity.[305] Although HA can be synthesised by precipitation, hydrolysis, hydrothermal (sol–gel), and microwave-assisted procedures using commercial phosphate salts,[306] the literature exhibits an increasing interest for biogenic hydroxyapatite (bio-HA) obtained from natural resources, particularly biowaste. Extraction methods of bio-HA have been described starting from many different residues from the processing of animal feedstocks of both terrestrial and marine origin.[307] Consistent with the aim of this review, here we focus on the preparation and applications and bio-HA from fish waste.

Fish bones are considered one of the major biological sources of calcium phosphate, being constituted by *ca.* 70% of inorganic matter, the majority of which is hydroxyapatite and minerals.[308] This subject has been recently examined in a review paper describing both the extraction of bio-HA and its potential applications in the biomedical field.[309] The resulting scenario highlighted how calcination was by far the most common procedure for the processing of a variety of fish bones derived from anchovy, barramundi, carp, cuttlefish, croaker, cod, conger eel, flat fish, amberjack, mackerel, sardine, shark, sierra, sea bass, sea bream, sword fish, trigger fish and tuna. Fig. 30 presents a flow chart outlining the basic operations for the thermal extraction of hydroxyapatite.

The treatment generally required the removal of residual proteins through washing and alkaline hydrolysis followed by high temperature calcination in the range of 600–1300 °C. It should be noted that this method produced either HA and β-TCP [β-tricalcium phosphate, β-$Ca_3(PO_4)_2$], with proportions depending on the nature of the starting fish bones and the temperature. However, with variations, increasing amounts of β-TCP were noticed at $T \geq 900$ °C. For example, calcination of tuna and sword fish bones (from North Atlantic) at 600 °C and 950 °C afforded HA and a mixture of HA/β-TCP (87/13, wt%), respectively,[310] while, starting from roho labeo fish (an Indian carp species), a bio-hydroxyapatite (HA) was produced with

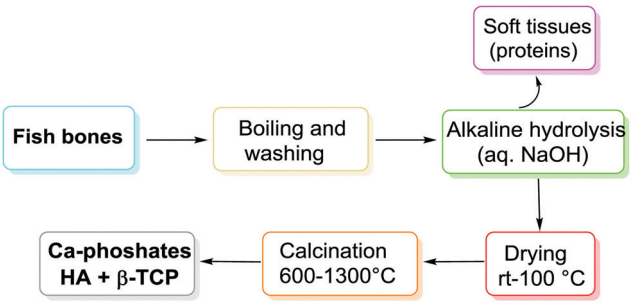

Fig. 30 Flowchart of the basic operations for the thermal extraction of hydroxyapatite from fish bones.

stability up to 1000 °C.[311] These differences were explained considering that naturally derived Ca-phosphates contain variable amounts of trace elements (Na, Cu, Fe, Mg, Mn, K, Sr, Zn, *etc.*), which alter the Ca/P ratio with respect to the stoichiometric value of synthetic HA and β-TCP solids (Ca/P = 1.67 and 1.50, respectively). Fish-derived phosphates also contain halide (Cl^- and F^-), SO_4^{2-}, and CO_3^{2-} species. Both cations and anions are reported to improve the material performance with beneficial effects on bioactivity and osteoblast growth.[312,313]

Other preparation protocols more often combine the initial calcination of fish bones with subsequent hydrothermal alkaline treatments (140–220 °C, NaOH or urea) to control the size and porosity of the nanometric HA particles. One example described the extraction of a mixture of whitlockite [$Ca_3(PO_4)_2$] and HA *via* the direct ablation of blue shark fish bone in the presence of a compressed gas jet, demonstrating that calcium phosphates could be obtained even without previous calcination.[314]

4.4.1 Bio-hydroxyapatite-based materials. The osteogenic activity of natural HA is crucial to assess its biocompatibility as a material for human bone implants. Accordingly, a recent work compared three biogenic HAs derived from the cheap fish bones of rainbow trout, cod and salmon.[315] After selecting the spine part, the solids were boiled in water, alkali-treated (NaOH, 1%), washed, dried, and ball milled (30 Hz, 2 min). The recovered powders were then calcined at 650 °C for 5 h. XRD and EDS characterisation proved the formation of HA with an average particle size of *ca.* 100, 250 and 200 nm from the trout, cod and salmon bones, respectively, and detected trace amounts of Mg^{2+} and Na^+ in all cases. However, a relevant difference was observed in the CO_3^{2-} substitution, which was present only for the trout- and salmon-derived materials, and likely responsible for their Ca/P ratio of 1.47 and 1.51, respectively, lower than that of the synthetic HA (1.67). The carbonate substitution proved critical for osteointegration, where MTT assays on MC3T3-E1 cells demonstrated the viability of osteoblasts for the trout and salmon HAs (200 μg mL^{-1}, 3 days, and 7 days incubation), but not for the corresponding solid obtained from cod. Notably, the natural apatite in the human body contains significant amounts of carbonate and trace elements, which promote the biological activity of osteoblasts.[316]

Another key factor for using HA in bone implant fabrication is its mechanical behaviour, particularly its response to sintering. This aspect together with bioactivity tests have been investigated for both a biphasic material comprised of hydroxyapatite/β-tricalcium phosphate (HAp/β-TCP) and a single-phase hydroxyapatite prepared from (Atlantic) cod fish bones.[317] These materials (CB and CB-Ca) were obtained *via* the calcination of fish bones at 700 °C, and after their treatment with aq. $CaCl_2$, respectively. The calcined solids were treated in a high-energy planetary ball mill (200 rpm, 24 h), pelletized, and sintered over a range of temperatures between 900 °C and 1250 °C. XRD confirmed that the CB powder was comprised of HA (73.2 wt%) and β-TCP (27.8 wt%), while CB-Ca was pure HA. The sintering behaviour was examined by SEM and illustrated in Fig. 31(a and b) for the CB sample.

After calcination and milling, the majority of the particles were smaller than 100 nm (a), while after sintering at 1250 °C, the grain sizes were in the order of 1 μm or less (b). The bioactivity was then investigated by soaking the pelletized solids in SBF (simulated body fluid). CB yielded the formation of a network of crystals in an irregular lattice, which, after only 3 days, covered most of the surface of the pellet (SEM image: Fig. 31c). By contrast, CB-Ca did not change within 7 days and it required 4 weeks in SBF to show evidence of the smaller grains forming and fusing into each other (SEM image: Fig. 31d). This provided clear evidence that the biphasic HAp/β-TCP material was comparably much more bioactive than single-phase HA.

Additionally, other tests of *in vitro* cytotoxicity on SaOs-2 cells and haemolysis confirmed that both phosphate CB and CB-Ca derived from cod fish bones were suitable as biomaterial components.

Fish scales (FS) rather than fish bones have also been investigated as a source of biogenic hydroxyapatite. Instead of calcination at high temperature, FS-waste required relatively mild treatment consisting of deproteinization with HCl (0.1–1 M, rt) and NaOH (5–50 wt%, 70–100 °C), and/or heating in boiling water to isolate hydroxyapatite.[318,319] In the

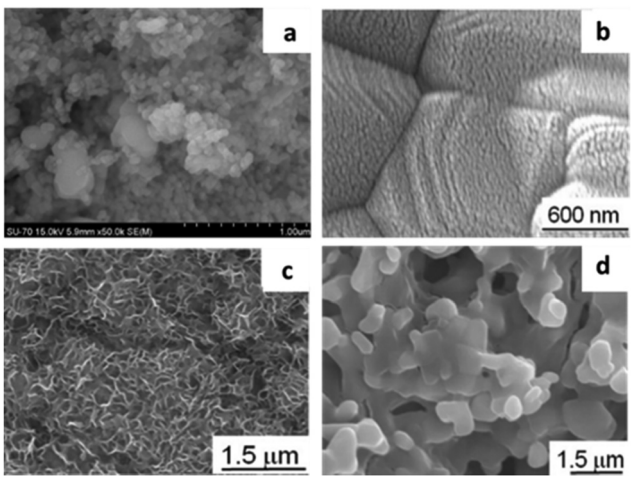

Fig. 31 SEM image of: (a) CB powder after calcination at 700 °C and ball milling; (b) CB powder after sintering at 1250 °C/2 h; (c) CB pellet after 3 days in SBF; and (d) CB-Ca pellet after 28 days in SBF. Adapted from ref. 317 with permission from Elsevier, Copyright 2015.

$$CaCO_3 \xrightarrow{\text{calcination}} CaO + CO_2$$

$$3\,Ca_3(PO_4)_2 + CaO + H_2O \longrightarrow Ca_{10}(PO_4)_6(OH)_2 \quad (a)$$

$$10\,CaO + K_2HPO_4 + 4H_2O \longrightarrow Ca_{10}(PO_4)_6(OH)_2 + 12\,KOH \quad (b)$$

Scheme 7 Preparation of HA from CaO and two phosphorous salts (a and b).

Table 11 Preparation and applications of fish-derived hydroxyapatite

Entry	Fish bone source	Prepared material	Ref.
1	Perch	Scaffold for bone graft material	323
2	Brazilian river fish	Bone tissue engineering	324
3	Cod	Additive to building material	325
4	Lizard fish	Stabilizer of heavy metals in fly ash	326
5	Whitemouth croaker bone	Bio-material	327
6	Cuttlefish	Cancellous bone regeneration	328
7	Tuna	Bio-material	329
8	Carp (fish scale)	Electrochemical sensing platforms	330
9	Tuna	Adsorbent for dye removal	331

first example, bio-HA extracted from FS of *Tilapia nilotica* proved to be 4-fold more efficient than commercial hydroxyapatite for the selective adsorption and removal of Se(IV) in the purification of drinking water. Even more remarkable were the properties of HA obtained from the FS of golden carp (*Probarbus jullieni*) with respect to synthetic HA, where the bio-HA improved the formation of tilapia apatite during incubation in simulated body fluid, and it showed a higher osteoblast-like cell adhesion on its surface, thereby proving its potential as a bioactive material for bone scaffolds and tissue regeneration. This behaviour was correlated to the results of the SEM, TEM, and EDX analyses, showing that the bio-derived hydroxyapatite had a larger surface area, higher Ca content, and higher surface roughness than synthetic HA, and it was comprised of rod-shaped (50 nm in diameter) and flat-plate (*ca.* 20 × 100 nm, width × length) nanocrystals, respectively.

Among the fish waste, sea- and mussel-shells and cuttlefish bone have been reported as sources for the preparation of bio-HA.[320–322] However, in this case, the starting shells and bone are calcined to obtain CaO, which in turn, is converted to HA by reaction with phosphorous salts [either $Ca_3(PO_4)_2$ or K_2HPO_4, Scheme 7]. The final HA product is therefore a synthetic material.

4.4.2 Additional examples. Besides the examples discussed in Sections 4.4 and 4.4.1, other relevant recent studies on fish-derived hydroxyapatite are summarized in Table 11.

5 Environmental impact of the valorisation of biowaste

Beyond the challenges associated with using unconventional resources as marine biowaste, a sustainability analysis on the valorisation of residual biomass should include the evaluation of the environmental impact of proposed treatment protocols according to the tools offered by the life cycle assessment (LCA) and other calculation methods. In this section, this subject will be introduced starting from model case studies selected from the current literature. However, it should be noted that a very little information is available related to the fish processing chain. A recent investigation on the organic fraction of municipal solid waste (OFMSW) offers a starting point to approach this problem.[332] After the generation of bio-pulp from OFMSW, lab- or pilot-scale experiments were used to explore many different scenarios including the production of: (i) biogas through anaerobic digestion followed by combustion or biological upgrading; (ii) single cell protein through the use of biogas to grow methane-oxidizing bacteria; and (iii) bio-succinic acid and bio-lactic acid through fermentation processes. A consequential life cycle assessment (CLCA) showed net environmental savings in the investigated indices from all evaluated platforms, indicating advantages from equivalent products they should substitute.

Another analysis described a model for circular bioresource management, in which the organic fraction of household waste (OFHW) was reallocated from combustion to co-digestion at manure- and sludge-based biogas plants producing natural organic biofertilizer products and energy.[333] The LCA study, performed in accordance with the international standards ISO 14040-44, was based on a functional unit covering an area of 2512 km^2 with 32 municipalities located in North Zealand (Denmark) producing 132 Gg dry weight biowaste per year. A net increase in renewable electricity of 39% was demonstrated at the expense of a reduction in heat production of 8%, corresponding to a greenhouse gas emission reduction of 100 kg CO_{2eq} per tonne of dry weight biowaste treated, *i.e.* a 10% reduction in total CO_2 emission. Moreover, both the depletion of fossil resources and impact on freshwater and marine eutrophication decreased by 11%, 4.8 t P eq. and 3.6 t N eq., respectively. In a totally different approach aimed to design green protocols for biomass waste valorisation, the catalytic conversion of model sugar-containing food biowaste (based on bread, rice, and fruits from Hong Kong airport) was explored under a total of 8 different experimental conditions, including combinations of solvents, catalysts, temperature and time.[334] The environmental performance of each procedure was compared by an LCA analysis (ISO 14040 standard) developed for the production of hydroxymethylfurfural (HMF), one of the most versatile platform chemicals of renewable origin. The investigation proved that the less polluting process was carried out at 140 °C for 30 min in the presence of a water-acetone medium and $AlCl_3$ as the catalyst.

One last case study examined here reported a comparative environmental assessment between a valorisation process of fish biowaste to produce fishmeal and oil, and different scenarios for the management of the same waste including composting, incineration and landfilling.[335] The Port of Vigo was selected as a representative case, which is one of the biggest fishing ports in Spain (Galicia), with an amount of

Table 12 Summary of the results for net EF and net LCA

Scenario	Net EF (ha/tonnes)	Net LCA (kg $CO_{2eq.}$/tonnes)
Fish waste valorization (fishmeal and oil)	−2.94	5.14
Composting	7.73	256.84
Incineration	8.16	−95.33
Landfilling	7.86	−2.27

landed fish of approximately 60.000 tonnes per year,[336] and related fish by-products used in the production of fishmeal and oil destined to animal feeds. Both EF (environmental footprint) and Life Cycle Impact Assessment (LCIA) were carried out, the first one through the conversion of mass flow into bio-productive areas, while the second approach considered the two most common categories used for the investigated scenarios, *i.e.* global warming and acidification potential. The salient results are summarized in Table 12.

Since EF is focused on the consumption of resources, while LCA is specific for the environmental impact of each phase or process, these two methods identified different situations, with opposite results. Indeed, valorisation was the best option for EF since both fishmeal and oil can be used in aquaculture, thereby reducing the need for fishing activity oriented to aquaculture feed and the pressure on marine resources. On the contrary, incineration and landfilling were the favoured routes for LCIA because especially the development of new strategies for waste treatment/management minimizes the major environmental impacts of these operations, and usually allows biomass recovery or energy reuse.

Overall, these investigations exemplify not only the vast and different scales at which the 'waste as a resource' paradigm can be analysed for its global impact on the environment, but also the further complexity of evaluation methods when they are extended using environmental/economic metrics for the market, requiring biowaste-derived end-products/materials and the development of new technologies devoted to this purpose.[337] Therefore, the results are largely subjected to the efficiency of the chosen biorefining platform, specifically to the degree of integration of different treatment technologies of biowaste with the market penetration of the obtained products, materials, and by-products.

6. Concluding remarks

The extensive discussion presented herein clearly highlights how fish waste should no longer be considered a problem or a worthless discard to be disposed of. Indeed, as part of the global trend towards the circular economy, fish waste represents a resource for a large variety of applications in the areas of food, nutraceuticals, medicine, electrical, optical and other functional materials. Aspects related to the bio-compatibility of the products obtained in this context are especially advantageous for high value use in human health. Key contributions are also expected to arise from the exploitation of other marine biomass, *e.g.* jelly fish, the productive use of which is attracting increasing attention.

Notwithstanding the huge potential emerging from these strategies, the input of fish waste biorefining to the sustainable growth of marine environments (blue growth) and to the needs of society is still in many respects in its infancy due to the limited technological transfer from academic scientific research to commercial market applications. Crucial to the advancement of the sector will be innovation through integration, *i.e.* the capability of integrating the best available experience (technology, skills, manufacturing methods, production samples, development of processes plus product descriptions and services) in plants with multiple inputs/outputs designed to select, collect and upgrade different types of fish discard by exploiting the economy of scale.

It is hoped that efforts made to collect and analyze the data, information, interpretations and insights in this review may be beneficial not only to inspire scientists and technologists sharing interests in the sustainable development of fishery and aquaculture, but also to inform policy makers regarding effective approaches for the conscious management of activities at sea and preservation of the coastal environment.

Conflicts of interest

There are no conflicts to declare.

Acknowledgements

MS acknowledges the receipt of a fellowship from the OECD Co-operative Research Programme, Biological Resource Management for Sustainable Agricultural Systems in (2019 contract no. JA00101597), for funding part of his sabbatical leave at the University of Sydney, Australia. RL acknowledges the Regione Veneto (project 2120-4-11-2018) for funding his two-months stay at Ca' Foscari University of Venice.

Notes and references

1 J. Cai and N. Hishamunda FAO Aquaculture Newsletter 2013, **51**, 34–36, and FAO Aquaculture Newsletter 2018, **58**, 49–51.
2 The state of the World fisheries and aquaculture, meeting the sustainable development goals, Food and Agriculture Organization of the United Nations, Rome 2108, ISBN 978-92-5-130562-1.
3 G. Caruso, *J. Fisheriessciences.com*, 2016, **10**, 12–015.
4 J. Guillen, S. J. Holmes, N. Carvalho, J. Casey, H. Dörner, M. Gibin, A. Mannini, P. Vasilakopoulos and A. Zanzi, *Sustainability*, 2018, **10**, 900.
5 D. Pauly and D. Zeller, *Nat. Commun.*, 2016, **7**, 10244, DOI: 10.1038/ncomms10244.
6 D. Zeller, T. Cashion, M. Palomares and D. Pauly, *Fish Fish*, 2018, **19**, 30–39.

7 E. Sala, J. Mayorga, C. Costello, D. Kroodsma, M. L. D. Palomares, D. Pauly, U. R. Sumaila and D. Zeller, *Sci. Adv.*, 2018, **4**, eaat2504.
8 https://www.abc.net.au/015-05-21/australia-commercial-fish-catch-bigger-than-official-reports/6485134, last access April 25th, 2019.
9 C. Xu, M. Nasrollahzadeh, M. Selva, Z. Issaabadi and R. Luque, *Chem. Soc. Rev.*, 2019, **48**, 4791–4822.
10 A. E. Ghaly, V. V. Ramakrishnan, M. S. Brooks, M. S. Budge and D. Dave, *J. Microb. Biochem. Technol.*, 2013, **5**, 107–129.
11 M. B. Esteban, A. J. García, P. Ramos and M. C. Márquez, *Waste Manag.*, 2007, **27**, 193–200.
12 F. M. Kerton, Y. Liu, K. W. Omari and K. Hawboldt, *Green Chem.*, 2013, **15**, 860–871.
13 K. Jayathilakan, K. Sultana, K. Radhakrishna and A. S. Bawa, *J. Food Sci. Technol.*, 2012, **49**, 278–293.
14 S. Maqsood, S. Benjakul and A. Kamal-Eldin, *Recent Pat. Food, Nutr. Agric.*, 2012, **4**, 141–147.
15 N. Yan and X. Chen, *Nature*, 2015, **524**, 155–157.
16 *From Waste to Value: Valorisation Pathways for Organic Waste Streams in Circular Bioeconomies*, ed. A. Klitkou and A. Fevolden, Taylor & Francis, 2019.
17 B. Iñarra, C. Bald, M. Cebrián, L. T. Antelo, A. Franco-Uría, J. A. Vázquez, R. I. Pérez-Martín and J. Zufía, What to Do with Unwanted Catches: Valorisation Options and Selection Strategies, in *The European Landing Obligation*, ed. S. S. Uhlmann, C. Ulrich, S. J. Kennelly, Springer, Cham, 2019.
18 K. de la Caba, P. Guerrero, T. Si Trung, M. Cruz-Romero, J. P. Kerry, J. Fluhr, M. Maurer, F. Kruijssen, A. Albalat, S. Bunting, S. Burt, D. Little and R. Newton, *J. Clean Prod.*, 2019, **208**, 86–98.
19 C. Lopes, L. T. Antelo, A. Franco-Uría, A. A. Alonso and R. Pérez-Martín, *Waste Manag.*, 2015, **46**, 103–112.
20 http://www.iffo.net, last access May 24, 2019.
21 A. E. Ghaly, D. Dave, S. Budge and M. S. Brooks Am, *J. Appl. Sci*, 2010, **7**, 859–877.
22 H. H. Huss, FAO Fisheries Technical Paper 348, Rome, 1995, ISBN 92-5-103507-5.
23 P. Dalgaard, H. L. Madsen, N. Samieian and J. Emborg, *J. Appl. Microbiol.*, 2006, **101**, 80–95.
24 F. Shahidi and Y. Zhong, *Chem. Soc. Rev.*, 2010, **39**, 4067–4079.
25 N. V. Toan, C.-H. Ng, K. N. Aye, T. S. Trang and W. F. Stevens, *J. Chem. Tech. Biotechnol.*, 2006, **81**, 1113–1118.
26 S. Sampels, *J. Food Process. Preserv.*, 2015, **39**, 1206–1215.
27 BBI work plan 2018, topic identifier BBI.2018.SO1.R1: http://ec.europa.eu/research/participants/portal/desktop/en/opportunities/h2020/topics/bbi.2018.so1.r1.html, last access January 24th, 2019.
28 J. Dyerberg and H. O. Bang, *Lancet*, 1979, **2**(8140), 433–435.
29 H. Tapiero, G. N. Ba, P. Couvreur and K. D. Tew, *Biomed. Pharmacother.*, 2002, **56**, 215–222.
30 C. H. S. Ruxton, S. C. Reed, M. J. A. Simpson and K. J. Millington, *J. Hum. Nutr. Dietet.*, 2004, **17**, 449–459.
31 R. T. Holman, *J. Nutr.*, 1998, **128**, 427S–433S.
32 W. E. M. Lands, in *Fish and Human Health*, Academic Press, Inc., Orlando, 1986.
33 *Omega-3 fatty acids: chemistry, nutrition and health effects, ACS Symposium Series 788*, ed. F. Shahidi and J. Finley, American Chemical Society, Washington, DC, 2001.
34 https://www.grandviewresearch.com/press-release/global-omega-3-market last access June 16, 2019.
35 https://www.mordorintelligence.com/industry-reports/fish-oil-omega-3-market last access June 16, 2019.
36 W. S. Harris, in *Omega-3 fatty acids, Encyclopedia of Dietary Supplements*, ed. P. M. Coates, J. M. Betz, M. R. Blackman, G. M. Cragg, M. Levine, J. Moss, J. D. White, Informa Healthcare, London and New York, 2nd edn, 2010, pp. 577–586.
37 T. Sun, W. Prinyawiwatkul and X. Zhimin, *J. Am. Oil Chem. Soc.*, 2006, **83**, 291–296.
38 C. Tyburczy Srigley and J. I. Rader, *J. Agric. Food Chem.*, 2014, **62**, 7268–7278.
39 M. I. Gurr, *Biochem. Soc. Trans.*, 1987, **15**(3), 336–338.
40 V. Fournier, F. Destaillats, P. Juaneda, F. Dionisi, P. Lambelet, J. L. Sebedio and O. Berdeaux, *Eur. J. Lipid Sci. Technol.*, 2006, **108**, 33–42.
41 C. Sciotto and S. A. Mjos, *Lipids*, 2012, **47**, 659–667.
42 S. Sathivel, W. Prinyawiwatkul and J. Huang, *J. Food Eng.*, 2008, **84**, 187–193.
43 P. J. Bechtel and A. C. M. Oliveira, *J. Food Sci.*, 2006, **71**, S480–S485.
44 K. Miyashita, R. Takahashi, T. Nishiyama, K. Fukunaga, M. Hosokawa and R. Noguchi, *J. Agric. Food Chem.*, 2004, **52**, 2372–2375.
45 V. Šimat, J. Vlahovic, B. Soldo, D. Skroza, I. Ljubenkov and M. Generalic, *Foods*, 2019, **8**, 125.
46 FAO, The production of fish meal and oil, Fisheries technical paper, 142, Rev.1, Rome, 1986.
47 H. Nygaard, Standard Norwegian fishmeal and fish oils process, heat treatment requirements, report 33/2010, Nofima Marine, Norway.
48 K. Chakraborty and D. Joseph, *J. Agric. Food Chem.*, 2015, **63**, 998–1009.
49 S. H. Suseno, N. Fitriana, A. M. Jacoeb and Saraswati, *Orient. J. Chem.*, 2015, **31**, 2507–2514.
50 R. Morales-Medina, G. De Leon, M. Munio, A. Guadix and E. Guadix, *J. Food Eng.*, 2016, **183**, 16–23.
51 M. L. Monte, M. L. Monte, R. S. Pohndorf, V. T. Crexi and L. A. A. Pinto, *Eur. J. Lipid Sci. Technol.*, 2015, **117**, 829–836.
52 C. Karahadian and R. C. Lindsay, *J. Am. Oil Chem. Soc.*, 1989, **66**, 953–960.
53 D. A. S. B. de Oliveira, M. G. Minozzo, S. Licodiedoff and N. Waszczynskyj, *Food Chem.*, 2016, **207**, 187–194.
54 P. Lembke, Omega 3 Directory, *Bioseutica*, 2011, 6–8.
55 R. Ciriminna, F. Meneguzzo, R. Delisi and M. Pagliaro, *Sustainable Chem. Pharm.*, 2017, **5**, 54–59.
56 https://www.kdpharmagroup.com; last access June 20, 2019.
57 P. Rossi, N. R. Grosso, M. C. Pramparo and V. Nepote, Fractionation and concentration of omega-3 by molecular distillation. Eicosapentaenoic Acid: Sources, Health Effects and Role, in *Disease Prevention*, ed. N. Gotsiridze-Columbus, Nova Science Pub., Inc., 2007, pp. 177–203.

58 https://www.kdpharmagroup.com/en/kdpharma/kd-pur-technology, last access June 20, 2019.
59 J. Neubronner, J. P. Schuchardt, G. Kressel, M. Merkel, C. von Schacky and A. Hahn, *Eur. J. Clin. Nutr.*, 2011, **65**, 247–254.
60 E. N. Frankel, *Lipid Oxidation*, Oily Press Lipid Library Series, Elsevier, 2nd edn, 2014.
61 F. Shahidi and P. Ambigaipalan, *J. Funct. Foods*, 2015, **18**, 820–897.
62 P. Kaushik, K. Dowling, C. J. Barrow and B. Adhikari, *J. Funct. Foods*, 2015, **19**, 868–881.
63 F. Shahidi, Extraction and Measurement of Total Lipids, *Current Protocols in Food Analytical Chemistry*, 2003, ch. 1, vol. 7, pp. D1.1.1–D1.1.11.
64 P. Mercer and R. E. Armenta, *Eur. J. Lipid Sci. Technol.*, 2011, **113**, 539–547.
65 S. C. Hathwar, B. Bijinu, A. K. Rai and B. Narayan, *Appl. Biochem. Biotechnol.*, 2011, **164**, 115–124.
66 O. J. Catchpole, S. J. Tallon, W. E. Eltringham, J. B. Grey, K. A. Fenton, E. M. Vagi, M. V. Vyssotski, A. N. MacKenzie, J. Ryan and Y. Zhu, *J. Supercrit. Fluids*, 2009, **47**, 591–597.
67 F. Sahena, I. S. M. Zaidul, S. Jinap, M. H. A. Jahurul, A. Khatib and N. A. N. Norulaini, *J. Food Eng.*, 2010, **99**, 63–69.
68 N. Rubio-Rodríguez, S. M. de Diego, S. Beltrán, I. Jaime, M. T. Sanz and J. Rovira, *J. Food Eng.*, 2012, **109**, 238–248.
69 A. P. Antunes Corrêa, C. Arantes Peixoto, L. A. Guaraldo Goncalves and F. A. Cabral, *J. Food Eng.*, 2008, **88**, 381–387.
70 R. Davarnejad, K. M. Kassim, A. Zainal and S. A. Sata, *J. Chem. Eng. Data*, 2008, **53**, 2128–2132.
71 S. Ferdosh, M. Z. I. Sarker, N. Norulaini, N. A. Rahman, M. J. H. Akanda, K. Ghafoor and M. O. A. Kadir, *J. Aquat. Food Prod. Technol.*, 2016, **25**, 230–239.
72 B. Nagy and B. Simandi, *J. Supercrit. Fluids*, 2008, **46**, 293–298.
73 B. L. F. Lopes, A. P. Sánchez-Camargo, A. L. K. Ferreira, R. Grimaldi, L. C. Paviani and F. A. Cabral, *J. Supercrit. Fluids*, 2012, **61**, 78–85.
74 T. T. Nguyen, W. Zhang, A. R. Barber, P. Su and S. He, *J. Agric. Food Chem.*, 2015, **63**, 4621–4628.
75 Y. Fang, S. Gu, S. Liu, J. Zhang, Y. Ding and J. Liu, *RSC Adv.*, 2018, **8**, 2723–2732.
76 V. V. Ramakrishnan, A. E. Ghaly, M. S. Brooks and S. M. Budge, *Enzyme Eng.*, 2013, **2**, 2.
77 M. Linder, J. Fanni and M. Parmentier, *Mar. Biotechnol.*, 2005, **15**, 70–76.
78 G. A. Gbogouri, M. Linder, J. Fanni and M. Parmentier, *Eur. J. Lipid Sci. Technol.*, 2006, **108**, 766–775.
79 W. Routray, D. Dave, V. V. Ramakrishnan and W. Murphy, *Waste Biomass Valorization*, 2018, **9**, 2003–2014.
80 M. Letisse, M. Rozieres, A. Hiol, M. Sergent and L. Comeau, *J. Supercrit. Fluids*, 2006, **38**, 27–36.
81 N. T. Dunford, F. Temelli and E. LeBlanc, *J. Food Sci.*, 1997, **62**, 289–294.
82 K. Ivanovs and D. Blumberga, *Energy Procedia*, 2017, **128**, 477–483.
83 M. Alkio, C. Gonzalez, M. Jäntti and O. Aaltonen, *J. Am. Oil Chem. Soc.*, 2000, **77**, 315–321.
84 H.-S. Roh, J.-Y. Park, S.-Y. Park and B.-S. Chun, *Biotechnol. Bioprocess Eng.*, 2006, **11**, 496–502.
85 F. Gironi and M. Maschietti, *Chem. Eng. Sci.*, 2006, **61**, 5114–5126.
86 (*a*) C. Vizetto-Duarte, H. Pereira, C. Bruno de Sousa, A. Pilar Rauter, F. Albericio, L. Custodio, L. Barreira and J. Varela, *Nat. Prod. Res.*, 2015, **29**, 1264–1270; (*b*) J. L. Harwood, *Biomolecules*, 2019, **9**, 708.
87 I. A. Adeoti and K. Hawboldt, *Biomass Bioenergy*, 2014, **63**, 330–340.
88 F. Preto, F. Zhang and J. Wang, *Fuel*, 2008, **87**, 2258–2268.
89 A. B. Fadhil, A. I. Ahmed and H. A. Salih, *Fuel*, 2017, **187**, 435–445.
90 G. I. Martins, D. Secco, L. K. Tokura, R. A. Bariccatti, B. Dresch Dolci and R. Ferreira Santos, *Renewable Sustainable Energy Rev.*, 2015, **42**, 234–239.
91 D. Madhu, B. Singh and Y. C. Sharma, *RSC Adv.*, 2014, **4**, 31462–31468.
92 D. Madhu, R. Arora, S. Sahani, V. Singh and Y. C. Sharma, *J. Agric. Food Chem.*, 2017, **65**, 2100–2109.
93 M. Vijaykrishnaraj and P. Prabhasankar, *RSC Adv.*, 2015, **5**, 34864–34877.
94 N. R. A. Halim, H. M. Yusof and N. M. Sarbon, *Trends Food Sci. Technol.*, 2016, **51**, 24–33.
95 L. Mora and M. Hayes, *J. Agric. Food Chem.*, 2015, **63**, 1319–1331.
96 J. Zamora-Sillero, A. Gharsallaoui and C. Prentice, *Mar. Biotechnol.*, 2018, **20**, 118–130.
97 S. Y. Lee and S. J. Hur, *Food Chem.*, 2017, **228**, 506–517.
98 F. Mahmoodani, M. Ghassem, A. S. Babji, S. M. Yusop and R. Khosrokhavar, *J. Food Sci. Technol.*, 2014, **51**, 1847–1856.
99 H. Fujita, T. Yamagami and K. Ohshima, *Nutr. Res.*, 2001, **21**, 1149–1158.
100 T. Kawasaki, E. Seki, K. Osajima, M. Yoshida, K. Asada, T. Matsui and Y. Osajima, *J. Hum. Hypertens.*, 2000, **14**, 519–523.
101 P. J. García-Moreno, F. J. Espejo-Carpio, A. Guadix and E. M. Guadix, *J. Funct. Foods*, 2015, **18**, 95–105.
102 M. Chalamaiah, B. Dinesh kumar, R. Hemalatha and T. Jyothirmayi, *Food Chem.*, 2012, **135**, 3020–3038.
103 A. Sila and A. Bougatef, *J. Funct. Foods*, 2016, **21**, 10–26.
104 P. Fernandes, *Front. Bioeng. Biotechnol.*, 2016, **4**, 59, DOI: 10.3389/fbioe.2016.00059.
105 I. Petrova, I. Tolstorebrov and T. Magne Eikevik, *Int. Aquat. Res.*, 2018, **10**, 223–241.
106 K.-C. Hsu, *Food Chem.*, 2010, **122**, 42–48.
107 R. Slizyte, K. Rommi, R. Mozuraityte, P. Eck, K. Five and T. Rustad, *Biotechnol. Rep.*, 2016, **11**, 99–109.
108 R. Abejón, M. P. Belleville, J. Sanchez-Marcano, A. Garea and A. Irabien, *Sep. Purif. Technol.*, 2018, **197**, 137–146.
109 D. F. Williams, *Biomaterials*, 2009, **30**, 5897–5909.
110 V. dos Santos, R. N. Brandalise and M. Savaris, *Engineering of Biomaterials, Biomaterials: characteristics and properties*, Springer AG, 2017.

111 S.-W. Chang and M. J. Buehler, *Mater. Today*, 2014, **17**, 70–76.
112 R. Mayne and R. G. Brewton, *Curr. Opin. Cell Biol.*, 1993, **5**, 883–890.
113 O. Pasvolsky, R. Umalsky, Y. Naparstek and A. Y. Hershko, in *Anticollagen Antibodies, Autoantibodies*, ed. Y. Shoenfeld, P. L. Meroni and M. E. Gershwin, Elsevier, 3rd edn, 2014.
114 A. Miller and J. S. Wray, *Nature*, 1971, **230**(5294), 437–439.
115 N. Annabi, S. M. Mithieux, G. Camci-Unal, M. R. Dokmeci, A. S. Weiss and A. Khademhosseini, *Biochem. Eng. J.*, 2013, **77**, 110–118.
116 C. H. Lee, A. Singla and Y. Lee, *Int. J. Pharm.*, 2001, **221**, 1–22.
117 R. Parenteau-Bareil, R. Gauvin and F. Berthod, *Materials*, 2010, **3**, 1863–1887.
118 S. Yamada, K. Yamamoto, T. Ikeda, K. Yanagiguchi and Y. Hayashi, *BioMed. Res. Int.*, 2014, 302932, DOI: 10.1155/2014/302932.
119 D. Swatschek, W. Schatton, J. Kellermann, W. E. Müller and J. Kreuter, *Eur. J. Pharm. Biopharm.*, 2002, **53**, 107–113.
120 D. Miranda-Nieves and E. L. Chaikof, *ACS Biomater. Sci. Eng.*, 2017, **3**, 694–711.
121 T. Nagai and N. Suzuki, *Food Chem.*, 2000, **68**, 277–281.
122 Y. Nomura, H. Sakai, Y. Ishii and K. Shirai, *Biosci., Biotechnol., Biochem.*, 1996, **60**, 2092–2094.
123 T. Ikoma, H. Kobayashi, J. Tanaka, D. Walsh and S. Mann, *Int. J. Biol. Macromolecules*, 2003, **32**, 199–204.
124 F. Pati, B. Adhikari and S. Dhara, *Biores. Technol.*, 2010, **101**, 3737–3742.
125 K. S. Silvipriya, K. K. Kumar, A. R. Bhat, B. D. Kumar, A. John and P. Lakshmanan, *J. Appl. Pharm. Sci.*, 2015, **5**, 123–127.
126 B. Hoyer, A. Bernhardt, A. Lode, S. Heinemann, J. Sewing, M. Klinger, H. Notbohm and M. Gelinsky, *Acta Biomater.*, 2014, **10**, 883–892.
127 L. T. Minh Thuy, E. Okazaki and K. Osako, *Food Chem.*, 2014, **149**, 264–270.
128 S. Mahboob, *J. Food Sci. Technol.*, 2015, **52**, 4296–4305.
129 P. K. Bhagwat and P. B. Dandge, *Biocatal. Agric. Biotechnol.*, 2016, **7**, 234–240.
130 B. Kumar and S. Rani, *J. Food Sci. Technol.*, 2017, **54**, 276–278.
131 J. Venkatesan, S. Anil, S.-K. Kim and M. S. Shim, *Mar. Drugs*, 2017, **15**, 143.
132 G. Kumar Pal and P. V. Suresh, *Mater. Sci. Eng.*, 2017, **C70**, 32–40.
133 P. G. Kumar, T. Nidheesh, K. Govindaraju, J. Anand and P. V. Suresh, *J. Sci. Food Agric.*, 2016, **97**, 1451–1458.
134 K.-M. Song, S. K. Jung, Y. H. Kim, Y. E. Kim and N. H. Lee, *Food Bioprod. Process.*, 2018, **110**, 96–103.
135 C. Bai, Q. Wei and X. Ren, *ACS Sustainable Chem. Eng.*, 2017, **5**, 7220–7227.
136 N. Muhammad, G. Gonfa, A. Rahim, P. Ahmad, F. Iqbala, F. Sharif, A. S. Khan, F. U. Khan, Z. U. H. Khan, F. Rehman and I. U. Rehman, *J. Mol. Liq.*, 2017, **232**, 258–264.
137 A. A. Barros, I. M. Aroso, T. H. Silva, J. F. Mano, A. R. C. Duarte and R. L. Reis, *ACS Sustainable Chem. Eng.*, 2015, **3**, 254–260.
138 J. C. Silva, A. A. Barros, I. M. Aroso, D. Fassini, T. H. Silva, R. L. Reis and A. R. C. Duarte, *Ind. Eng. Chem. Res.*, 2016, **55**, 6922–6930.
139 G. K. S. Arumugam, D. Sharma, R. M. Balakrishnan and J. B. P. Ettiyappan, *Sustainable Chem. Pharm.*, 2018, **9**, 19–26.
140 Z. Dong, D. Liu and J. K. Keesing, *Mar. Pollut. Bull.*, 2010, **60**, 954–963.
141 Z. Rastian, S. Pütz, Y. Wang, S. Kumar, F. Fleissner, T. Weidner and S. H. Parekh, *ACS Biomater. Sci. Eng.*, 2018, **4**, 2115–2125.
142 C. Y. Huang, J. M. Kuo, S. J. Wub and H. T. Tsai, *Food Chem.*, 2016, **190**, 997–1006.
143 (*a*) https://clearmedicine.com/top-ten-benefits-marine-collagen/; (*b*) https://www.justvitamins.co.uk/blog/bovine-collagen-vs-marine-collagen/#.XMkIA6TA82w, last access May 1, 2019.
144 J. Liang, X. Pei, Z. Zhang, N. Wang, J. Wang and Y. Li, *J. Food Sci.*, 2010, **75**, H230–H238.
145 E. Proksch, D. Segger, J. Degwert, M. Schunck, V. Zague and S. Oesser, *Skin Pharmacol. Physiol.*, 2014, **27**, 47–55.
146 A. L. Alves, A. L. P. Marques, E. Martins, T. H. Silva and R. L. Reis, *Cosmetics*, 2017, **4**, 39.
147 C. Liu and J. Sun, *Biomacromolecules*, 2014, **15**, 436–443.
148 F. Subhan, M. Ikram, A. Shehzad and A. Ghafoor, *J. Food Sci. Technol.*, 2015, **52**, 4703–4707.
149 H. Ma, J. Shen, Q. Yang, J. Zhou, S. Xia and J. Cao, *Ind. Eng. Chem. Res.*, 2015, **54**, 10945–10951.
150 T. Mitra, P. Jana Manna, S. T. K. Raja, A. Gnanamani and P. P. Kundu, *RSC Adv.*, 2015, **5**, 98653–98665.
151 T. Zhou, N. Wang, Y. Xue, T. Ding, X. Liu, X. Mo and J. Sun, *Colloids Surf., B*, 2016, **143**, 415–422.
152 S. K. Ghosh and D. Mandal, *ACS Sustainable Chem. Eng.*, 2017, **5**, 8836–8843.
153 S. K. Ghosh and D. Mandal, *Nano Energy*, 2016, **28**, 356–365.
154 T. Muthukumar, P. Prabu, K. Ghosh and T. P. Sastry, *Colloids Surf., B*, 2014, **113**, 207–212.
155 T. I. Mredha, N. Kitamura, T. Nonoyama, S. Wada, K. Goto, X. Zhang, T. Nakajima, T. Kurokawa, Y. Takagi, K. Yasuda and J. P. Gong, *Biomaterials*, 2017, **132**, 85–95.
156 (*a*) G. Ramanathan, T. Muthukumar and U. T. Sivagnanam, *Eur. J. Pharmacol.*, 2017, **814**, 45–55; (*b*) G. Ramanathan, S. Singaravelu, M. D. Raja, N. Nagiah, P. Padmapriya, K. Ruban, K. Kaveri, T. S. Natarajan, U. T. Sivagnanam and P. T. Perumal, *RSC Adv.*, 2016, **6**, 7914–7922.
157 C. Ferrario, L. Leggio, R. Leone, C. Di Benedetto, L. Guidetti, V. Cocce, M. Ascagni, F. Bonasoro, C. A. M. La Porta, M. D. Candia Carnevali and M. Sugni, *Mar. Environ. Res.*, 2017, **128**, 46–57.
158 J. Chen, K. Gao, S. Liu, S. Wang, J. Elango, B. Bao, J. Dong, N. Liu and W. Wu, *Mar. Drugs*, 2019, **17**, 33.
159 C. Liu, X. Liu, Y. Xue, T. Ding and J. Sun, *RSC Adv.*, 2015, **5**, 30727–30736.

160 S. Zhu, Z. Gu, S. Xiong, Y. An, Y. Liu, T. Yin, J. Youa and Y. Hu, *RSC Adv.*, 2016, **6**, 66180–66190.
161 B. Hoyer, A. Bernhardt, S. Heinemann, I. Stachel, M. Meyer and M. Gelinsky, *Biomacromolecules*, 2012, **13**, 1059–1066.
162 A. Mandal, S. Sekar, K. M. Seeni Meera, A. Mukherjee, T. P. Sastry and A. B. Mandal, *Phys. Chem. Chem. Phys.*, 2014, **16**, 20175–20183.
163 J. Zhang, Y. Sun, Y. Zhao, B. Wei, C. Xu, L. He, C. L. P. Oliveira and H. Wang, *Soft Matter*, 2017, **13**, 9220–9228.
164 S. K. Ghosh and D. Mandal, *Appl. Phys. Lett.*, 2016, **109**, 103701.
165 C. K. S. Pillai, W. Paul and C. P. Sharma, *Prog. Polym. Sci.*, 2009, **34**, 641–678.
166 A. Verlee, S. Mincke and C. V. Stevens, *Carbohydr. Polym.*, 2017, **164**, 268–283.
167 S. Kaur and G. S. Dhillon, *Crit. Rev. Biotechnol.*, 2015, **35**, 44–61.
168 R. Vani and S. A. Stanley, *Adv. Biotechnol.*, 2013, **12**, 12–15.
169 C. Peniche, W. Argüelles-Monal and F. M. Goycoolea, Chitin and Chitosan: Major Sources, Properties and Applications, In *Monomers, Polymers and Composites from Renewable Resources*, ed. M. N. Belgacem and A. Gandini, Elsevier, 2008.
170 I. Hamed, F. Ozogul and J. M. Regenstein, *Trends Food Sci. Technol.*, 2016, **48**, 40–50.
171 R. Jayakumar, M. Prabaharan, P. T. Sudheesh Kumar, S. V. Nair and H. Tamura, *Biotechnol. Adv.*, 2011, **29**, 322–337.
172 L. Wang, B. Yang, B. Yan and X. Yao, *Food Sci. Emerg. Technol.*, 2012, **13**, 120–127.
173 K. Prameela, K. Venkatesh, S. B. Immandi, A. P. K. Kasturi, C. R. Krishna and C. M. Mohan, *Food Chem.*, 2017, **237**, 121–132.
174 X. Mao, N. Guo, J. Sun and C. Xue, *J. Clean. Prod.*, 2017, **143**, 814–823.
175 V. Zargar, M. Asghari and A. Dashti, *Chem. Bio. Eng. Rev.*, 2015, **2**, 204–226.
176 A. Anitha, S. Sowmya, P. T. Sudheesh Kumar, S. Deepthi, K. P. Chennazhi, H. Ehrlich, M. Tsurkan and R. Jayakumar, *Prog. Polym. Sci.*, 2014, **39**, 1644–1667.
177 M. Yadav, P. Goswami, K. Paritosh, M. Kumar, N. Pareek and V. Vivekanand, *Bioresour. Bioprocess.*, 2019, **6**, 8.
178 H. K. No and E. Y. Hur, *J. Agric. Food Chem.*, 1998, **46**, 3844–3846.
179 E. Khor, in *The Sources and Production of Chitin In Chitin*, ed. E. Khor, Elsevier Science Ltd, 2001, ch. 5, pp. 63–72, DOI: 10.1016/B978-008044018-7/50005-1.
180 Y. Qin, X. Lu, N. Sun and R. D. Rogers, *Green Chem.*, 2010, **12**, 968–971.
181 Mari Signum, LLC. https://www.marisignum.com, last access May 9, 2019.
182 J. L. Shamshina, P. Berton and R. D. Rogers, *ACS Sustainable Chem. Eng*, 2019, **7**, 6444–6457.
183 J. L. Shamshina, P. S. Barber, G. Gurau, C. S. Griggs and R. D. Rogers, *ACS Sustainable Chem. Eng*, 2016, **4**, 6072–6081.
184 T. Uto, S. Idenoue, K. Yamamoto and J.-I. Kadokawa, *Phys. Chem. Chem. Phys.*, 2018, **20**, 20669–20677.
185 H. Yang, G. Gözaydın, R. R. Nasaruddin, J. R. G. Har, X. Chen, X. Wang and N. Yan, *ACS Sustainable Chem. Eng.*, 2019, **7**, 5532–5542.
186 D. Ramamoorthy and D. Raghavachari, *ACS Sustainable Chem. Eng.*, 2018, **6**, 846–853.
187 S. Reinwald, C. M. Weaver and J. J. Kester, The Health Benefits of Calcium Citrate Malate: A Review of the Supporting Science, ed. S. L. Taylor, *Advances in Food and Nutrition Research*, Academic Press, 2008, ch. 6.
188 A. Jardine and S. Sayed, *Curr. Opin Green Sustainable Chem.*, 2016, **2**, 34–39.
189 O. S. Hammond, D. T. Bowron and K. J. Edler, *Angew. Chem., Int. Ed.*, 2017, **56**, 9782–9785.
190 K. Radošević, M. C. Bubalo, V. G. Srček, D. Grgas, T. L. Dragičević and I. Radojčić Redovniković, *Ecotoxicol. Environ. Saf.*, 2015, **112**, 46–53.
191 P. Zhu, Z. Gu, S. Hong and H. Lian, *Carbohydr. Polym.*, 2017, **177**, 217–223.
192 S. Hong, Y. Yuan, Q. Yang, P. Zhu and H. Lian, *Carbohydr. Polym.*, 2018, **201**, 211–217.
193 W.-C. Huang, D. Zhao, N. Guo, C. Xue and X. Mao, *J. Agric. Food Chem.*, 2018, **66**, 11897–11901.
194 D. Zhao, W.-C. Huang, N. Guo, S. Zhang, C. Xue and X. Mao, *Polymers*, 2019, **11**, 409.
195 T. Kokubo, M. Hanakawa, M. Kawashita, M. Minoda, T. Beppu, T. Miyamoto and T. Nakamura, *Biomaterials*, 2004, **25**, 4485–4488.
196 P. Hassanzadeh, M. Kharaziha, M. Nikkhah, S. R. Shin, J. Jin, S. He, W. Sun, C. Zhong, M. R. Dokmeci, A. Khademhosseini and M. Rolandi, *J. Mater. Chem. B*, 2013, **1**, 4217–4224.
197 P. Hassanzadeh, W. Sun, J. P. de Silva, J. Jin, K. Makhnejia, G. L. W. Cross, M. Rolandi, J. Mater. Chem. B, 2014, **2**, 2461–2466.
198 F. Ding, H. Deng, Y. Du, X. Shi and Q. Wang, *Nanoscale*, 2014, **6**, 9477.
199 P. S. Barber, C. S. Griggs, J. R. Bonner and R. D. Rogers, *Green Chem.*, 2013, **15**, 601–607.
200 Y. Huang, Z. Zhong, B. Duan, L. Zhang, Z. Yang, Y. Wang and Q. Yeb, *J. Mater. Chem. B*, 2014, **2**, 3427–3432.
201 N. A. Hoque, P. Thakur, P. Biswas, M. M. Saikh, S. Roy, B. Bagchi, S. Das and P. P. Ray, *J. Mater. Chem. A*, 2018, **6**, 13848–13858.
202 J. A. Gonzalez, M. F. Mazzobre, M. E. Villanueva, L. E. Diaz and G. J. Copello, *RSC Adv.*, 2014, **4**, 16480–16488.
203 S. Gopi, P. Balakrishnan, C. Divya, S. Valic, E. G. Bajsic, A. Pius and S. Thomas, *New J. Chem.*, 2017, **41**, 12746–12755.
204 C. C. Satam, C. W. Irvin, A. W. Lang, J. C. R. Jallorina, M. L. Shofner, J. R. Reynolds and J. Carson Meredith, *ACS Sustainable Chem. Eng.*, 2018, **6**, 10637–10644.
205 J. J. Vilatela and D. Eder, *ChemSusChem*, 2012, **5**, 456–478.
206 S. K. Rastogi, A. Kalmykov, N. Johnson and T. Cohen-Karni, *J. Mater. Chem. B*, 2018, **6**, 7159–7178.
207 C. Tang, M.-M. Titirici and Q. Zhang, *J. Energy Chem.*, 2017, **26**, 1077–1093.

208 A. Bhati, G. K. M. Tripathi, A. Singh, S. Sarkar and S. K. Sonkar, *New J. Chem.*, 2018, **42**, 16411–16427.
209 J. B. Essner and G. A. Baker, *Environ. Sci.: Nano*, 2017, **4**, 1216–1263.
210 R. Wang, K.-Q. Lu, Z.-R. Tang and Y.-J. Xu, *J. Mater. Chem. A*, 2017, **5**, 3717–3734.
211 Y. Zhao, R. Nakamura, K. Kamiya, S. Nakanishi and K. Hashimoto, *Nat. Commun.*, 2013, **4**, 2390.
212 T.-D. Nguyen, K. E. Shopsowitz and M. J. MacLachlan, *J. Mater. Chem. A*, 2014, **2**, 5915–5921.
213 Y. Gao, X. Chen, J. Zhang and N. Yan, *ChemPlusChem*, 2015, **80**, 1556–1564.
214 S. Kumari, P. Rath, A. S. H. Kumar and T. N. Tiwari, *Environ. Technol. Innov.*, 2015, **3**, 77–85.
215 G. Wu, M. Feng and H. Zhan, *RSC Adv.*, 2015, **5**, 44636–44641.
216 R. Devi and R. Dhamodharan, *ACS Sustainable Chem. Eng.*, 2018, **6**, 11313–11325.
217 X. Gao, X. Chen, J. Zhang, W. Guo, F. Jin and N. Yan, *ACS Sustainable Chem. Eng.*, 2016, **4**, 3912–3920.
218 X. Chen, S. L. Chew, F. M. Kerton and N. Yan, *Green Chem.*, 2014, **16**, 2204–2212.
219 X. Chen, S. L. Chew, F. M. Kerton and N. Yan, *RSC Adv.*, 2015, **5**, 20073–20080.
220 M. V. Tzoumaki, D. Karefyllakis, T. Moschakis, C. G. Biliaderisc and E. Scholten, *Soft Matter*, 2015, **11**, 6245–6253.
221 Y. Fang, R. Zhang, B. Duan, M. Liu, A. Lu and L. Zhang, *ACS Sustainable Chem. Eng.*, 2017, **5**, 2725–2733.
222 P. S. Saravana, T. C. Ho, S.-J. Chae, Y.-J. Cho, J.-S. Park, H.-J. Lee and B.-S. Chun, *Carbohydr. Polym.*, 2018, **195**, 622–630.
223 C. J. Raj, M. Rajesh, R. Manikandan, K. H. Yu, J. R. Anusha, J. H. Ahn, D.-W. Kim, S. Y. Park and B. C. Kim, *J. Power Sources*, 2018, **386**, 66–76.
224 G. Margoutidis, V. H. Parsons, C. S. Bottaro, N. Yan and F. M. Kerton, *ACS Sustainable Chem. Eng*, 2018, **6**, 1662–1669.
225 C. A. King, J. L. Shamshina, O. Zavgorodnya, T. Cutfield, L. E. Block and R. D. Rogers, *ACS Sustainable Chem. Eng.*, 2017, **5**, 11660–11667.
226 A. Zhang, G. Wei, X. Mo, N. Zhou, K. Chen and P. Ouyanga, *Green Chem.*, 2018, **20**, 2320–2327.
227 Y. Zou and E. Khor, *Carbohydr. Polym.*, 2009, **77**, 516–525.
228 E. Castagnino, M. F. Ottaviani, M. Cangiotti, M. Morelli, L. Casettari and R. A. Muzzarelli, *Carbohydr. Polym.*, 2008, **74**, 640–647.
229 H. Liu, Q. Yang, L. Zhang, R. Zhuo and X. Jiang, *Carbohydr. Polym.*, 2016, **137**, 600–607.
230 M. N. V. R. Kumar, R. A. A. Muzzarelli, C. Muzzarelli, H. Sashiwa and A. J. Domb, *Chem. Rev.*, 2004, **104**, 6017–6084.
231 M. Hamdi, R. Nasri, S. Hajji, M. Nigen, S. Li and M. Nasri, *Food Hydrocolloids*, 2019, **87**, 48–60.
232 K. L. B. Chang, G. Tsai, J. Lee and W. R. Fu, *Carbohydr. Res.*, 1997, **303**, 327–332.
233 L. Bekale, D. Agudelo and H. A. Tajmir-Riahi, *Colloids Surf., B*, 2015, **125**, 309–317.
234 A. Fiamingo, J. A. de Moura Delezuk, S. Trombotto, L. David and S. P. Campana-Filho, *Ultrason. Sonochem.*, 2016, **32**, 79–85.
235 M. Mazza, D. A. Catana, C. V. Garcia and C. Cecutti, *Cellulose*, 2009, **16**, 207–215.
236 M. Shimo, M. Abe and H. Ohno, *ACS Sustainable Chem. Eng.*, 2016, **4**, 3722–3727.
237 T. Di Nardo, C. Hadad, A. N. Van Nhien and A. Moores, *Green Chem.*, 2019, **21**, 3276–3285, DOI: 10.1039/c9gc00304e.
238 Z. Amoozgar, J. Park, Q. Lin and Y. Yeo, *Mol. Pharmaceutics*, 2012, **9**, 1262–1270.
239 C. Lim, D. W. Lee, J. N. Israelachvili, Y. S. Jho and D. S. Hwang, *Carbohydr. Polym.*, 2015, **117**, 887–894.
240 X. Chen, H. Yang, Z. Zhong and N. Yan, *Green Chem.*, 2017, **19**, 2783–2792.
241 G. Margoutidis, V. Parsons, C. S. Bottaro, N. Yan and F. M. Kerton, *ACS Sustainable Chem. Eng.*, 2018, **6**, 1662–1669.
242 M. Yabushita, H. Kobayashi, K. Kuroki, S. Ito and A. Fukuoka, *ChemSusChem*, 2015, **8**, 3760–3763.
243 R. S. C. M. de Queiroz Antonino, B. R. P. L. Fook, V. A. de Oliveira Lima, R. Í. de Farias Rached, E. P. N. Lima, R. J. da Silva Lima, C. A. P. Covas and M. V. L. Fook, *Mar. Drugs*, 2017, **15**, 141.
244 N. Pacheco, M. Garnica-Gonzalez, M. Gimeno, E. Bárzana, S. Trombotto, L. David and K. Shirai, *Biomacromolecules*, 2011, **12**, 3285–3290.
245 T. S. Tan, H. Y. Chin, M. L. Tsai and C. L. Liu, *Carbohydr. Polym.*, 2015, **122**, 321–328.
246 C. T. G. V. M. T. Pires, J. A. P. Vilela and C. Airoldi, *Procedia Chem.*, 2014, **9**, 220–225.
247 A. Sahu, P. Goswami and U. Bora, *J. Mater. Sci.: Mater. Med.*, 2009, **20**, 171–175.
248 C. Peniche, W. Argüelles-Monal and F. M. Goycoolea Chitin and Chitosan: Major Sources, Properties and Applications, In Monomers, in *Polymers and Composites from Renewable Resources*, ed. M. N. Belgacem and A. Gandini, Elsevier, 2008.
249 N. Kubota, N. Tatsumoto, T. Sano and K. Toya, *Carbohydr. Res.*, 2000, **324**, 268–274.
250 C. Qin, H. Li, Q. Xiao, Y. Liu, J. Zhu and Y. Du, *Carbohydr. Polym.*, 2006, **63**, 367–374.
251 E. Khor and L. Y. Lim, *Biomaterials*, 2003, **24**, 2339–2349.
252 I. Younes and M. Rinaudo, *Mar. Drugs*, 2015, **13**, 1133.
253 J. Duan, X. Liang, Y. Cao, S. Wang and L. Zhang, *Macromolecules*, 2015, **48**, 2706–2714.
254 J. You, S. Xie, J. Cao, H. Ge, M. Xu, L. Zhang and J. Zhou, *Macromolecules*, 2016, **49**, 1049–1059.
255 A. Konwar, S. Kalita, J. Kotoky and D. Chowdhury, *ACS Appl. Mater. Interfaces*, 2016, **8**, 20625–20634.
256 J. H. Ryu, S. Hong and H. Lee, *Acta Biomater.*, 2015, **27**, 101–115.
257 S. S. Silva, J. F. Mano and R. L. Reis, *Green Chem.*, 2017, **19**, 1208–1220.
258 M. Lee, B.-Y. Chen and W. Den, *Appl. Sci.*, 2015, **5**, 1272–1283.
259 Z. Ma, A. Garrido-Maestu and K. C. Jeong, *Carbohydr. Polym.*, 2017, **176**, 257–265.

260 I. M. El-Sherbiny and N. M. El-Baz, A Review on Bionanocomposites Based on Chitosan and Its Derivatives for Biomedical Applications, in *Eco-friendly Polymer Nanocomposites, Chemistry and Applications*, ed. V. K. Thakus and M. K. Thakur, Spinger, 2015.
261 M. Ahmad, K. Manzoor and S. Ikram, *Int. J. Biol. Macromol.*, 2017, **105**, 190–203.
262 G. Kerch, *Mar. Drugs*, 2015, **13**, 2158–2182.
263 V. K. H. Bui, D. Park and Y.-C. Lee, *Polymers*, 2017, **9**, 21.
264 L. A. M. van den Broek, R. J. I. Knoop, F. H. J. Kappen and C. G. Boeriu, *Carbohydr. Polym.*, 2015, **116**, 237–242.
265 B. Cheng, B. Pei, Z. Wang and Q. Hu, *RSC Adv.*, 2017, **7**, 42036–42046.
266 A. El Kadib, *ChemSusChem*, 2015, **8**, 217–244.
267 S. Dimassi, N. Tabary, F. Chai, N. Blanchemain and B. Martel, *Carbohydr. Polym.*, 2018, **202**, 382–396.
268 V. Patrulea, V. Ostafe, G. Borchard and O. Jordan, *Eur. J. Pharm. Biopharm.*, 2015, **97**, 417–426.
269 H. Hamedi, S. Moradi, S. M. Hudson and A. E. Tonelli, *Carbohydr. Polym.*, 2018, **199**, 445–460.
270 M. A. Elgadir, M. S. Uddin, S. Ferdosh, A. Adam, A. J. K. Chowdhury and M. Z. I. Sarker, *J. Food Drug Anal.*, 2015, **23**, 619–629.
271 M. C. G. Pellá, M. K. Lima-Tenório, E. T. Tenório-Neto, M. R. Guilherme, E. C. Muniz and A. F. Rubira, *Carbohydr. Polym.*, 2018, **196**, 233–245.
272 G. Z. Kyzas and D. N. Bikiaris, *Mar. Drugs*, 2015, **13**, 312–337.
273 P. M. Pakdel and S. J. Peighambardoust, *Carbohydr. Polym.*, 2018, **201**, 264–279.
274 J. Carneiro, J. Tedim and M. G. S. Ferreira, *Prog. Org. Coat.*, 2015, **89**, 348–356.
275 D. R. Perinelli, L. Fagioli, R. Campana, J. K. W. Lam, W. Baffone, G. F. Palmieri, L. Casettari and G. Bonacucina, *Eur. J. Pharm. Sci.*, 2018, **117**, 8–20.
276 G. Kerch, *Trends Food Sci. Technol.*, 2015, **46**, 159–166.
277 A. Ali and S. Ahmed, *Int. J. Biol. Macromol.*, 2018, **109**, 273–286.
278 S. Ahmed and S. Ikram, *Achiev. Life Sci.*, 2016, **10**, 27–37.
279 H. El Knidri, R. Belaabed, A. Addaou, A. Laajeb and A. Lahsini, *Int. J. Biol. Macromol.*, 2018, **120**, 1181–1189.
280 A. Khalil H. P. S., C. K. Saurabh, A. S. Adnan, M. R. Nurul Fazita, M. I. Syakir, Y. Davoudpour, M. Rafatullah, C. K. Abdullah, M. K. M. Haafiz and R. Dungani, *Carbohydr. Polym.*, 2016, **150**, 216–226.
281 S. Ahmed, Annu, A. Ali and J. Sheikh, *Int. J. Biol. Macromol.*, 2018, **116**, 849–862.
282 R. LogithKumar, A. KeshavNarayan, S. Dhivya, A. Chawla, S. Saravanan and N. Selvamurugan, *Carbohydr. Polym.*, 2016, **151**, 172–188.
283 H. Wang, J. Qian and F. Ding, *J. Agric. Food Chem.*, 2018, **66**, 395–413.
284 S. Olivera, H. B. Muralidhara, K. Venkatesh, V. K. Guna, K. Gopalakrishna and K. Yogesh Kumar, *Carbohydr. Polym.*, 2016, **153**, 600–618.
285 I. Aranaz, N. Acosta, C. Civera, B. Elorza, J. Mingo, C. Castro, M. de los Llanos Gandía and A. Heras Caballero, *Polymers*, 2018, **10**, 213.
286 M. I. A. Echazú, M. V. Tuttolomondo, M. L. Foglia, A. M. Mebert, G. S. Alvarez and M. F. Desimone, *J. Mater. Chem. B*, 2016, **4**, 6913–6929.
287 H. Li, C. Hu, H. Yu and C. Chen, *RSC Adv.*, 2018, **8**, 3736–3749.
288 N. Islam and V. Ferro, *Nanoscale*, 2016, **8**, 14341–14358.
289 R. Antony, T. Arun, S. Theodore and D. Manickam, *Int. J. Biol. Macromol.*, 2019, **129**, 615–633.
290 R. Yang, H. Li, M. Huang, H. Yang and A. Li, *Water Res.*, 2016, **95**, 59–89.
291 M. Mujtaba, R. E. Morsi, G. Kerch, M. Z. Elsabee, M. Kaya, J. Labidi and K. M. Khawar, *Int. J. Biol. Macromol.*, 2019, **121**, 889–904.
292 P. Sahariah and M. Masson, *Biomacromolecules*, 2017, **18**, 3846–3868.
293 E. Avcu, F. E. Baştan, H. Z. Abdullah, M. A. U. Rehman, Y. Y. Avcu and A. R. Boccaccini, *Progr Mater. Sci.*, 2019, **103**, 69–108.
294 P. Kanmani, J. Aravind, M. Kamaraj, P. Sureshbabu and S. Karthikeyan, *Biores. Technol.*, 2017, **242**, 295–303.
295 M. Vakili, S. Deng, G. Cagnetta, W. Wang, P. Meng, D. Liu and G. Yu, *Sep. Purif. Technol.*, 2019, **224**, 373–387.
296 M. A. M. Rocha, M. A. Coimbra and C. Nunes, *Curr. Opin. Food Sci.*, 2017, **15**, 61–69.
297 A. Kassem, G. M. Ayoub and L. Malaeb, *Sci. Total Environ.*, 2019, **668**, 566–576.
298 J. Liu, H. Pu, S. Liu, J. Kan and C. Jin, *Carbohydr. Polym.*, 2017, **174**, 999–1017.
299 X. Jing, H.-Y. Mi, B. N. Napiwocki, X.-F. Peng and L.-S. Turng, *Carbon*, 2017, **125**, 557–570.
300 W. Jiang, W. Wang, B. Pan, Q. Zhang, W. Zhang and L. Lv, *ACS Appl. Mater. Interfaces*, 2014, **6**, 3421–3426.
301 L. Zhang, T. Zhu, X. Liu and W. Zhang, *J. Hazard. Mater.*, 2016, **308**, 1–10.
302 W. Cai, W. Xue and Y. Jiang, *ACS Omega*, 2018, **3**, 5725–5734.
303 G. L. Dotto, J. M. N. Santos, E. H. Tanabe, D. A. Bertuol, E. L. Foletto, E. C. Lima and F. A. Pavan, *J. Clean. Prod.*, 2017, **144**, 120–129.
304 X. Wang, J. Shi, Z. Li, S. Zhang, H. Wu, Z. Jiang, C. Yang and C. Tian, *ACS Appl. Mater. Interfaces*, 2014, **6**, 14522–14532.
305 Y. Yan, X. Zhang, C. Li, Y. Huanga, Q. Dinga and X. Pang, *Appl. Surf. Sci.*, 2015, **332**, 62–69.
306 A. Szcześ, L. Hołysz and E. Chibowski, *Adv. Colloid Interface Sci.*, 2017, **249**, 321–330.
307 M. Akram, R. Ahmed, I. Shakir, W. Aini, W. Ibrahim and R. Hussain, *J. Mater. Sci.*, 2014, **49**, 1461–1475.
308 T. Nagai and N. Suzuki, *Food Chem.*, 2000, **68**, 277–281.
309 P. Terzioğlu, H. Öğüt and A. Kalemtaş, *Mater. Sci. Eng., C*, 2018, **91**, 899–911.
310 M. Boutinguiza, J. Pou, R. Comesaña, F. Lusquiños, A. de Carlos and B. León, *Mater. Sci. Eng., C*, 2012, **32**, 478–486.
311 B. Ratna Sunil and M. Jagannatham, *Mater. Lett.*, 2016, **185**, 411–414.
312 J. S. Cho, D. S. Yoo, Y. C. Chung and S. H. Rhee, *J. Biomed. Mater. Res., Part A*, 2014, **102**, 455–469.

313 L. Stipniece, K. Salma-Ancane, N. Borodajenko, M. Sokolova, D. Jakovlevs and L. BerzinaCimdina, *Ceram. Int.*, 2014, **40**, 3261–3267.
314 M. Boutinguiza, F. Lusquiños, R. Comesaña, A. Riveiro, F. Quintero and J. Pou, *Appl. Surf. Sci.*, 2007, **254**, 1264–1267.
315 P. Shi, M. Liu, F. Fan, C. Yu, W. Lu and M. Du, *Mater. Sci. Eng., C*, 2018, **90**, 706–712.
316 R. Astala and M. J. Stott, *Chem. Mater.*, 2005, **17**, 4125–4133.
317 C. Piccirillo, R. C. Pullar, E. Costa, A. Santos-Silva, M. M. E. Pintado and P. M. L. Castro, *Mater. Sci. Eng., C*, 2015, **51**, 309–315.
318 S. Kongsri, K. Janpradit, K. Buapa, S. Techawongstien and S. Chanthai, *Chem. Eng. J.*, 2013, **215–216**, 522–532.
319 W. Pon-Ona, P. Suntornsaratoon, N. Charoenphandhu, J. Thongbunchoo, N. Krishnamra and I. M. Tang, *Mater. Sci. Eng., C*, 2016, **62**, 183–189.
320 G. Karunakaran, E.-B. Cho, G. S. Kumar, E. Kolesnikov, G. Janarthanan, M. M. Pillai, S. Rajendran, S. Boobalan, M. V. Gorshenkov and D. V. Kuznetsov, *ACS Appl. Bio. Mater.*, 2019, **2**(5), 2280–2293.
321 A. Shavandi, A. El-Din, A. Bekhit, A. Ali and Z. Sun, *Mater Chem Phys.*, 2015, **149–150**, 607–616.
322 J. Venkatesan, P. D. Recka, S. Anil, I. Bhatnagar, P. N. Sudha, C. Dechsakulwatana, S.-K. Kim and M. S. Shim, *Biotechnol. Bioprocess Eng.*, 2018, **23**, 383–393.
323 S. M. Naga, H. F. El-Maghraby, E. M. Mahmoud, M. S. Talaat and A. M. Ibrhim, *Ceram. Int.*, 2015, **41**, 15010–15016.
324 T. G. M. Bonadio, V. F. Freitas, T. T. Tominaga, R. Y. Miyahara, J. M. Rosso, L. F. Cotica, M. L. Baesso, W. R. Weinand, I. A. Santos, R. Guo and A. S. Bhalla, *Curr. Appl. Phys.*, 2017, **17**, 767–773.
325 M. Saeli, C. Piccirillo, D. M. Tobaldi, R. Binions, P. M. L. Castro and R. C. Pullar, *J. Clean Prod.*, 2018, **193**, 115–127.
326 Y. Mu, A. Saffarzadeh and T. Shimaoka, *J. Clean Prod.*, 2018, **172**, 3111–3118.
327 H. Yamamura, V. H. Pereira da Silva, P. L. Menin Ruiz, V. Ussui, D. Ribeiro Ricci Lazar, A. C. Muniz Renno and D. Araki Ribeiro, *J. Mech. Behav. Biomed. Mater.*, 2018, **80**, 137–142.
328 K. Hadagalli, A. K. Panda, S. Mandal and B. Basu, *ACS Appl. Bio. Mater.*, 2019, **2**, 2171–2184.
329 C. Sudip Mondal, G. Hoang, P. Manivasagan, M. S. Moorthy, H. H. Kim, T. T. Vy Phan and J. Oh, *Mater. Chem. Phys.*, 2019, **228**, 344–356.
330 Y. Zhang, W. Zhang, Q. Zhang, K. Li, W. Liu, Y. Liu and C. E. Banks, *Analyst*, 2014, **139**, 5362–5366.
331 Q. Peng, F. Yu, B. Huang and Y. Huang, *RSC Adv.*, 2017, **7**, 26968–26973.
332 B. Khoshnevisan, M. Tabatabaei, P. Tsapekos, S. Rafiee, M. Aghbashlo, S. Lindeneg and I. Angelidaki, *Renewable Sustainable Energy Rev.*, 2020, **117**, 109493.
333 M. Thomsen, M. Seghetta, M. H. Mikkelsen, S. Gyldenkærne, T. Becker, D. Caro and P. Frederiksen, *J. Clean Prod.*, 2017, **142**, 4050–4058.
334 C.-M. Lam, I. K. M. Yu, S.-C. Hsu and D. C. W. Tsang, *J. Clean Prod.*, 2018, **199**, 840–848.
335 C. Lopes, L. T. Antelo, A. Franco-Uría, A. A. Alonso and R. Pérez-Martín, *Waste Manag.*, 2015, **46**, 103–112.
336 https://www.portseurope.com/spain-puertos-del-estado-october-2018-fish-landed-by-port-authority/, last access, December 12, 2019.
337 C. R. Lohri, S. Diener, I. Zabaleta, A. Mertenat and C. Zurbrugg, *Rev. Environ. Sci. Biotechnol.*, 2017, **16**, 81–130.